EPA'S COMPOSITE MODEL FOR LEACHATE
MIGRATION WITH TRANSFORMATION PRODUCTS

BACKGROUND DOCUMENT FOR EPACMTP: METALS TRANSPORT IN THE SUBSURFACE

Volume 1: Methodology

United States Environmental Protection Agency
Office of Solid Waste
Washington, DC 20460

August 1996

ABSTRACT

This report documents the implementation of the metals modeling procedure in EPACMTP. The modeling procedure for metals combines the finite source methodology with a metal-specific procedure for handling geochemical interactions that affect the subsurface fate and transport of metals. The latter procedure has been developed at the EPA-ORD Environmental Research Laboratory in Athens, GA and has been adopted for incorporation into EPACMTP.

This document provides a brief overview of the metals modeling procedure. It discusses modifications that were made to the EPACMTP computer code, and presents results of representative verification examples.

ACKNOWLEDGMENTS

TABLE OF CONTENTS

TABLE OF CONTENTS

LIST OF FIGURES

LIST OF FIGURES

LIST OF TABLES

1.0 INTRODUCTION

To support the Toxicity Characteristic (TC) Rule, promulgated in 1990, EPA has developed a methodology to set regulatory standards for wastes based on the expected groundwater quality impact of constituents leaching from the waste when disposed in an unlined, subtitle D municipal landfill. Wastes whose Toxicity Characteristic Leaching Procedure (TCLP) constituent concentrations exceed any of the corresponding Toxicity Characteristic (TC) regulatory limits are classified as hazardous waste.

The original rule considered only a limited number of constituents. Not included were: compounds for which a finite source assumption is appropriate, organic compounds subject to biochemical transformation and daughter product formation, and metals which are subject to complex geochemical interactions in the subsurface.

This report documents a finite source methodology applicable to the Hazardous Waste Identification Rule (HWIR). The methodology incorporates metal-specific geochemical interactions controlling the mobility of metals in the subsurface. The procedure for including geochemical interactions for metals was developed at the National Exposure Research Laboratory, Ecosystems Research Division (formerly U.S. EPA Environmental Research Laboratory) at Athens, GA. The methodology utilizes nationwide distributions of key geochemical parameters that impact metal mobility in the subsurface.

In this methodology, the MINTEQA2 metals speciation code was used to generate nonlinear adsorption isotherms for each individual metal. For each metal, a set of isotherms was produced reflecting the range in geochemical environments that is expected to be encountered at waste sites across the nation. The variability in geochemical environments was represented by four geochemical master variables: pH, concentration of iron oxide adsorption sites, concentration of dissolved and particulate natural organic matter, and concentration of anthropogenic organic acids in the leachate. The set of isotherms were made available to the fate and transport model, EPACMTP. In the fate and transport modeling for a particular metal, EPACMTP is executed for each Monte Carlo selection of possible combinations of the four master variables. For a given metal, the known or assumed probability distributions for these four variables form the basis for the Monte-Carlo selection of the appropriate adsorption isotherm. A detailed discussion of the MINTEQA2 simulation procedure for generating the metals sorption isotherms is provided in Allison et al. (1992).

Sorption isotherms have been developed for ten RCRA metals. These are: barium, cadmium, chromium (III), copper (II), mercury (II), nickel, lead, vanadium, and zinc. Beryllium is assumed to have the same isotherm as barium. Five additional metals of concern in this study could not be modeled using MINTEQA2 because adsorption reactions describing the interaction of the metal with an adsorbing surface are not reliably known. These metals are antimony (V), arsenic (III), chromium (VI), selenium (VI), and thallium (I). Because MINTEQA2 could not be used, empirical relationships due to Loux et al. (1990), which give the adsorption distribution coefficient as a function of pH, were used for these metals.

The sorption isotherms for the MINTEQA2 metals are nonlinear in that the adsorption distribution coefficient (K_d, the ratio of metal concentration in the sorbed phase (C_s) versus metal concentration in the dissolved phase (C_d) at equilibrium) is a function of metal concentration. Modifications in the fate and transport model (EPACMTP) to accommodate transport with nonlinear sorption are described in this report. The implementation of nonlinear sorption is based on the assumption that the nonlinearity of the isotherms is most important in the unsaturated zone where metals concentrations are relatively high. Upon reaching the water table and mixing of the leachate with ambient groundwater, the metals concentration is considered

to be low enough that a linear isotherm (single K_d value not dependent on metal concentration) can always be used. The appropriate saturated zone retardation factor is determined based on the maximum groundwater concentration underneath the source.

In addition to the nonlinear treatment of unsaturated zone metals transport, options to linearize the sorption isotherms have also been implemented and are discussed later in this document.

In addition to accounting for complex sorption behavior, metals modeling also requires application of the finite source methodology. The infinite source, steady state modeling methodology is not applicable to metals since at steady state, sorption, whether linear or nonlinear, would have no effect on the predicted receptor well concentration. If the steady-state, infinite source methodology was applied to metals, the model would yield results that are the same as for conservative contaminants, i.e., those considered in the 1990 TC Rule.

This report is organized as follows: Chapter 2 discusses modifications to the unsaturated zone transport module for handling nonlinear metals isotherms; Chapter 3 provides an overview of the MINTEQA2 modeling procedure for generating metal-specific sorption isotherms; Chapter 4 presents the nationwide probability distributions of the geochemical master variables that control metals mobility and discusses the linearization procedure for nonlinear isotherms; Chapter 5 discusses the modifications to the EPACMTP data input for metals; Chapter 6 discusses the implementation of the finite source methodology for metals in EPACMTP; and Chapter 7 presents a number of representative verification test cases that were analyzed to test the correctness and robustness of the EPACMTP code modifications for metals modeling.

2.0 METALS TRANSPORT MODELING

2.1   GENERAL

The fate and transport of metal species in the subsurface can be modeled using the conventional advection-dispersion equation. Therefore, most of the mathematical techniques used for simulating the transport of conservative and organic contaminants are applicable to simulation of metals. In this report, we present modifications made on the EPACMTP model specifically for simulation of metals. For more complete description of the model, the reader is referred to the EPACMTP background document (EPA, 1996a).

For the simulation of metals, the major modifications involve altering the unsaturated-zone transport module to accommodate the metal-specific nonlinear isotherms obtained by applying the geochemical speciation model MINTEQA2 (Allison et al., 1991). The nonlinear isotherms can be expressed as a dependence of K_d on metal concentration (Figure 2.1). The dependence can be depicted equally well as a dependence on the dissolved metal concentration (C_d), the sorbed metal concentration (C_s), or the total metal concentration ($C_T = C_d + C_s$). The typical behavior shown in Figure 2.1 indicates that at low total metal concentrations, K_d is relatively constant. However, as total metal concentration increases beyond some concentration threshold (dependent on the pH and other master variables, as well as the affinity of the metal for the adsorbing surface) K_d begins to decrease markedly. This tendency of apparent linear behavior at low metal concentrations has been noted by others (Stumm and Morgan, 1996). These observations have led to the following modeling approach for simulating the transport of metals: the full nonlinear isotherms (K_d depends on total concentration) are used for the unsaturated-zone transport and linear isotherms (a single K_d value suitable for low total metal concentrations) is used for the saturated-zone transport. This approach is based on the assumption that after migrating through the unsaturated zone, concentrations in the saturated zone will be low enough to justify the use of linear isotherms.

The main modification of the EPACMTP fate and transport model introduced by the simulation of metals is that the governing advection-dispersion equation in the unsaturated zone becomes nonlinear. In order to handle the nonlinearity in a computationally efficient way, two metals transport solution options have been added to the unsaturated zone module of EPACMTP.

2.2   UNSATURATED-ZONE TRANSPORT MODULE

The general advection-dispersion solute transport equation can be written as:

$$\frac{\partial C_d}{\partial t} \% \frac{\rho_b}{\theta} \frac{\partial C_s}{\partial t} \% V \cdot \nabla C_d \quad ' \quad D \nabla^2 C_d \tag{2.1}$$
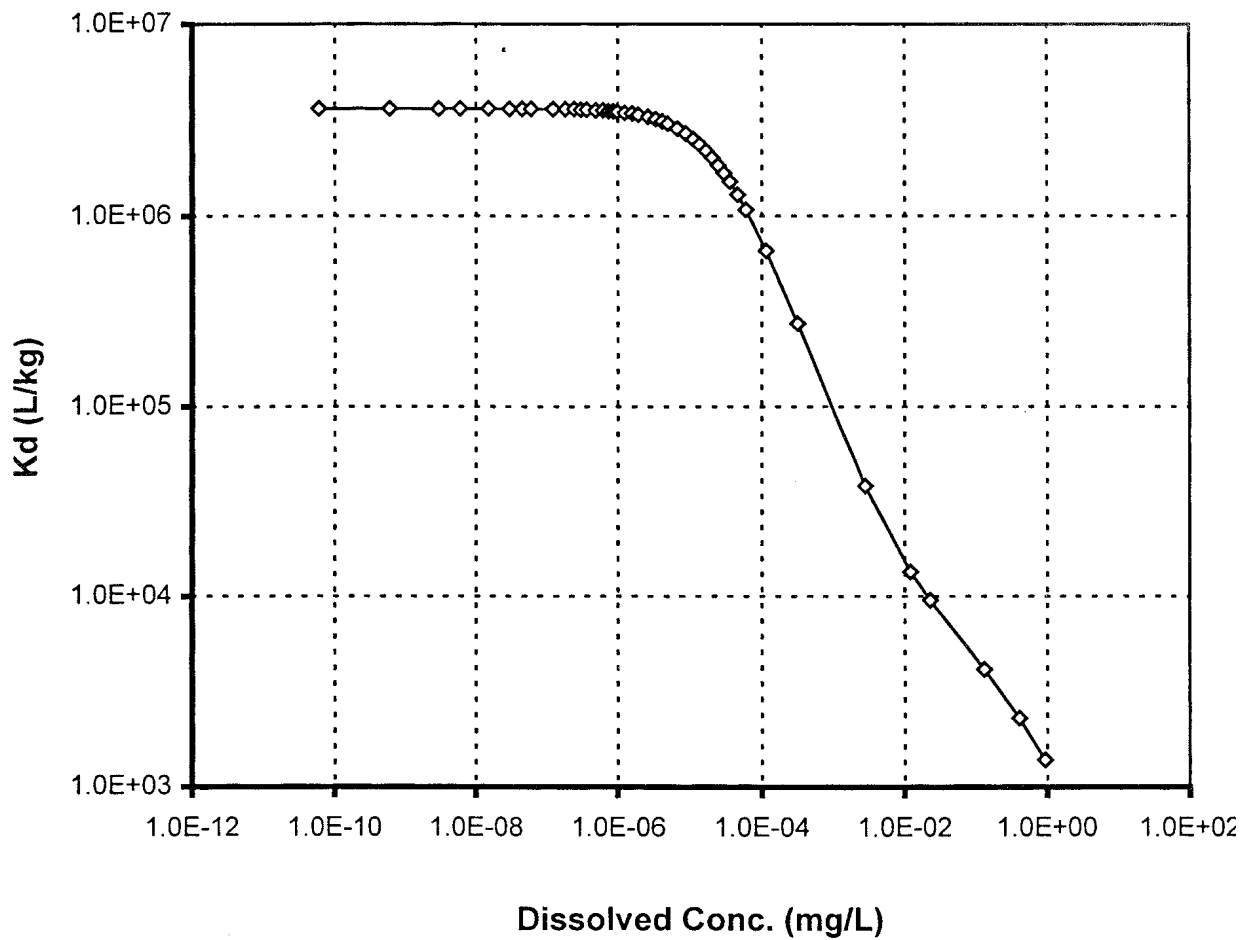
Figure 2.1 K_d is a function of metal concentration for a particular system.

where C_d is the dissolved phase concentration (mg/l), C_s is the sorbed phase concentration (mg/kg), D_b is the bulk density of soil, θ is the moisture content, V is the pore-water velocity vector, and D is the dispersion coefficient. Assuming equilibrium and reversible sorption, the sorbed phase and dissolved phase concentrations are related through:

$$C_s = K_d C_d \tag{2.2}$$

where K_d is the equilibrium partitioning coefficient (1/kg). Note that when K_d is a function of C_d, as in the metals case, the governing equation (2.1) becomes nonlinear.

EPACMTP treats flow and transport in the unsaturated zone as one-dimensional in the vertical direction. Then the spatial derivatives in (2.1) reduce to simpler forms, resulting in the following equation:

$$\frac{\partial C_d}{\partial t} + \frac{D_b}{\theta}\,\frac{\partial C_s}{\partial t} + V_u\,\frac{\partial C_d}{\partial z} = D_u\,\frac{\partial^2 C_d}{\partial z^2} \tag{2.3}$$

where z increases downward from the soil surface, and the subscript u indicates unsaturated zone properties.

The governing equation is supplemented by initial and boundary conditions. Initially, the unsaturated-zone is assumed to be free of contaminant:

$$C_d(z,0) = 0 \tag{2.4}$$

The following boundary conditions are used at the source (z= 0) and the water table (z= L):

$$\dot{M}_c = \theta\, V_u\, C_d\, - \theta D_u\,\frac{\partial C_d}{\partial z} \qquad , z = 0 \tag{2.5}$$

$$\frac{\partial C_d}{\partial z} = 0 \qquad\qquad , z = L \tag{2.6}$$

where $\dot{M}_c$ is the specified contaminant mass flux at the source.

Modifications of the unsaturated zone transport module of EPACMTP for nonlinear conditions are presented in the following sections.

2.2.1 Numerical Transport Module

Traditionally, the transport equation is solved in terms of dissolved concentration after the sorbed phase concentration is eliminated by using (2.2). However, numerical difficulties may be experienced when highly nonlinear adsorption isotherms are used. These potential difficulties are circumvented in the modified EPACMTP by using the solution approach recommended by Yeh and Tripathi (1989). They examined various numerical approaches for solving nonlinear transport equations and recommended the use of total concentration as the primary unknown. The total concentration is defined as follows:

$$C_t = C_d + \frac{D_b}{2} C_s \tag{2.7}$$

The factor $D_b/2$ before C_s is to convert from mass of sorbed metal per kilogram soil to mass of sorbed metal per liter of porewater.

Substitution of (2.7) into (2.3) results in the following equation:

$$\frac{\partial C_t}{\partial t} + V_u \frac{\partial C_t}{\partial z} - D_u \frac{\partial^2 C_t}{\partial z^2} = \frac{V_u D_b}{2} \frac{\partial C_s}{\partial z} - \frac{D_u D_b}{2} \frac{\partial^2 C_s}{\partial z^2} \tag{2.8}$$

Note that the left hand side of (2.8) is identical to the conventional transport equation written in terms of the total concentration. The right hand side of (2.8) are the correction terms for the immobile sorbed phase concentration. In the next section, the numerical techniques employed to solve (2.8) are described briefly.

2.2.2 Solution Techniques

The governing equation (2.8) supplemented by initial and boundary conditions (2.4)-(2.6) can be solved numerically, in the general case with nonlinear adsorption. EPACMTP uses the upstream Galerkin finite element method. Applying the weighted residual scheme and performing integration by parts to the dispersion terms, the following equation results:

$$\int_m dz \left[\frac{w_i}{\partial t} C_t^{k+1} + w_i \theta V_u \frac{\partial C_t^{k+1}}{\partial z} + \theta D_u \frac{\partial C_t^{k+1}}{\partial z} \frac{\partial w_i}{\partial z} \right]$$

$$= \int_m dz \left[\frac{w_i}{\partial t} C_t^k + w_i (1 - \theta) V_u \frac{\partial C_t^k}{\partial z} + (1 - \theta) D_u \frac{\partial C_t^k}{\partial z} \frac{\partial w_i}{\partial z} \right]$$

$$+ \int_m dz \left[\theta \left(w_i V_u \frac{\partial C_s^{k+1}}{\partial z} + D_u \frac{\partial w_i}{\partial z} \frac{\partial C_s^{k+1}}{\partial z} \right) + (1 - \theta) \left(w_i V_u \frac{\partial C_s^k}{\partial z} + D_u \frac{\partial w_i}{\partial z} \frac{\partial C_s^k}{\partial z} \right) \right]$$

$$+ \theta w_i D_u \frac{\partial C_d^{k+1}}{\partial z} \bigg|_0^L + (1 - \theta) w_i D_u \frac{\partial C_d^k}{\partial z} \bigg|_0^L \tag{2.9}$$

where w_i is the weighting function for node i, ∂t is the time step size, and θ is the time weighting factor.

The primary unknown in (2.9) is the total concentration at the next time level k+ 1. The sorbed phase concentration at time level k+ 1 is also not known; the solution therefore can be obtained only through iteration. Note that the boundary terms in (2.9) resulting from the integration by parts, are expressed in terms of dissolved concentration. The gradient of the dissolved phase concentration at the water table is explicitly specified as a boundary condition (2.6). However, the gradient of the water phase concentration at the source is not known. The term can be expressed in terms of the specified mass flux, as given by (2.5) and using the total concentration and sorbed concentration to eliminate C_d from (2.5).

The resulting system of algebraic equations are nonlinear. Picard iteration is used to treat the nonlinearity.

2.2.3 Analytical Transport Module

An exact analytical solution to (2.3) in general form is intractable because of the nonlinear adsorption term. In order to solve the problem, some approximations must be resorted to. If the solute transport is advection-dominated, we may ignore the dispersion term in (2.3). In that case, the transport equation (2.3) can be written as

$$V_u \frac{\partial C_d}{\partial z} \% \left[1 \% f\aleph(C_d) \right] \frac{\partial C_d}{\partial t} \quad ' \quad 0 \tag{2.10}$$

where

$$f\aleph(C_d) \quad ' \quad \frac{df(C_d)}{dC_d} \tag{2.11}$$

and $f(C_d)$ is a dimensionless nonlinear function representing the adsorption isotherm.

Alternatively, for nonlinear metals transport, the adsorption function $f(C_d)$ can be defined using tabulated isotherm data, generated by the MINTEQA2 speciation model. The initial and boundary conditions for the one-dimensional transport problem may be expressed as

Initial condition:

$$C_d \ (z, \ t \, ' \, 0) \quad ' \quad C_i \qquad (z > 0) \tag{2.12}$$

Boundary conditions:

$$C_d \ (z \, ' \, 0, \ t \, \# \, t_p) \quad ' \quad C_o \qquad (C_o \, ... \, C_i) \tag{2.13}$$

and

$$C_d \ (z \, ' \, 0, \ t > t_p) \quad ' \quad 0 \tag{2.14}$$

where C_i is the constant initial concentration of solute; C_o is a constant source concentration of the time period of $t \# t_p$; and t_p is the time period during which a constant concentration source is applied at the surface boundary.

Equation (2.10) is a quasi-linear first-order differential equation, which describes traveling of different concentrations at different characteristic speeds given by (Hildebrand, 1976)

$$\left(\frac{dz}{dt}\right)_c \quad ' \quad \frac{V_u}{1 \% f \mathbb{N}(C_d)} \tag{2.15}$$

The complete solution of concentration can then be obtained by integration of equation (2.15), subject to the initial and boundary conditions.

Equation (2.15) indicates that the traveling velocity for a particular concentration, C_d, is constant. Upon integration for a particular concentration, C_d, the penetration position or depth, z_c, of the concentration will be obtained at any time t ($t > t_s$) from

$$\int_{z_s}^{z_c} dz \quad ' \quad \int_{t_s}^{t} \frac{V_u \, dt}{1 \% f \mathbb{N}(C_d)}$$

which yields

$$z_{C_d} \quad ' \quad \frac{V_u (t \& t_s)}{1 \% f \mathbb{N}(C_d)} \% z_s \tag{2.16}$$

if C_d starts traveling from $z = z_s$ at $t = t_s$.

The above analytical solution is a direct application of chromatographic transport theory to the solute transport problem (Hirasaki, 1981; and Fredrick, 1981). As in the Buckley-Leverett theory for multiphase flow, a shock front may form during the concentration propagation. The occurrence of the shock concentration front depends on the initial and boundary conditions (van Der Zee, 1990).

In order to use the above frontal advance solution to describe solute transport with nonlinear adsorption effects, one has to recognize the conditions under which a shock front will develop, otherwise, a non-physical solution may be proposed. There are two common situations for the occurrence of the shock front. If the initial concentration is constant, C_i, and a step increase of the concentration, C_o, is injected into the fluid at $z=0$, a shock front will develop under the following two conditions (van Der Zee, 1990)

Situation 1:

$$\left.\begin{array}{c} C_o > C_i \\[1em] \dfrac{d\,f(C_d)}{dC_d} > 0 \\[1.5em] \dfrac{d^2\,f(C_d)}{dC_d^2} < 0 \end{array}\right\} \qquad (2.17)$$

Situation 2:

$$\left.\begin{array}{c} C_o < C_i \\[1em] \dfrac{d\,f(C_d)}{dC_d} > 0 \\[1.5em] \dfrac{d^2\,f(C_d)}{dC_d^2} > 0 \end{array}\right\} \qquad (2.18)$$

The two conditions of (2.17) and (2.18) can be better understood physically using the Freundlich adsorption isotherm as an example. For a Freundlich isotherm, we have

$$f(C_d) \quad ' \quad \frac{D_b}{2}\, k_1\, C_d^0 \qquad (2.19)$$

where the coefficient k_1 (L^{30}/M^0) and 0 (dimensionless) are nonlinear Freundlich parameters. When the exponent $0 = 1$, the Freundlich isotherm becomes linear, and the parameter k_1 is then the same as the partition coefficient K_d for a linear adsorption case.

For a case of continuous release of solute with concentration C_o, and constant initial concentration, C_i, in the system, we have

$$\left.\begin{array}{c} C_o > C_i \\[1em] \dfrac{d\,f(C_d)}{dC_d} \quad ' \quad \dfrac{D_b\,k}{2}\,0\,C_d^{0\&1} > 0 \\[1.5em] \dfrac{d^2\,f(C_d)}{dC_d^2} \quad ' \quad \dfrac{D_b\,k}{2}\,0\,(0\,\&\,1)\,C_d^{0\&2} < 0 \\[1.5em] for \quad (0 < 0 < 1) \end{array}\right\} \qquad (2.20)$$

When the condition of (2.17) is satisfied, a shock front for the solute plume will develop during the transport process. Using equation (2.15), the traveling velocity for a particular concentration, C_d, is

$$\left(\frac{dz}{dt}\right)_{C_d} \; ' \; \frac{V_u}{1 \% \dfrac{D_b k}{2} 0\, C_d^{0\&1}} \qquad for \;\; (0 < 0 < 1) \tag{2.21}$$

For C_d 6 0, $C_d^{0\&1}$ 6 4, and

$$\left(\frac{dz}{dt}\right)_{C_d} 6\; 0 \tag{2.22}$$

For C_d 6 4, $C_d^{0\&1}$ 6 0,

$$\left(\frac{dz}{dt}\right)_{C_d} 6\; V_u \tag{2.23}$$

Therefore, the higher the concentration is, the higher the velocity. Physically, this is impossible across the concentration front because of the adsorption effect, and a sharp front will form for the concentration plume. In this case, the velocity of the shock front is described by

$$\left(\frac{)z}{)t}\right)_{)C_d} \; ' \; \frac{V_u}{1 \% \dfrac{)\, f(C_d)}{)\, C_d}} \tag{2.24}$$

where $) C_d = C_o - C_i$, represents the concentration difference across the front. The penetration depth of the sharp front at time t is given by

$$z_f \; ' \; \frac{2 V_u t \; (C_o \& C_i)}{2 \; (C_o \& C_i) \% D_b K_1 \; (C_o^0 \& C_i^0)} \tag{2.25}$$

For a pulse release and the same range of the Freundlich exponent, $0 < 0 < 1$, the condition (2.20) will not be satisfied at the entrance boundary when $t > t_p$. Consequently, adsorption according to the Freundlich isotherm will result in a sharp leading edge and diffuse trailing of the solute concentration profile when the exponential parameter is in the range of $0 < 0 < 1$.

The second situation for the occurrence of the shock front (condition 2.18) is illustrated using the Freundlich isotherm, $O > 1$. This corresponds to a pure water displacement front following a pulse solute injection. Then

$$\left.\begin{array}{l} C_o \; ' \; 0 < \; C_i \\[2ex] \dfrac{d\,f(C_d)}{dC_d} \; ' \; \dfrac{D_b\,k}{2}\,O\;C_d^{O\&1} \; > \; 0 \\[3ex] \dfrac{d^2\,f(C_d)}{dC_d^2} \; ' \; \dfrac{D_b\,k}{2}\,O\;(O\&1)\;C_d^{O\&2} \; > \; 0 \end{array}\right\} \qquad (2.26)$$

This satisfies condition (2.18), resulting in a concentration profile that exhibits a dispersed front and a sharp trail edge (sharp tail). The location of the sharp tail is given by:

$$z_f \;\; ' \;\; \frac{2\,V_u t\;C_i}{2C_i \; \% \; D_b\,k\,C_i^0} \qquad (2.27)$$

3.0 DETERMINATION OF ADSORPTION ISOTHERMS FOR METALS

The fate of metals in the subsurface is governed by a number of transport mechanisms. EPACMTP takes into account transport by advection and dispersion and includes the retardation effect of sorption processes. Advection and dispersion are essentially mechanical processes that do not, for all practical purposes, depend on the type of solute, except for molecular diffusion which is usually negligible. However, the adsorption of metals is metal-specific. The assumption is made here that the rate of adsorption reactions is fast relative to the transport rate, and the result of the adsorption process can be described by equilibrium adsorption isotherms. In EPACMTP, adsorption distribution coefficients (K_d's) are provided for the metals antimony, arsenic, barium, beryllium, cadmium, chromium, copper, mercury, lead, nickel, selenium, silver, thallium, vanadium, and zinc. Table 3.1 provides a complete list of metals considered in this report and an explanation of shorthand notation by which they are hereafter referenced.

The notation employs a Roman numeral superscript (e.g., Cr^{III}) to avoid the confusion that may accompany the use of Cr^{3+}. The latter is commonly used to refer to free chromium(III) in solution. The Cr^{III} designation should be taken as referring to chromium with a $+3$ oxidation state, regardless of the particular species. Thus, Cr^{3+}, $Cr_2O_3(s)$, and $Cr(OH)_3(s)$ are all Cr^{III} species. Note that Cr^{III} typically behaves as a cation in aqueous solution and Cr^{VI} typically behaves as an anion.

Table 3.1   Notation used for metals considered in this report.

Metal	Oxidation State	Notation
Typically behaving as cations in aqueous solution		
Barium	$+2$	Ba
Beryllium	$+2$	Be
Cadmium	$+2$	Cd
Chromium	$+3$	Cr^{III}
Copper	$+2$	Cu
Mercury	$+2$	Hg
Lead	$+2$	Pb
Nickel	$+2$	Ni
Silver	$+1$	Ag
Zinc	$+2$	Zn
Thallium	$+1$	Tl
Typically behaving as anions in aqueous solution		
Antimony	$+3$ and $+5$	Sb^{III} and Sb^V
Arsenic	$+3$ and $+5$	As^{III} and As^V

Metal	Oxidation State	Notation
Chromium	$+6$	Cr^{VI}
Selenium	$+4$ and $+6$	Se^{IV} and Se^{VI}
Vanadium	$+5$	V

For the eleven metals: Ag, Ba, Be, Cd, Cr^{III}, Cu, Hg, Ni, Pb, V, and Zn the K_d values used in EPACMTP were computed using a modified version of the U.S. EPA geochemical speciation model, MINTEQA2 (Allison et al., 1991). The specific modifications to MINTEQA2 relative to the currently distributed version (v3.11) are detailed in section 3.1.5. The motivation for using a speciation model is to capture the variation in K_d due to variability in geochemical conditions and due to the extent of metal loading. The geochemical parameters whose variability is included in the modeling are: pH, concentration of hydrous ferric oxide adsorption sites, concentration of dissolved and particulate natural organic matter, and concentration of leachate organic acids. The method used to account for nationwide variability in these four master variables is discussed in separate sections below. To compute the adsorption distribution coefficient (K_d) values for a particular metal, a value was selected for each of the four master variables and the MINTEQA2 model was executed over a range of total metal concentrations. The result is a nonlinear adsorption isotherm that can be represented by the variation in K_d with total metal concentration (or, with equilibrium dissolved concentration). This procedure was repeated (separately for each metal) for numerous combinations of master variable settings. The final result from MINTEQA2 was nonlinear K_d versus metal concentration curves for combinations of master variable settings spanning the range of reasonable values.

In determining the adsorption isotherms via MINTEQA2 modeling, surface adsorption reactions are included in the equilibrium speciation calculations. The surface reactive sites at which metal adsorption occurs are in competition with metal-complexing solution ligands for the available metal. Numerous other species in the system (e.g., H^+, OH^-, Ca^{2+}, etc.) may be in simultaneous competition for adsorption sites and solution ligands resulting in a complicated web of competitive interactions. For a particular total concentration of a metal in a given system, the equilibrium partitioning between the sorbed and solution phases is dependent on the relative affinities of surface sites and solution ligands for the metal and for the numerous other species involved in the competition. The K_d is determined as the concentration ratio at equilibrium of metal bound in the sorbed phase versus metal in solution. For a particular interaction in the speciation web, the relative affinities are regulated by the form of the chemical reaction and the magnitude of the associated equilibrium constant. MINTEQA2 inherently includes chemical reactions and their equilibrium constants for solution phase interactions. However, it does not inherently include adsorption reactions or constants; the user must supply them prior to executing the model run. Adsorption reactions pertinent to a hydrous ferric oxide (HFO) surface were available for the contaminant cationic metals: Ag, Ba, Cd, Cr^{III}, Cu, Hg, Pb, Ni, and Zn (Dzombak, 1986; Dzombak and Morel, 1990). Reactions were also available from the same source for the anionic metals: As^{III}, As^V, Cr^{VI}, and V. However, the results of calibration tests in which MINTEQA2 along with the hydrous ferric oxide adsorption reactions was used to predict the extent of adsorption in lab experiments indicated that those species that typically behave as anions in solution are not as well represented by the model as cationic species (Loux et al., 1990). Therefore, experimentally determined empirical relationships giving K_d as a function of pH only were used for the anionic species. An exception was V; MINTEQA2 was used for this anionic metal because no pH-dependent empirical relationship was available. Conversely, MINTEQA2 was not used for the cationic metal Tl because no HFO adsorption reactions were available. An pH-dependent empirical relationship was used instead. Neither the appropriate adsorption reactions for MINTEQA2 nor an empirical relationship was available for

Be. In lieu of a better alternative, it was assumed that Be adsorption could be conservatively approximated by that of its fellow Group II-A element Ba, and the K_d values computed for Ba were used for Be as well.

For some metals modeled using MINTEQA2, adsorption onto particulate organic matter (POM) was included in the model calculations by including as POM reactions a database of reactions developed for dissolved organic matter (DOM) (Susetyo et al., 1991). "Borrowed" DOM reactions were available for the contaminant metals Ba, Cd, Cr^{III}, Cu, Pb, Ni, and Zn.

Empirical relationships in which K_d is expressed as a function of pH only were used for the metals As^{III}, Cr^{VI}, Sb^V, Se^{VI}, and Tl. These relationships, presented in Loux et al. (1990), were determined statistically from experimental data on a collection of groundwater/aquifer samples. The experiments were repeated at various pH values to develop empirical expressions giving K_d as a function of pH. This approach makes no assumption regarding the exact identity of the species adsorbed. K_d is determined solely on the basis of total metal adsorbed versus total dissolved. Also, for antimony, arsenic, and selenium, there are two oxidation states relevant to environmental concerns. No empirical relation was available for Sb^{III}; the Sb^V relationship is used for both in this study. The As^{III} species is adsorbed less strongly than As^V, but the contrast is not nearly as pronounced as for Cr^{III} versus Cr^{VI}. Therefore, the As^{III} relationship was used for both oxidation states. Likewise, Se^{VI} is expected to be adsorbed less strongly than Se^{IV}, so the Se^{VI} relationship was used for both.

3.1   MINTEQA2 DERIVED ADSORPTION ISOTHERMS

The geochemical equilibrium speciation model MINTEQA2 is designed to calculate the mobile fraction of a metal species and the effective distribution coefficient (K_d) between dissolved and adsorbed fractions for a user-specified geochemical system. The system-specific K_d can then be used in transport modeling to account for attenuation of metal concentration due to adsorption along the transport path. MINTEQA2 was used to compute K_d's for the ten metals: Ag, Ba, Cd, Cr^{III}, Cu, Hg, Ni, Pb, V, and Zn. (The K_d values for Be were actually the Ba results.)

3.1.1   Overview of Speciation Modeling with MINTEQA2

The data required to predict the equilibrium composition (i.e., the mass distribution among dissolved, adsorbed, and precipitated phases) consists of chemical analysis information from the system to be modeled. The chemical analysis information is expressed in terms of total system concentrations of a set of components sufficient to represent the system. For example, a system may be characterized by the pH and system totals for calcium, magnesium, iron, carbonate, and other major ions. The general description of the system is used in MINTEQA2 to calculate a specific description of the system at equilibrium: concentrations of all dissolved species (CO_3^{2-}, HCO_3^-, $H_2CO_3^0$, Ca^{2+}, etc.), concentrations of all adsorbed species, and concentrations of all precipitates. The pH may also be calculated if the system total for hydrogen is known.

The component is the fundamental entity used to describe the system whose equilibrium composition is to be calculated. The user selects from a pre-defined set of components needed to describe a specific system. MINTEQA2 includes a database of reaction products in which components are reactants in over 900 dissolved species, 500 solid species, and 21 gas species. When requested by the user, a database of reaction products representing a hydrous ferric oxide adsorption surface (Dzombak, 1986; Dzombak and Morel, 1990) may be included in the calculations. Upon execution, the database of reaction products is searched for all species pertinent to the set of components that the user has selected to represent the system. All species in the system are then assigned to one of the categories or types shown in Table 3.2.

Table 3.2   Species types in MINTEQA2 speciation calculations.

Type	Description
I	Dissolved and surface species that also serve as components
II	Other dissolved and surface species (i.e., not components)
III	Any species whose equilibrium activity is established by a user-imposed constraint
IV	Solid species precipitated at equilibrium
V	Solid species undersaturated (not precipitated) at equilibrium
VI	Any species excluded from impacting the equilibria

The general sequence of calculations in a single MINTEQA2 model execution is depicted in Figure 3.1. After acquiring the system-specific fundamental description of the system from the user and accessing the appropriate thermodynamic data from its own database, the aqueous phase is equilibrated. The degree of saturation is computed with respect to the solution for each possible solid. The most supersaturated solid is precipitated (or, if previously precipitated solids have become undersaturated, the most undersaturated is dissolved). The aqueous phase is re-equilibrated, and supersaturation and undersaturation are again checked and dealt with. This procedure continues until the aqueous phase is equilibrated without supersaturation or undersaturation. The equilibrium mass distribution in the three phases: dissolved, adsorbed, and precipitated are tabulated and written to an output file along with the concentrations of all species in each phase.

3.1.2   Application of MINTEQA2 in Adsorption Modeling for HWIR

Adsorption of metals depends on a number of geochemical factors, and chemical speciation modeling with MINTEQA2 requires that the controlling chemical parameters be supplied as input. These parameters characterize various subsurface geochemical conditions and a single characteristic of the leachate itself, namely, the concentration of leachate organic acids. The parameters pertinent to modeling for K_d can be classified into three types: 1) those that have a primary (direct) impact on adsorption and for which the range of variability is so great as to significantly alter the results (e.g., the pH); 2) those that
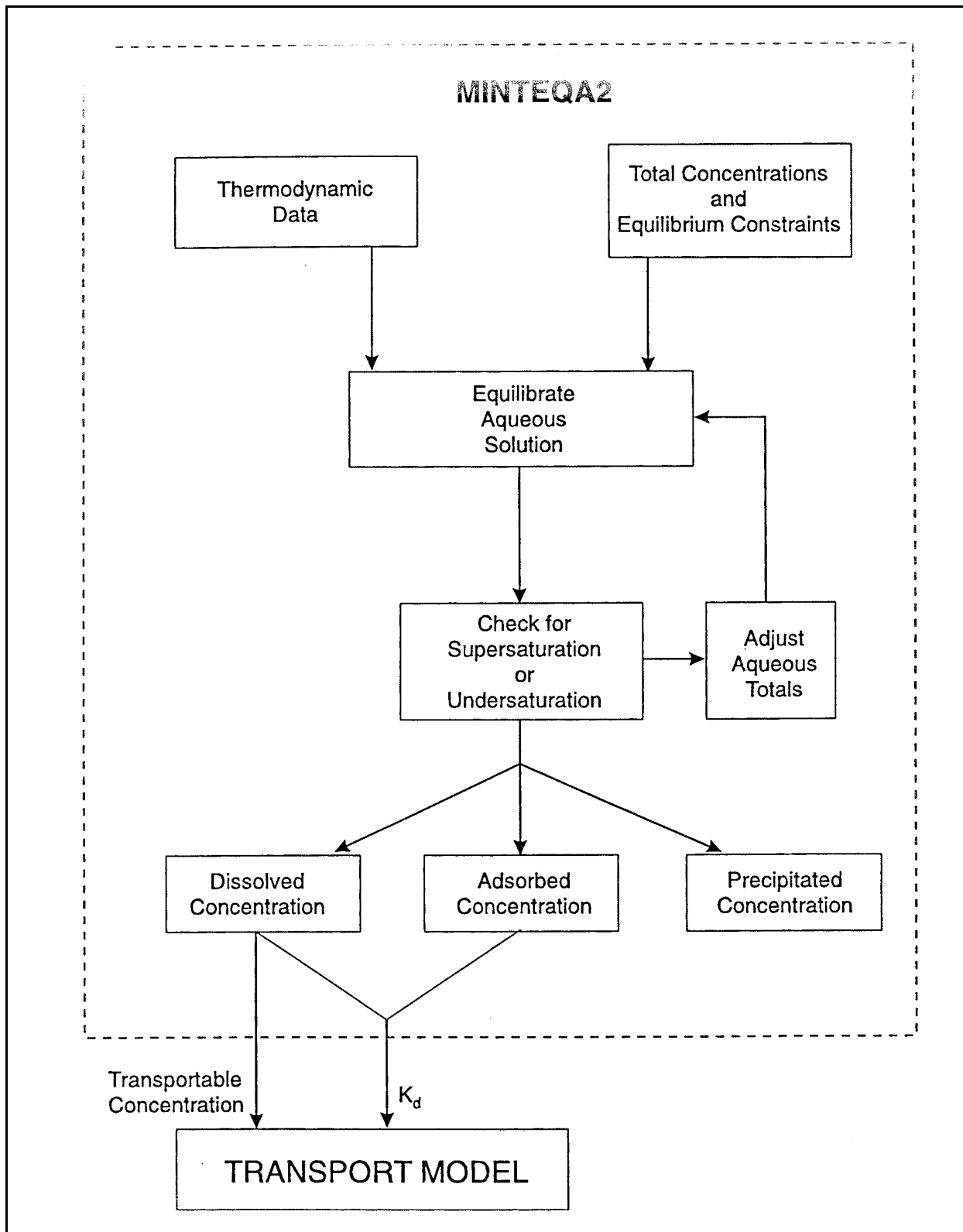
Figure 3.1   Flowchart of MINTEQA2 calculations and results applicable transport model (From Allison et al., 1992)

have secondary (indirect) effects, but for which the range of variability is relatively small or insignificant to the results (e.g., sodium and chloride concentrations); and 3) those that may have a primary impact on the results, but for which neither the variability nor its significance is known. Perhaps the most important example of the third kind of parameters is the oxidation-reduction (redox) potential or E_H.

Although the groundwater E_H is an important factor in the partitioning of metals into dissolved, adsorbed, and precipitated phases, it is not treated as a master variable in this modeling. This is because of limitations in measuring E_H in groundwater systems. Two factors that limit the efficacy of such measurements are pH-dependent response from surface oxide coatings that form on electrodes used to measure E_H and changes in sample E_H over a short time interval during and immediately after sample collection. Changes in sample E_H may be due to contamination with atmospheric oxygen or microbial activity. These problems render reported E_H measurements in databases such as the U.S. EPA Storage and Retrieval System (STORET) unreliable as indicators of groundwater redox potential (Whitfield, 1974 and Lindberg and Runnels, 1984). In the absence of a reliable probability distribution for groundwater redox potential, oxidation-reduction reactions were excluded from equilibrium calculations. Multiple oxidation states of groundwater constituents that occur in more than one state (e.g., sulfide and sulfate) are treated as separate components and no transformation from one to the other was allowed. Contaminant metals that occur in more that one oxidation state were treated as separate metals. In fact, for reasons already discussed, K_d's for Cr^{III} were obtained from MINTEQA2 modeling and K_d's for Cr^{VI} were obtained from an empirical relationship. As indicated in Table 3.1, for mercury and vanadium, only one oxidation state was considered (+2 and +5, respectively). This was due to a lack of adsorption information necessary to include other forms.

In generating the K_d values for metals, the primary and secondary parameters were considered, but parameters which could not be reliably quantified were ignored. For the primary parameters, variability in the subsurface environment (or variability expected in the landfill scenario) was explicitly considered by including probability distributions as described below. For the secondary parameters, variability was ignored and a constant value was used to represent each parameter. The characterization of primary and secondary parameters and their use in the MINTEQA2 modeling are described in more detail below.

3.1.3   Primary Geochemical Factors

Geochemical factors that are known to have direct impact on adsorption in groundwater systems are: (1) subsurface pH, (2) hydrous ferric oxide adsorbent content of the soil/aquifer in the subsurface, (3) natural soil organic matter content of the soil/aquifer in the subsurface (particulate and dissolved), and (4) concentration of organic acids in the leachate. For a given metal at a given total concentration, the propensity for adsorption changes greatly as these parameters vary. For the MINTEQA2 modeling, the natural variability of these parameters was divided into three ranges: high, medium, and low. Furthermore, each of these parameters was assigned values corresponding (approximately) to the midpoint of each range, and one isotherm (as a function metal concentration) was developed for each combination of the three possible values for the four master variables. Therefore, a set of 81 (3^4) isotherms was developed for both the unsaturated and saturated zones. The data source for each of the four master variables along with the values used in the MINTEQA2 modeling is described briefly below.

Master variable: pH

The low, medium, and high values of pH (4.9, 6.8, and 8.0) used in the MINTEQA2 modeling represent the 7.5, 50.0, and 92.5 percentiles respectively from a distribution of 24,921 field measured

groundwater pH values obtained from the U.S. EPA STORET database (EPA, 1985). Because the STORET database has unrealistic extreme values (presumably from errors in instrument calibration or reading, or in data entry), the upper and lower bounds of the distribution were established by reference to reported values in the open literature. The pH distribution is shown in Figure 3.2. In this modeling methodology, it is assumed that the groundwater/aquifer system is well buffered with respect to pH. That is, in the modeling there is no effect on the ambient pH from the landfill leachate. The only impact of the leachate on the groundwater system is that it carries the metal and certain anthropogenic organic acids that complex the metal (see the leachate organic acids section below).

Master variable: Hydrous ferric oxide (HFO) adsorbent content

The low, medium, and high values associated with the hydrous ferric oxide adsorbent content are expressed in the MINTEQA2 modeling as molar site concentrations for two site types: a high population, low binding-energy site and a low population high binding-energy site. A corresponding value of adsorbent concentration in g liter^{-1} is also a model parameter. The source data for the selection and specification of these parameters is a set of 12 aquifer/soil material samples collected from across the United States by the U.S. EPA. The characteristics of these samples are described in "Soil/Sediment Properties Influencing Lead Mobility in the Environment" by Loux et al. (publication pending). Specialized wet chemical methods were used in measuring the extractable (reactive) iron in these samples (see aforementioned work). The iron content (weight percent) of the 12 samples served as the source data for the MINTEQA2 modeling parameters. Specifically, the three lowest iron contents among the 12 samples were averaged to provide a basis for the low MINTEQA2 values, the iron content of all 12 samples were averaged to provide a medium value, and the three highest values were averaged for the high value.

MINTEQA2 performs all calculations on a per liter basis. Therefore, the amount of reactive iron solid with which one liter of groundwater/leachate solution is equilibrated is critical in determining the proper inputs for the model. The total mass of soil/aquifer material whose pore space will hold one liter of solution for a given water content (referred to as the phase ratio, *a*) is given by $D_b/2$ where D_b is the soil dry bulk density and 2 is the water content. Although these parameters are themselves presented as distributions to be Monte Carlo'ed in the transport modeling, it was necessary to select representative values in order to scale the input parameters in MINTEQA2. For this purpose, D_b was set to 1.6 kg liter^{-1} and 2 was set to 0.35 in the unsaturated zone and 0.45 in the saturated zone. The water content of 0.35 in the unsaturated zone reflects a value of 77% for water saturation (the mean value from a distribution of water saturations in EPACMTP) and a porosity of 0.45 (the mean value from the EPACMTP porosity distribution). The same porosity was used for the saturated zone except with a water saturation of 100%. These values give a soil mass phase ratio appropriate for one liter of solution as 4.57 kg in the unsaturated zone and 3.56 kg in the saturated zone.

Once the total mass of aquifer/soil material and weight percent reactive iron were determined as per the foregoing, it was necessary to derive parameters specifically for the particular adsorption sub-
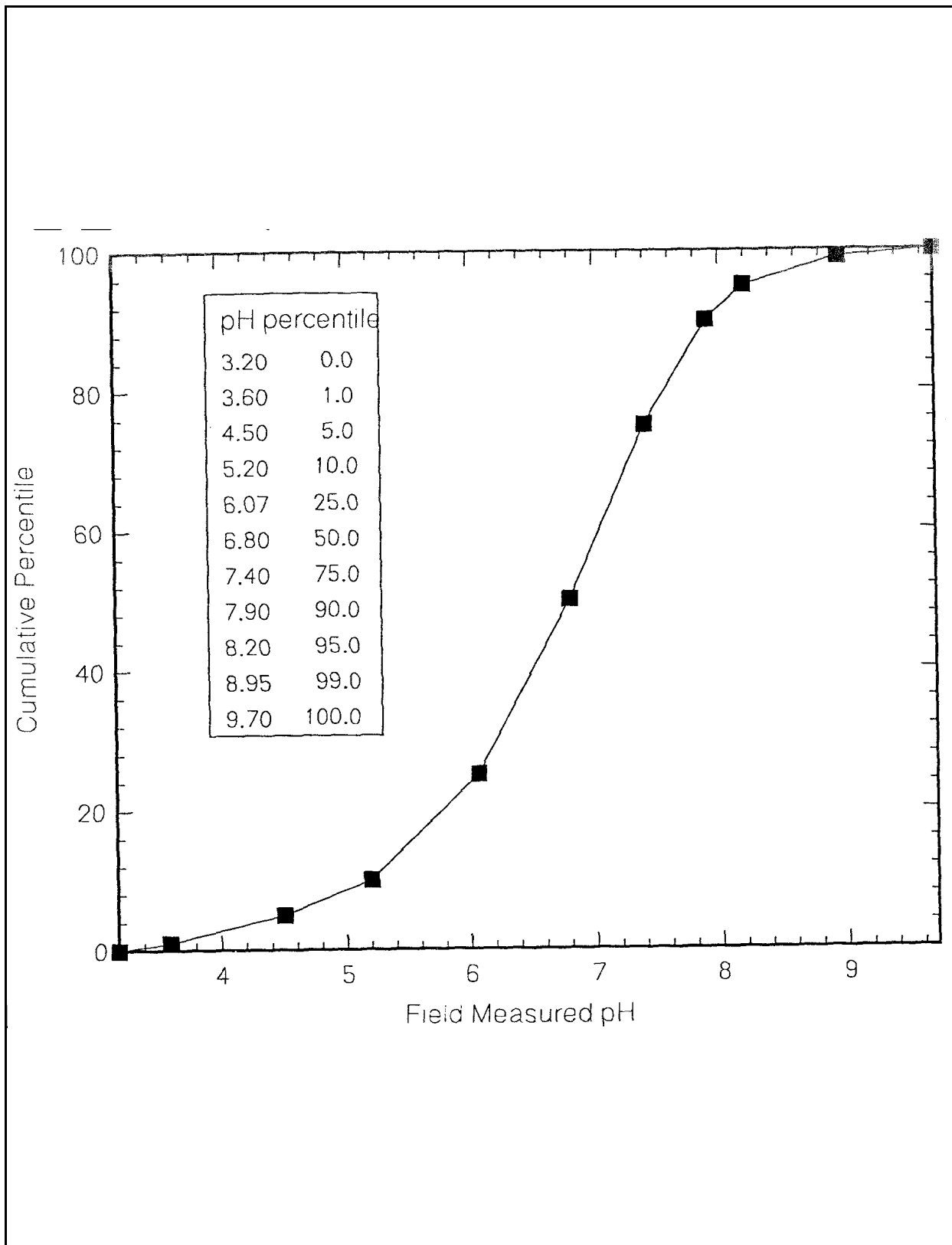
Figure 3.2   Frequency distribution for field measured pH.

model to be used. MINTEQA2 provides seven different sub-models for adsorption calculations. The sub-model used in this work was the diffuse-layer model (Dzombak, 1986; Dzombak and Morel, 1990). This sub-model provides a database of adsorption reactions that describe the equilibria between two adsorption sites on the HFO and the metals Ag, Ba, Cd, Cr^{III}, Cu, Hg, Pb, Ni, V, and Zn. Protonation/deprotonation reactions and reactions with various other constituents from the groundwater background chemistry are included as well. (The chemical makeup of the groundwater is discussed later; all adsorption reactions pertaining to the HFO surface are shown in Appendix A.) As specified by Dzombak, the diffuse-layer model presumes that the iron is in the form FeOOH with molar mass 89 g. Also, the site density of the high population, low energy site (MINTEQA2 component number 812) is 0.2 moles of sites / mol Fe; the low population, high energy site (MINTEQA2 component number 811) is 0.005 moles of sites / mol Fe. Table 3.3 presents the low, medium and high values of weight percent (wt%) reactive iron, molar site concentrations for both sites (mol sites liter^{-1}), and the mass of adsorbing solid (g liter^{-1}) used in the modeling. The values differ in the unsaturated and saturated zones only because the water saturation differs, and so too does the mass of soil that one liter of porewater is in equilibrium with.

Table 3.3   MINTEQA2 parameters associated with the hydrous ferric oxide (HFO) surface.

	Fe wt%	HFO (g liter^{-1})	Site 811 (mol liter^{-1})	Site 812 (mol liter^{-1})
Unsaturated Zone				
LOW	8.830×10^{-3}	0.643	3.613×10^{-5}	1.445×10^{-3}
MEDIUM	2.094×10^{-1}	15.250	8.568×10^{-4}	3.427×10^{-2}
HIGH	4.964×10^{-1}	36.152	2.031×10^{-3}	8.124×10^{-2}
Saturated Zone				
LOW	8.830×10^{-3}	0.501	2.814×10^{-5}	1.125×10^{-3}
MEDIUM	2.094×10^{-1}	11.880	6.674×10^{-4}	2.670×10^{-2}
HIGH	4.964×10^{-1}	28.163	1.582×10^{-3}	6.329×10^{-2}

Master variable: Natural organic matter content

The low, medium, and high concentrations for components representing particulate and dissolved natural organic matter in the MINTEQA2 model runs were based on the distribution of solid organic matter in EPACMTP and on dissolved organic carbon measurements retrieved from the U.S. EPA STORET database. EPACMTP includes solid organic matter distributions for three soil types in the unsaturated zone: silty clay loam, sandy loam, and silty loam. The silty loam soil type is intermediate in weight percent organic matter in comparison with the other two. Therefore, low, medium, and high values for particulate organic matter in the unsaturated zone were determined from the silty loam distribution. In the saturated zone, EPACMTP includes a distribution of solid organic matter that is identical to that for the sandy loam soil type in the unsaturated zone. All organic matter distributions in EPACMTP are SB-Johnson frequency distributions. As was the case for the HFO adsorbent distribution described above, it was necessary to scale the amount of solid organic matter to be included in the MINTEQA2 modeling as appropriate for one liter of porewater solution. As before, we assume a phase ratio of 4.57 kg of soil per liter of groundwater-leachate solution in the unsaturated zone and 3.56 kg per liter in the saturated zone. The silty loam and sandy

loam distributions were used to calculate the appropriate MINTEQA2 concentration of particulate organic matter (POM) adsorption sites in the unsaturated and saturated zones, respectively. Table 3.4 shows the weight percent organic matter and the POM concentration (mg liter^{-1}) for both zones. The low, medium, and high values correspond to the 7.5, 50.0, and 92.5 percentile values, respectively, from the distributions.

Table 3.4 POM weight percent (wt%) and POM and DOM concentrations used in deriving MINTEQA2 modeling parameters.

	POM wt%	Concentration POM (mg liter^{-1})	Concentration DOM (mg liter^{-1})
Unsaturated Zone			
LOW	0.034	1553.8	6.58
MEDIUM	0.105	4798.5	20.32
HIGH	0.325	14852.5	62.90
Saturated Zone			
LOW	0.020	712.0	3.00
MEDIUM	0.074	2634.4	14.40
HIGH	0.275	9790.0	69.38

A dissolved organic carbon (DOC) distribution for the saturated zone was obtained from the U.S. EPA STORET database. This distribution is based on 1343 groundwater samples and is approximated by a log normal distribution with a median $\log_e$ DOC of 1.974 (corresponding to 7.2 mg liter^{-1}) and $\log_e$ standard deviation of 1.092. Assuming DOM is approximately 50% organic carbon, the DOC values are multiplied by two to approximate DOM concentrations. The low, medium and high values corresponding to the 7.5, 50.0, and 92.5 percentiles, respectively, of the approximated DOM distribution are shown in mg liter^{-1} in Table 3.4. An important point to note is that POM and DOM were not treated as independent: the high DOM value was associated in the MINTEQA2 modeling with the high POM value, the medium DOM with the medium POM, etc. The reason for doing this is that to do otherwise would have increased the number of MINTEQA2 runs from 81 per metal in each zone (unsaturated and saturated zones) to 243 runs per metal for each zone. (Because there would be five independent master variables rather than four; the number of possible combinations of low, medium, and high values would be 3^5 rather that 3^4). Also, that there should be some dependence between POM and DOM concentrations in a system at equilibrium is not without logic.

In the unsaturated zone, there was no direct measurement of DOM (or DOC) available. Therefore, the assumption was made that the ratio of POM to DOM for the three concentration levels (low, medium, high) in the unsaturated zone is the same as for the saturated zone. Unsaturated zone DOM values (mg liter^{-1}) are also shown in Table 3.4.

As was the case for the HFO adsorbent, a specialized sub-model within MINTEQA2 was used for calculations involving the POM and DOM. This sub-model, called the Gaussian distribution model or composite-ligand model, assumes that natural organic matter is a mixture of various functional groups having a *mean* log K for binding metals and a standard deviation in log K. This is in contrast to all other reactants in MINTEQA2 which are implicitly treated as pure substances with a single equilibrium constant for a

particular metal. A database of DOM reactions proposed by Susetyo et al. (1991) for the contaminant metals Ba, Cd, Cr^{III}, Cu, Pb, Ni, and Zn and for various other MINTEQA2 components is included with v3.11 of the model. Adsorption of metals onto POM was included in the model calculations by assuming that the reactions were identical to those for metal complexation with DOM. Appendix A shows all POM reactions added to the MINTEQA2 database for this work.

The Gaussian distribution sub-model assumes that the input concentrations for POM and DOM are in terms of moles of sites per liter. The conversion from the mg $liter^{-1}$ values shown in Table 3.4 to the entries in mol sites $liter^{-1}$ used in the MINTEQA2 modeling was by means of a total acidity estimate of 1.2 μmol sites per mg organic matter. Table 3.5 shows the actual site concentrations in mol $liter^{-1}$ for POM (MINTEQA2 component number 146) and DOM (MINTEQA2 component number 145).

Table 3.5   MINTEQA2 input parameters for POM and DOM.

	POM Concentration Site 146 (mol liter^{-1})	DOM Concentration Site 145 (mol liter^{-1})
Unsaturated Zone		
LOW	1.865×10^{-3}	7.896×10^{-6}
MEDIUM	5.758×10^{-3}	2.439×10^{-5}
HIGH	1.782×10^{-2}	7.548×10^{-5}
Saturated Zone		
LOW	8.544×10^{-4}	3.600×10^{-6}
MEDIUM	3.161×10^{-3}	1.728×10^{-5}
HIGH	1.175×10^{-2}	8.326×10^{-5}

Master variable: Leachate organic acid concentration

In addition to the metal contaminants, the leachate exiting a landfill may contain elevated concentrations of anthropogenic leachate organic acids. These acids may represent primary disposed waste or may result from the breakdown of more complex organic substances. Many organic acids found in landfill leachate have significant metal-complexing capacity that may influence metal mobility. In an effort to incorporate in the K_d modeling the solubilizing effect of organic acids, three representative monoprotic acids were included as components. Leachates from six landfills from across the U.S. as analyzed and reported by Gintautas et al. (1993) were used to select and quantify the organic acids. Those analyses indicated the presence of over 30 different acids; most were carboxylic. The three acids: acetic, propanoic (propionic), and butanoic (butyric) were chosen to represent the complex mixture. The three were selected based on structure/activity relationships, comparison of equilibrium constants, and relative concentrations in the analyzed leachates. The low, medium, and high values were based on the lowest, the average, and the highest measured TOC among the six landfill leachates. The relative concentrations of the three representative acids were scaled in accordance with their relative concentrations as measured in the "Wisconsin sample" described in the Gintautas study. The same set of three acids was used in both the unsaturated and saturated zones; in the latter, their concentrations were only one-seventh of their unsaturated

zone values to account for the effects of dispersion and diffusion. Table 3.6 gives the low, medium, and high concentrations in mg liter^{-1} used in the MINTEQA2 modeling for each of the three acids in each zone. Further details concerning the representation of leachate organic acids can be found in Allison et al. (1992). (The designation "LOA" is used in some figures in this report to specify the concentration of leachate organic acids.)

Table 3.6   MINTEQA2 concentrations in mg liter^{-1} for acetic, propanoic, and butanoic acids.

	Acetic acid	Propanoic acid	Butanoic acid
Unsaturated Zone			
LOW	24.80	14.61	15.68
MEDIUM	111.00	64.30	67.94
HIGH	274.60	158.60	169.00
Saturated Zone			
LOW	3.54	2.09	2.24
MEDIUM	15.86	9.19	9.71
HIGH	39.23	22.66	24.14

For the U.S. EPA's HWIR proposal, industrial waste management scenarios were modeled rather than municipal. Because industrial waste management units are expected to have a lower anthropogenic organic acid content than municipal units, only the K_d values corresponding to *low* organic acid concentration was used in the EPACMTP simulations.

3.1.4   Secondary Geochemical Factors

The concentrations of several geochemical constituents common in groundwater are included in the modeling as secondary parameters. The impact on the amount of metal adsorbed by constituents treated as secondary factors is less pronounced than those treated as primary. In consequence, and also because of the computational burden of doing otherwise, only a single constant value was used to depict their concentrations. Table 3.7 lists 13 groundwater constituents and their background (ambient) concentrations. The values in Table 3.7 represent median values obtained from the STORET database (EPA, 1985). The concentrations of these constituents were treated as constant throughout the modeling.

Table 3.7   MINTEQA2 components representing groundwater background chemistry. Concentrations are median values from the U.S.EPA STORET database.

Constituent	Concentration (mg liter^{-1})	MINTEQA2 component
Aluminum	0.20	Al^{3+}
Calcium	48.00	Ca^{2+}
Iron (III)	0.20	Fe^{3+}

Constituent	Concentration (mg liter^{-1})	MINTEQA2 component
Magnesium	14.00	Mg^{2+}
Manganese (II)	0.04	Mn^{2+}
Potassium	2.90	K^+
Sodium	22.00	Na^+
Carbonate	187.00	CO_3^{2-}
Bromine	0.30	Br^-
Chlorine	15.00	Cl^-
Nitrate	1.00	NO_3^-
Phosphate	0.09	PO_4^{3-}
Sulfate	25.00	SO_4^{2-}

There are a large number of chemical constituents that might reasonably be included in a "recipe" for groundwater; yet the number of components and species available for use in a MINTEQA2 model run is limited. Some constituents are included in the modeling because of their importance as metal complexers or as competitors with metals for ligands or adsorption sites. Examples are carbonate, sulfate, calcium, and magnesium. Others were included, not because of their direct effect on metal speciation, but because of their impact on ionic strength, and thus on the calculated activity coefficients of all solution species. Examples include sodium, chloride, and nitrate.

3.1.5 MINTEQA2 Model Revisions

The MINTEQA2 model used to develop the K_d values for this work is a revision of MINTEQA2, version 3.11 (v3.11) currently being distributed by the U.S. EPA. It differs from v3.11 in the following respects:

1)   Provision has been made to represent POM as an adsorbing surface. This task required four steps:

   a)   The v3.11 component database file COMP.DBS was supplemented with an additional component (number 146) to represent POM. The POM component is envisioned as chemically the same as the dissolved organic matter (DOM) (component number 145) already in the MINTEQA2 database. The charge specified for the new POM component was the same as for the existing DOM component: -2.8. All other entries in COMP.DBS for the POM component are zero.

   b)   The v3.11 thermodynamic database COMPLIG.DBS was supplemented with reactions between the new POM component and the metals Al, Ba, Ca, Cd, Cr^{III}, Cu, Fe^{III}, Mg, Ni, Pb, and Zn. The reactions entered in COMPLIG.DBS were duplicates of the corresponding DOM reactions already existing in that file except that every occurrence of the component number "145" was changed to "146", and every occurrence of "DOM" was changed to "POM". The result was a COMPLIG.DBS file that contained identical reactions for DOM

and POM. The complete set of metal-POM reactions as they appear in COMPLIG.DBS is given in Appendix A.

    c)   The source code for the v3.11 subroutine OUTPUT was modified so that the equilibrium mass of metal bound with POM (component number 146) is attributed to the adsorbed phase. Subroutine OUTPUT already had logic to attribute the metal complexed with the HFO surface (component number's 811 and 812) to the adsorbed category. This modification causes the mass distribution shown as "SORBED" under PART 5 of the output file to represent metal bound with both sorbents (HFO and POM). Without this modification, metal bound with POM would be counted in the "DISSOLVED" column.

    d)   The source code for the v3.11 subroutines COMPOSIT, INIT, and INPUT and the include file MINTEQA2.INC were modified to provide for the possibility of two components that behave in accordance with the Gaussian distribution model. As previously noted, v3.11 contained provision for treating DOM as a complex substance that exhibits a distribution of log K values for binding a particular metal. The distribution results from the complex collection of different ligands of which humic substances are composed and may also reflect steric and electrostatic effects that influence the binding affinity at specific sites. In v3.11, the distribution of log K values for a particular metal is treated as Gaussian and is characterized by a mean log K and standard deviation in log K. The modification for this work involved providing for the newly created POM component to behave in the same way. Version 3.11 allowed only one component to behave according to the Gaussian model in a given MINTEQA2 run.

2)   Other modifications were made in the v3.11 source code as follows:

    a)   An error in subroutine INPUT was corrected. The error could allow the standard deviation in log K values for composite ligand species (such as metal-DOM species) to be erroneously treated as standard enthalpy of reaction. This would result in an improper (though small) adjustment in log K for temperatures other than 25° C. Had this correction not been made, the error in computed K_d values would have been slight.

    b)   Subroutines INPUT and OUTPUT were modified to provide for a new input parameter, SOILKG. This parameter, the mass of soil (in kg) that one liter of solution is equilibrated with, is given by $D_b/2$. Additionally, subroutine OUTPUT was modified to calculate and write K_d from the equilibrated results to the output file. The K_d written out is the ratio of total metal sorbed over total metal dissolved, and has been normalized using SOILKG. It has units of liters kg^{-1}.

3)   The general thermodynamic database file THERMO.DBS and the database of solid species TYPE6.DBS have been updated with new thermodynamic data for many aqueous and solid species of particular interest in this modeling. New unformatted renditions of the modified files were generated for use in MINTEQA2. Log K values were updated for reactions between each of the ligands in the groundwater (see Table 3.7) and the metals: Ag, Ba, Cd, Cr^{III}, Hg, Ni, Pb, V, and Zn. Reactions between these metals and the leachate acids used in this work (acetic, propanoic, and butanoic) were also updated. The data source of the updates was the National Institute of Standards and Technology (NIST) Reference Database 46, *Critical Stability Constants for Metals Complexes, version 1.0*. The modifications and additions are presented in detail in Appendix B.

3.1.6   Ancillary MINTEQA2 Model Parameters and Example Input File

In addition to the concentrations of chemical constituents specified in the above sections, the MINTEQA2 model input file consists of settings for program options and directives. Some options affect the format or quantity of output and have no impact on the computed results. Others do affect results (e.g., selection of activity coefficient equation). All program settings and options not already discussed are shown in Table 3.8.

Table 3.8   Other MINTEQA2 settings and program options

Parameter or Option	Setting	Comment
Temperature	14	^{o}C; this is an average for U.S. groundwater obtained from the U.S. EPA STORET database
Units of concentration	MG/L	HFO, DOM, and POM in mol sites liter^{-1}
Ionic strength (I.S.) option	I.S. to be computed	
Solids option	Solids allowed	Print equilibrium results after all solids have precipitated
Iterations (maximum)	200	
Activity coefficient equation	Davies	
Output completeness option	Full output	
Sweep option	On	48 points individually specified
Sweep parameter	Total concentration	Of contaminant metal
Auxiliary importable output option	On	Output equilibrated distribution of metal dissolved, sorbed, and precipitated
Diffuse-layer adsorption	On	One HFO surface with two site types; Attach HFO database (FEO-DLM.DBS) to input file
Specific surface area (HFO)	600.0 m^2 g^{-1}	
User imposed equilibrium constraints	1	pH is specified as per above description
User imposed excluded species	2	Species number 2003002 (Diaspore) and number 3028100 (Hematite) excluded
Alkalinity	Not specified	Inorganic carbon specified as total dissolved carbonate (component 140)
Charge balance option	Off	Do not terminate due to charge imbalance

An example MINTEQA2 input file for the generation of K_d's for Pb is shown in Appendix C. This example corresponds to the unsaturated zone with the geochemical master variables set as follows: low pH, medium HFO and POM concentrations, and low leachate organic acid concentrations. The set of total input

concentrations for Pb shown in the example file was the same for all metals throughout the modeling. Specifically, the speciation problem was solved at a series of 48 total metal concentrations beginning with 0.001 mg liter^{-1} and ending with 100,000 mg liter^{-1}. This range begins at a low enough value to capture the apparent linear response characteristic of low total metal, and goes high enough to insure that the nonlinear character (in which K_d tends toward a small limiting value) is included as well. The full set of 48 metal concentrations were included for execution in one input file by means of the sweep option to simulate titration of the system with metal. Interpretation of the output was made easier by use of the output option allowing the total dissolved, adsorbed, and precipitated concentration of metal (Pb in the example) to be written to a separate file for each of the 48 points in the titration. The resulting file (PbLMMLux.prn in the example) can be imported by popular spreadsheet programs for analysis.

3.1.7 Example MINTEQA2 K_d Results

Selected examples of the MINTEQA2 K_d results are shown in Figures 3.3, 3.4, and 3.5. These figures show the computed K_d versus dissolved Pb concentration for a number of master variable combinations in the unsaturated zone. Figure 3.3 shows the K_d curves corresponding to low, medium, and high pH values when HFO and POM concentrations are set to medium. Figure 3.4 shows the effect of variations in HFO concentrations when pH and POM are set to medium. Figure 3.5 shows the effect of variation in POM when pH and HFO are set to medium. The concentration of leachate organic acids was low in all of these examples (as it was for all HWIR transport modeling).
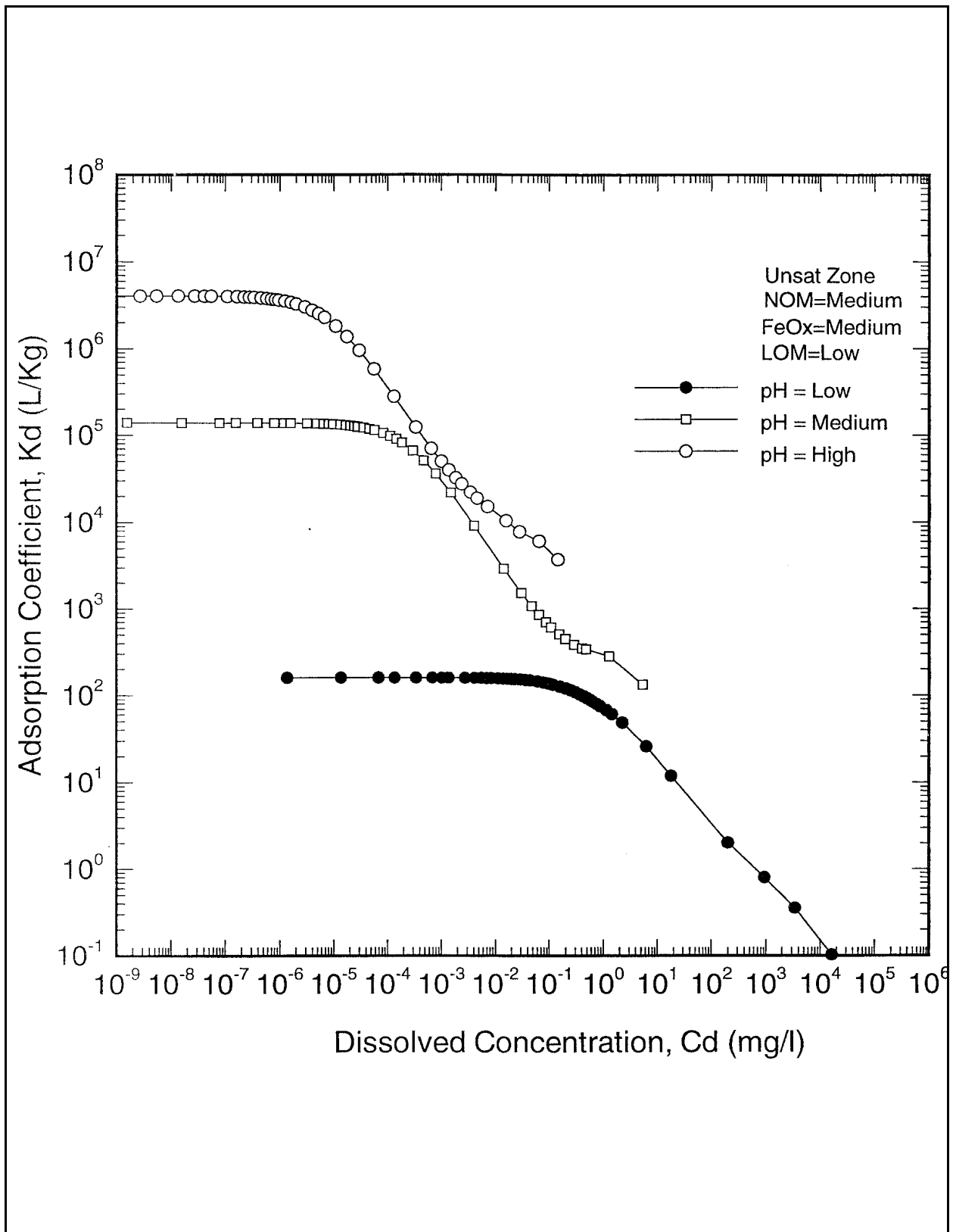
Figure 3.3   Effect of varying pH and MINTEQA2 derived adsorption isotherm for lead.
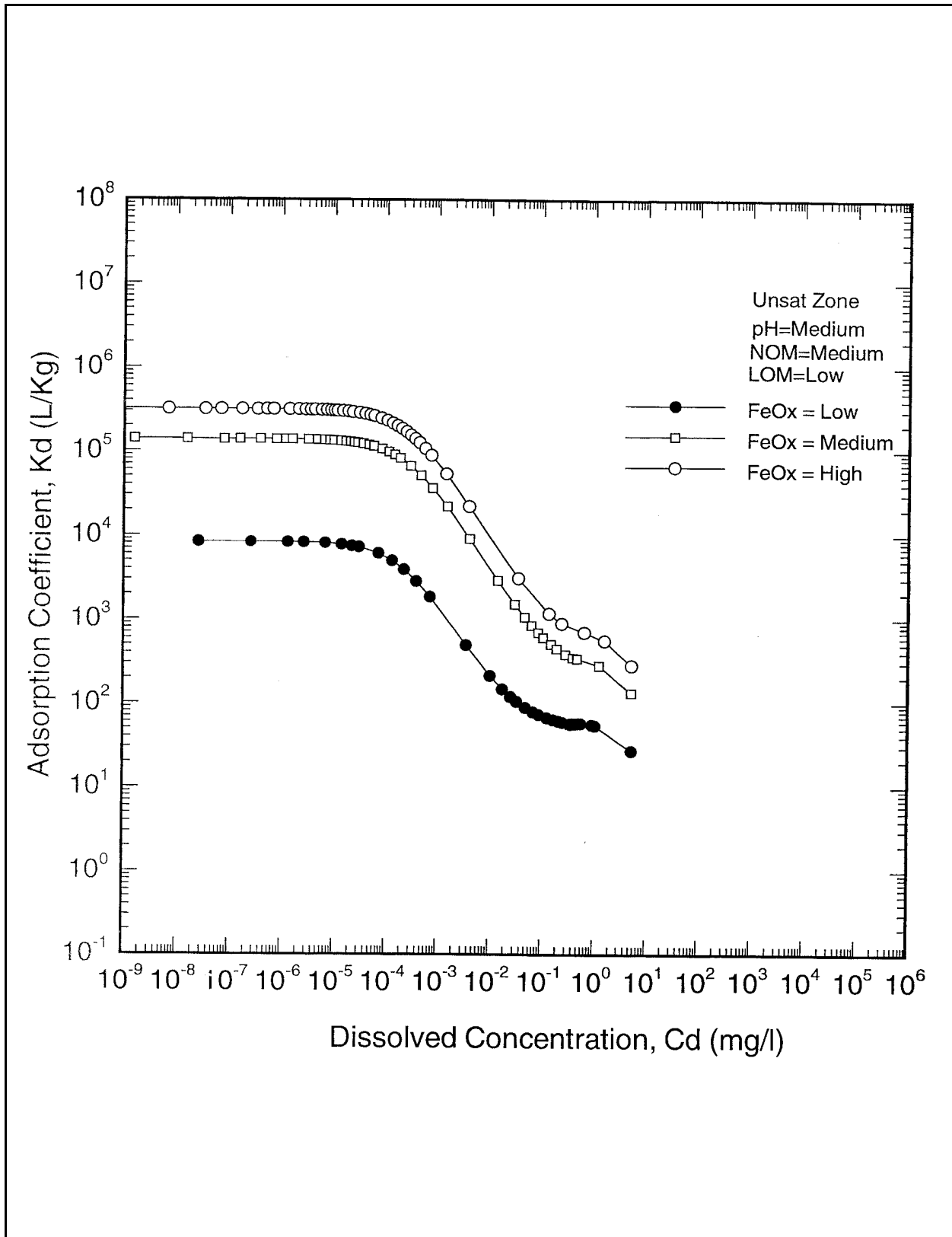
Figure 3.4   Effect of varying FeOx on MINTEQA2 derived isotherm for lead.
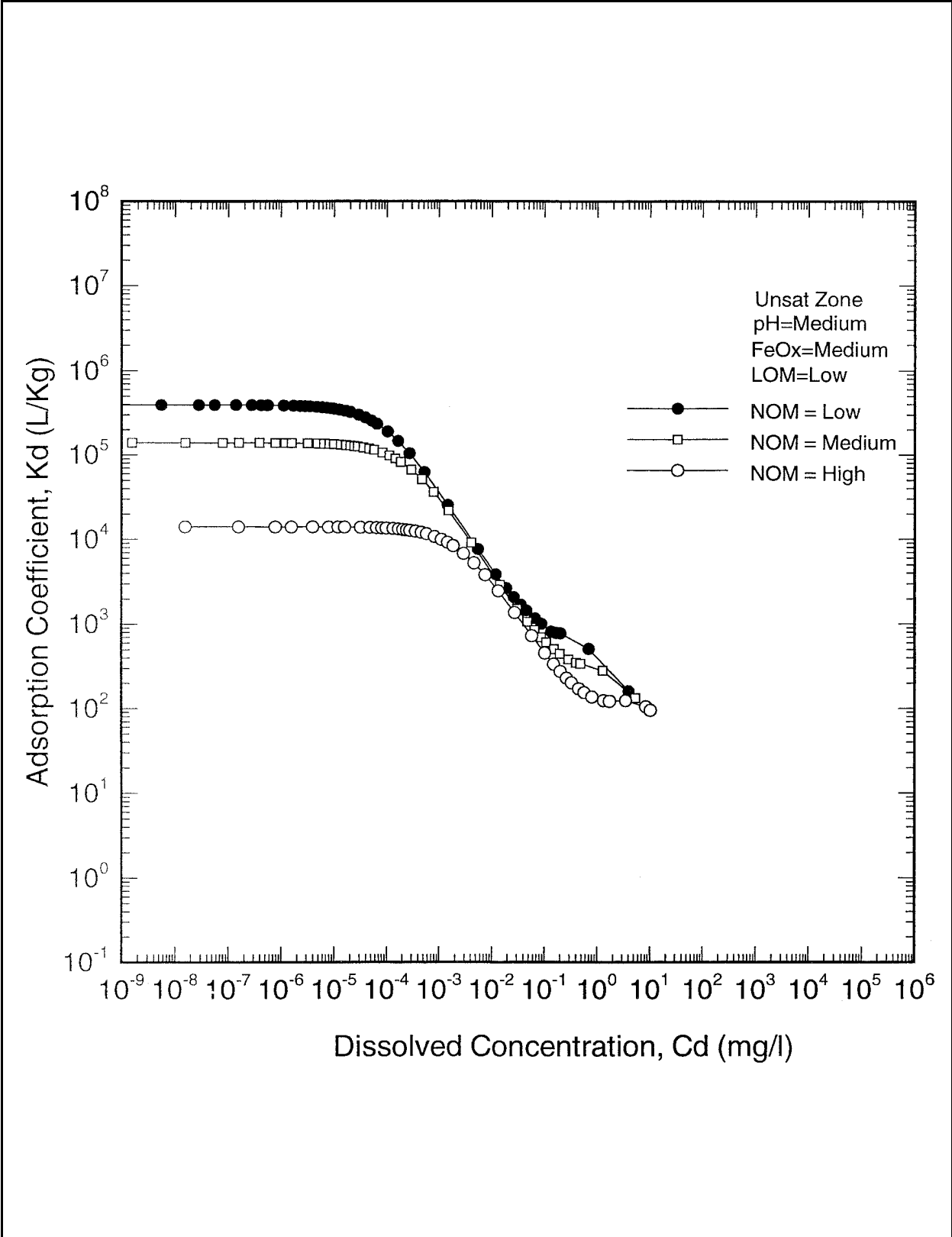
Figure 3.5   Effect of varying natural organic matter or MINTEQA2 derived isotherm for lead.

3.2 EMPIRICAL ADSORPTION ISOTHERMS

Distribution coefficients for As^{III}, Cr^{VI}, Sb^{V}, Se^{VI}, and Tl were determined from empirical relationships due to Loux et al. (1990). With the exception of Tl, these metals form anions or neutral species in aqueous solution (e.g., $HAsO_3^{2-}$, $H_2AsO_3^{-}$, and $H_3AsO_3^{0}$). As previously mentioned, adsorption modeling with the HFO database in MINTEQA2 works best for cationic species. Although Tl behaves as a cation, no HFO or POM reactions with Tl were available for use in MINTEQA2. The pH-dependent empirical relationships were determined from linear least squares analysis of laboratory measurements from aquifer materials and their corresponding groundwater and leachate samples collected from six municipal landfills, as well as other published data. In these experiments, the concentrations of trace metal contaminants in the groundwater/aquifer material samples were augmented with additions (spikes), and the spiked samples were allowed to equilibrate for 48 hours. After equilibration, the trace metal remaining in solution was measured. The difference between the total trace metal in the system (the metal originally in the sample plus the amount added) and the amount remaining in solution at equilibrium was regarded as adsorbed. The distribution coefficient was determined as the ratio of amount of trace metal adsorbed to the amount remaining in solution. The resulting relationships give K_d as a function of pH only; the inherent nonlinear character of metal adsorption as a function of total metal concentration is not represented. In EPACMTP Monte Carlo analyses for nationwide assessments, a different pH value is generated for each Monte Carlo iteration. Upon the selection of a pH, the corresponding K_d is calculated from the appropriate empirical relationship.

As previously mentioned, no empirical relation was available for Sb^{III}; the Sb^{V} relationship is used for both the +3 and +5 state. Also, the As^{III} species is adsorbed somewhat less strongly than As^{V}, and Se^{VI} is adsorbed less strongly than Se^{IV}. The contrast in adsorption affinity between different oxidation states for these metals is not nearly so marked as the contrast in Cr^{III} and Cr^{VI}. Therefore, the As^{III} and Se^{VI} relationships were used to represent both oxidation states for these metals. The empirical relationships are presented in Table 3.9.

Table 3.9   Empirical pH-dependent Adsorption Relations (Loux et al., 1990)

Metal Species	K_d (liters kg^{-1})
As^{III}	$10^{(0.0322\,pH\,+\,1.24)}$
Cr^{VI}	$10^{(-0.117\,pH\,+\,2.07)}$
Sb^{V}	$10^{(-0.207\,pH\,+\,2.996)}$
Se^{VI}	$10^{(-0.296\,pH\,+\,2.71)}$
Tl	$10^{(0.110\,pH\,+\,1.102)}$

4.0 INCORPORATION OF MINTEQA2 ADSORPTION ISOTHERMS IN EPACMTP

Monte Carlo modeling of metals transport requires, for each Monte Carlo iteration, selecting one out of 81 adsorption isotherms for each metal species, for both the unsaturated and saturated zones. The selection of the appropriate MINTEQA2 generated adsorption isotherm for each Monte Carlo iteration depends on the values of the four geochemical master variables, as discussed in the preceding chapter. These values are generated randomly from given distributions. This section describes how EPACMTP selects and prepares adsorption isotherms for use in the transport simulations. Subsequently, a range (low, medium, or high) is determined for each parameter value. In this section, distributions and range-determination criteria are described. EPACMTP-metals provides an option to linearize the nonlinear MINTEQA2 generated isotherms. The linearization scheme is also presented in this section.

4.1   DISTRIBUTION OF FIRST-TYPE PARAMETERS

4.1.1   pH Distribution

An empirical distribution of pH was obtained from an analysis of 24,921 field measured pH values available from the US EPA STORET (1985) database. The distribution is presented in Chapter 3.

From this distribution, a pH value is generated for each Monte Carlo iteration. Then, the range of pH is determined as follows: low if the generated pH value is less than 5.85, high if greater than 7.4, and medium otherwise. The same value of pH is used for both unsaturated and saturated zones.

4.1.2   Leachate Organic Content

Data on leachate organic matter content has been obtained from six leachate samples collected over a wide geographic area-Florida, New Jersey, Oregon, Texas, Utah, and Wisconsin (Loux et al., 1990). Since the number of samples is insufficient for meaningful statistical analyses, the distribution of leachate organic content was assumed to be uniform for Monte Carlo purposes. The minimum and maximum values of the uniform distribution are 0.00117 and 0.00878 (mole/l), respectively for the unsaturated zone (Tetra Tech, 1993). For a given random value of leachate organic content, the range is determined as follows: low if the value is less than 0.00236, high if greater than 0.00616, and medium otherwise.

For the saturated zone, the leachate organic content value is estimated to be one seventh of that of the unsaturated zone to account for dilution and dispersion. The range is determined using the same criteria as is in the unsaturated zone.

4.1.3   Amorphous Iron Hydroxide Adsorbent

Six samples obtained from the six areas were used to determine the range of variability of amorphous iron hydroxide adsorbent (FeOx). These samples are a subset of the samples used in the MINTEQA2 modeling. Again a uniform distribution was assumed with minimum and maximum values of 0.01258 and 1.11497, respectively. An FeOx value is low if it is less than 0.1636, high if greater than 0.7148, and medium otherwise. The same FeOx value is used for both unsaturated and saturated zones.

4.1.4 Natural Organic Matter

The distribution of natural organic matter in the unsaturated zone is a function of soil type. For the purpose of Monte Carlo simulations, one distribution is obtained for each of three main soil type: silty clay loam (SCL), sandy loam (SL), and silty loam (SIL). The frequency distribution of organic matter for each soil type is described by the Johnson-SB distribution. Table 4.1 presents the statistical parameters of natural organic matter in the unsaturated zone for each soil type.

Table 4.1   Distribution and cut-off values of natural organic matter (weight %) in the unsaturated zone

Soil Type	Distribution	Mean	Std. dev.	Min	Max
SCL	SB	0.11	5.91	0.0	8.35
SL	SB	0.0744	7.86	0.0	11.00
SIL	SB	0.105	5.88	0.0	8.51

For the unsaturated zone an organic content is considered high when greater than 0.2149, low when less than 0.06945, medium otherwise.

For the saturated zone, one distribution is used (Table 4.2). The distribution is identical to that of a sandy loam soil. However, the distribution is specified as fraction organic carbon, not as weight percent of organic matter.

Table 4.2   Distribution and cut-off values of natural organic matter (as fraction organic carbon) in the saturated zone

Distribution	Mean	Std. dev.	Min	Max
SB	4.32E-4	0.0456	0.0	0.0638

For the saturated zone a fraction organic carbon is considered high when greater than 7.355E-4, low when less than 2.92E-4, and medium otherwise.

4.2   INCORPORATION OF MINTEQA2 ISOTHERMS

In the Monte Carlo transport simulations, one isotherm is selected for each combination of the four geochemical master variables generated by the random number routines. Isotherms are selected independently for the unsaturated and saturated zones. The isotherm curves generated by running MINTEQA2 are provided to EPACMTP in tabular form. The table of values consists of one set of dissolved concentration and associated distribution coefficient (K_d) pairs for each isotherm. There are 162 isotherms for each metal (81 for the unsaturated zone and 81 for the saturated zone). Each isotherm is indexed to the particular values of the four geochemical variables used in its generation by MINTEQA2, and to the zone (unsaturated or saturated) to which it applies. The complete set of isotherms is presented in Volume 2 of this report. Note that the unit of concentration used in MINTEQA2, and hence presented in the isotherms, is mol

liter^{-1}, while EPACMTP uses mg liter^{-1}. EPACMTP converts isotherm units to mg liter^{-1} using the atomic weights shown in Table 4.3.

Table 4.3　　　Atomic weight of metals (CRC, 1970)

Metals	Atomic Weight
Ba^{2+}	137.34
Cd^{2+}	112.40
Cr^{3+}	51.995
Hg^{2+}	200.59
Ni^{2+}	58.71
Pb^{2+}	207.19
Ag^{+4}	107.89
Zn^{+2}	16.38
Cu^{+2}	63.55
V^{+4}	50.94

4.2.1　Precipitation Effects

In the EPACMTP Monte Carlo transport simulations, the effect of adsorption is incorporated through a partition coefficient K_d, defined as the ratio of the metal bound on the soil (C_s, expressed in mass of metal per mass soil) to dissolved phase concentration (C_d, expressed in mass of metal per volume of solution). In EPACMTP, K_d has the units liter kg^{-1}. The K_d values computed from the MINTEQA2 output are dimensionless, because in that model the equilibrium mass of metal in each phase (dissolved, sorbed, and precipitated) is expressed relative to a liter of solution. Here, the sorbed metal should be regarded as the mass of metal that has been *sorbed from the liter of solution.* Hence, dimensionless K_d, called K_d', can be expressed:

$$K_d' \ ' \ \frac{C_s}{C_d} \tag{4.1}$$

where C_s and C_d have, as in MINTEQA2, the same units. (Conversion of K_d' to K_d is discussed in Section 4.2.2.) Because the output from the MINTEQA2 model simulations includes the equilibrium mass of metal in each of the three phases: dissolved, adsorbed, and precipitated (C_p), the effect of precipitation can, in principle, be incorporated into the transport simulations by defining K_d' (which becomes K_d after units conversion in the transport model) as the ratio of immobile concentration ($C_s + C_p$) to mobile concentration (C_d). However, if K_d' is defined in this way, rather than as in (4.1), the form of the isotherm relating dissolved concentration and K_d is no longer monotonic. The K_d initially will decrease with increasing metal concentration, but when the solubility product is exceeded and precipitation occurs, K_d will begin to increase (Figure 4.1). The slope of the K_d curve may change again as total metal concentration increases if the anion with which the metal is co-precipitating becomes depleted. In the Monte Carlo transport
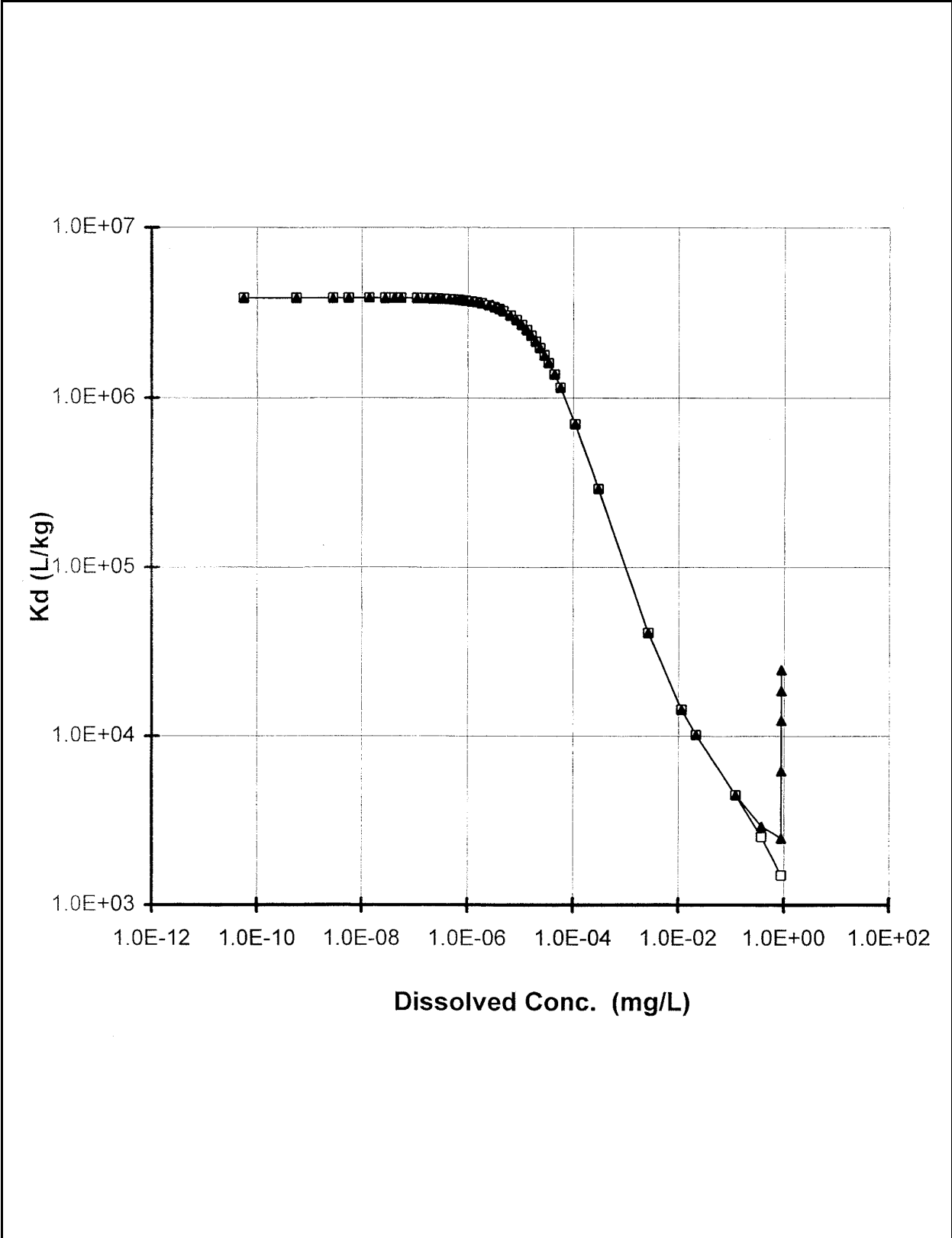
Figure 4.1   Lead Sorption isotherm with and without consideration of precipitation.

analysis, EPACMTP uses a robust and computationally efficient analytical solution technique for the unsaturated zone simulations (see Section 2.2.3). This solution method requires a monotonic isotherm; it cannot accommodate the non-monotonic isotherms that result when precipitation is included. Therefore, precipitation is not included in the EPACMTP transport analysis. This is justified somewhat by the fact that precipitation, when it does occur, is restricted to the high end of the concentration range for the metals simulated using MINTEQA2. At lower concentrations, precipitation does not occur. Also, to include precipitation would require making assumptions about the availability of the anion(s) with which the metal is precipitating. Ignoring precipitation in the transport simulations will, for those cases where it does occur in the MINTEQA2 simulations, lead to a more conservative model outcome.

4.2.2   Variable Soil Moisture Content

The partition coefficient needed in the EPACMTP transport simulations has units of volume per mass (liters kg^{-1}), but the K_d' values provided by MINTEQA2 are dimensionless. As mentioned in the preceding section, this is simply because the sorbed mass in MINTEQA2 is expressed in terms of mass of metal sorbed *from* a liter of the solution rather than mass of metal sorbed *onto* the mass of soil with which one liter is equilibrated. The partition coefficient can be transformed to the units appropriate for the transport model (i.e., liters kg^{-1}) by normalizing the MINTEQA2 sorbed concentration (in mg $liter^{-1}$) by the phase ratio (the mass of soil with which one liter is equilibrated, given in kg $liter^{-1}$). As explained in Chapter 3, the phase ratio was always 4.57 kg $liter^{-1}$ in the unsaturated zone and 3.56 kg $liter^{-1}$ in the saturated zone. These values were determined from the median values of water content (2) and soil dry bulk density (D_b) from EPACMTP distributions for these parameters. The phase ratio (*a*) is used in calculating the concentration of HFO and POM adsorption sites specified in the MINTEQA2 model runs. It follows that the dimensionless K_d' values should be normalized by 4.57 and 3.56 kg $liter^{-1}$, respectively, for the unsaturated and saturated zones to provide the input K_d for EPACMTP:

$$ K_d \; ' \; \frac{K_d^)}{a} \; ' \; K_d^) \; \frac{2^M}{D_b^M} $$

where 2^M and D_b^M are the median water content and dry bulk density. In the subsequent EPACMTP calculations, sorption is incorporated through the retardation factor R, defined as:

$$ R \; ' \; 1 \; \% \; \frac{D_b}{2} \; K_d $$

where 2 and D_b are selected from their corresponding distributions for each particular Monte Carlo iteration.

4.3   LINEARIZATION OF MINTEQA2 ADSORPTION ISOTHERM

Although EPACMTP can be run using nonlinear adsorption in both the unsaturated and saturated zones in the deterministic case (in other words, for a single set of hydrogeological parameters), the computer processing time required for a Monte Carlo analysis that includes nonlinear adsorption in both zones is prohibitive. For that reason, a technique was developed that calculates a single value of K_d from a nonlinear isotherm. This "linearized" single K_d value can then be used as a linear partition coefficient in the model,

which decreases computer processing time dramatically. Obviously, when the original nonlinear isotherm from which the linear K_d is calculated is almost linear to begin with, the impact of reducing it to a linear K_d is small. Conversely, the error associated with using a linear approximation is increased for highly nonlinear isotherms.

In EPACMTP, two methods are provided for approximating a linear isotherm from a nonlinear isotherm. In the first method, a concentration-interval weighted approach is used to compute a single K_d from the nonlinear K_d versus C_d curve. In effect, the technique simply calculates an average K_d over the range of dissolved metal concentration represented by the isotherm. Concentration-interval weighting is used to account for the fact that the dissolved concentration values are not evenly spaced on the isotherm. This option is provided for use in the unsaturated zone. In the second method (for use in the saturated zone), the K_d corresponding to the peak water table metal concentration is used for linear partitioning. The procedure involves the following steps: First, a saturated zone isotherm is specified by Monte Carlo selection of values for the four geochemical master variables. Then, the peak dissolved metal concentration at the water table is determined, and the K_d corresponding to this dissolved concentration is obtained from the isotherm by interpolation. If the peak concentration at the water table is lower than the minimum dissolved concentration given by the isotherm, the K_d value corresponding to the minimum concentration is used. Likewise, if the peak concentration is higher than the maximum concentration on the isotherm, the K_d corresponding to the isotherm maximum is used.

The specific options used in HWIR modeling pertaining to linearizing isotherms and further discussion of the implications of linearized isotherms is presented in Section 5.2.

5.0 IMPLEMENTATION OF EPACMTP FOR METALS

The EPACMTP computer code was modified to include capabilities to simulate fate and transport of metals. Most of the existing algorithms in the EPACMTP model are applicable to the simulation of metals. However, significant modifications were necessary to simulate metals adsorption with nonlinear sorption isotherms as discussed in Chapter 2. Additional modifications were made to the data input module and the Monte Carlo module for assigning values to each model parameter.

5.1   ADDITIONAL INPUT DATA FOR METALS

Several input parameters were added to EPACMTP for metal simulations. A control parameter (a FORTRAN logical variable) was added to indicate if the contaminant of interest is a metal species. Additional parameters, specifying the type of adsorption isotherm to be used and the distributions of the geochemical waste variables were also included.

5.1.1   Control Parameters

The following parameters were added to the General Parameter (GP01) record.

Table 5.1   Additional Control Parameters for Metals Simulation

Variable	Type	Column	Descriptions
IF-METAL	logical	41-45	Enter 'T' for metals simulations and 'F' otherwise.
KDEVAL	integer	46-50	Isotherm type; (required only when IF_METAL= 'T') = 1 for pH-dependent linear isotherm = 2 for linearized MINTEQA2 isotherm = 3 for nonlinear MINTEQA2 isotherm

Note that the KDEVAL= 1 option is available only for the five metals: As^{III}, Cr^{VI}, Se^{VI}, Sb^{V}, T1. The other two options are available for the ten metals: Ag, Ba, Cd, Cr^{III}, Cu, Hg, Ni, Pb, V and Zn. Also note that for the HWIR modeling, certain other metals were assumed to behave like one of the above metals as detailed in Section 3 (e.g., K_d results for Be were assumed to be the same as for Ba; As^{III} results were assumed to apply to As^{V}, etc.)

5.1.2   Metal Specific Data

A separate data group was added to specify additional parameters for metals simulations. This data group is identified in the input data file with the code 'MT'. The first variable in this group specifies the identification number for the metal species to be simulated. The remaining variables specify the distributions of the geochemical master variables for the unsaturated and saturated zones.

Table 5.2   Additional input parameters for metals specific (MT) group

Variable No.	Description
1	Metal identification number (1-12, Table 5.3)
2	pH for both unsaturated and saturated zones
3	HFO for both unsaturated and saturated zones
4	Leachate organic acids for unsaturated zone
5	POM for unsaturated zone
6	POM for saturated zone

Each metal species is identified using a numerical code, which is shown in Table 5.3. The table also shows the isotherm selection options available for the different metal species.

Table 5.3   METAL_ID and corresponding metal species

METAL_ID	1	2	3	4	5	6	7	8	9	10	13	14	15	16	17
Metal species	Ba	Cd	Cr^{III}	Hg	Ni	Pb	Ag	Zn	Cu	V	As^{III}	Cr^{VI}	Se^{VI}	Tl	Sb^{V}
KDEVAL available					2 and 3								1		

The remaining parameters in the metals group specify distributions of the geochemical master variables for the unsaturated and saturated zones. The distributions of the parameters were presented in Section 3. Note that the distributions of pH and natural organic matter (NOM) are also required for degrading chemicals (organics) as part of the unsaturated zone and saturated zone data groups. However, they are duplicated in the metal-specific data input group to emphasize the dependence of metals on these parameters. For the HWIR analyses of industrial waste management units, the leachate organic matter is always assigned a value of <u>low</u>.

5.2   EVALUATION OF APPROACHES FOR HANDLING METALS ISOTHERMS

The partitioning of metals between aqueous and soil components through adsorption is generally a nonlinear function of metal concentration. However, including nonlinear adsorption in metals transport simulations in a Monte Carlo framework places great demands on computer processing resources. In fact, accounting for nonlinear adsorption in both the unsaturated and saturated zone simulations is not feasible. Three different adsorption schemes for metals transport are included in EPACMTP, one of which is intended to provide faster transport simulations. For unsaturated zone transport simulations, all three metals adsorption options are available: (1) a coefficient for linear partitioning calculated by the model from the empirical pH-K_d relationship described by Loux et al. (1990), (2) a coefficient for linear partitioning calculated by the model by linearizing the MINTEQA2 isotherms as described in Section 4.3. and (3) a nonlinear partitioning isotherm developed using MINTEQA2 ,or determined by the user from Freundlich isotherm parameters. For options 1 and 2, an analytical transport solution algorithm is implemented. For option 3, the nonlinear adsorption case, either analytical or numerical transport solutions may be used, as discussed in Section 2. Obviously, option 1 should only be used for the five metals for which pH-K_d relationships are available. Options 2 and 3 were compared for modeling adsorption in the unsaturated zone. Results were evaluated in terms of model response and computational efficiency, leading to the following conclusions:

- Linearization of the adsorption isotherm to produce a linear partition coefficient and subsequent use of the analytical unsaturated zone transport solution (option 2) is computationally efficient, but produces significantly different water table concentrations than using nonlinear adsorption (option 3). Option 2 should only be used for unsaturated zone transport when the concentration range being modeled corresponds to a segment of the isotherm that is approximately linear (relatively low concentrations).

- The use of nonlinear adsorption with the numerical unsaturated zone transport solution can lead to convergence problems in the model, especially if the isotherm has a high degree of nonlinearity. In that case, the transport time step must be made very small to insure convergence, but this leads to long computer simulation times.

- The use of nonlinear adsorption with the analytical unsaturated zone transport solution is both fast and accurate. Only minor differences were found between this solution technique and the numerical technique, which includes dispersion. The nonlinearity of the isotherm itself creates a contaminant profile with a sharp front and a long (dispersed) tail. For typical MINTEQA2 isotherms, this effect was found to be more pronounced than for cases involving hydrodynamic dispersion alone.

For HWIR metals simulations in the unsaturated zone, option 1 was used for the five metals for which pH-K_d relationships are available. Option 3, nonlinear adsorption isotherms, was used with the analytical transport solution for the unsaturated zone simulations. The nonlinear isotherms were developed using the MINTEQA2 simulations.

For saturated zone transport, a linear partition coefficient must always be used in EPACMTP, regardless of the unsaturated zone adsorption option selection. Linear partitioning must be used because including nonlinear partitioning in the saturated zone requires a numerical solution, which in turn requires small time steps to insure convergence. This places an insupportable demand on computational resources, given the Monte Carlo framework of the problem to be solved. Further, there is some justification for its use in that, at low concentration ranges, most of the MINTEQA2 adsorption isotherms are linear. Also, the maximum saturated zone metal concentrations are expected to be lower than the leachate concentrations of metal leaving the waste disposal unit due to adsorption in the unsaturated zone and initial dilution in the groundwater. This provides some logical basis for the use of linear partitioning in the saturated zone. EPACMTP determines the K_d value to be used in the saturated zone from the selected MINTEQA2 isotherm after the unsaturated zone simulation has been completed. This permits the saturated zone K_d to be determined as a function of the peak metal concentration exiting the unsaturated zone. The method is described in Section 4.3.

6.0 FINITE SOURCE METHODOLOGY

6.1   LINEAR ADSORPTION MODELING

For those cases in which a linear metals adsorption isotherm is used, i.e., a pH-derived isotherm using the method of Loux (1990), the EPACMTP finite source methodology developed for hydrolyzing contaminants (EPA, 1996b) can be applied to metals without modification. The key feature of the finite source methodology is that for a fixed pulse duration, t_p, the receptor well concentration C_{rw}, is a linear function of the leachate concentration C_L. This requires a linear transport equation. The methodology can accommodate biochemical transformation (degradation) and linear sorption. In the case of metals, there is no degradation, but the effect of adsorption, as expressed in an effective retardation factor, may be highly significant.

For those metals with high effective retardation coefficients, the elapsed time required for the receptor well concentration to reach its peak and begin to decline for a given leachate pulse duration may be very large, on the order of several hundred-thousand to million years. To allow some consideration to be given to the time factor, the finite source methodology was modified to incorporate a maximum time value, for determining the maximum receptor well concentration. The implementation of this factor is as follows: If the receptor well concentration has reached a peak and started to decline by a time less than some fixed cut off time called t_c, the model returns the peak receptor well concentration. If, on the other hand, the receptor well concentration has not reached a peak, but is still increasing at time t_c, then the well concentration at time t_c is returned. If t_c is set to a very large value, the effect will be the same as using no time limit. If t_c is set to a relatively small value, it will result in smaller receptor well values being returned by the model for use in determining allowable leachate and total waste concentrations for a given protection level. The procedure is graphically illustrated in Figure 6.1. For the HWIR analyses, the value of t_c was set to 10,000 years.

6.2   NONLINEAR ADSORPTION MODELING

If the metals fate and transport modeling is performed using nonlinear MINTEQA2 isotherms, the finite source implementation as documented in EPA (1996b) for linearly sorbing chemicals can no longer be used because the relationship between leachate concentration, C_L, and receptor well concentration, C_{rw}, becomes nonlinear also. A fundamental premise of the finite source implementation for EPACMTP (EPA, 1996b) is the linear relationship between leachate concentration and receptor well concentration, all other model parameters being constant. Under linear transport conditions, all model simulations are run using a fixed leachate concentration, and a limited range of different ratios between leachate concentration, C_L, and total waste concentration, C_w. Typically eight to ten different ratios of C_w/C_L are needed, resulting in an equal number of separate Monte Carlo runs. From this, the frequency of exceedance of the health-based groundwater standard can be determined for any combination of C_L and C_w, which in turn allows the specific combinations of C_L and C_w which correspond to a specified protection level, e.g., 85th percentile, to be calculated. Instead, it is necessary to perform separate Monte Carlo simulations for specific metal leachate concentrations (C_L) within the overall leachate concentration range of interest (which extends from a C_L near the health-based standard to a C_L many times that value), stepping through an appropriate set of C_w/C_L ratios within each simulation. The percentage exceedance of the appropriate health-based groundwater standard is   recorded   at   the   end   of   each   Monte   Carlo   simulation   for   each C_W/C_L
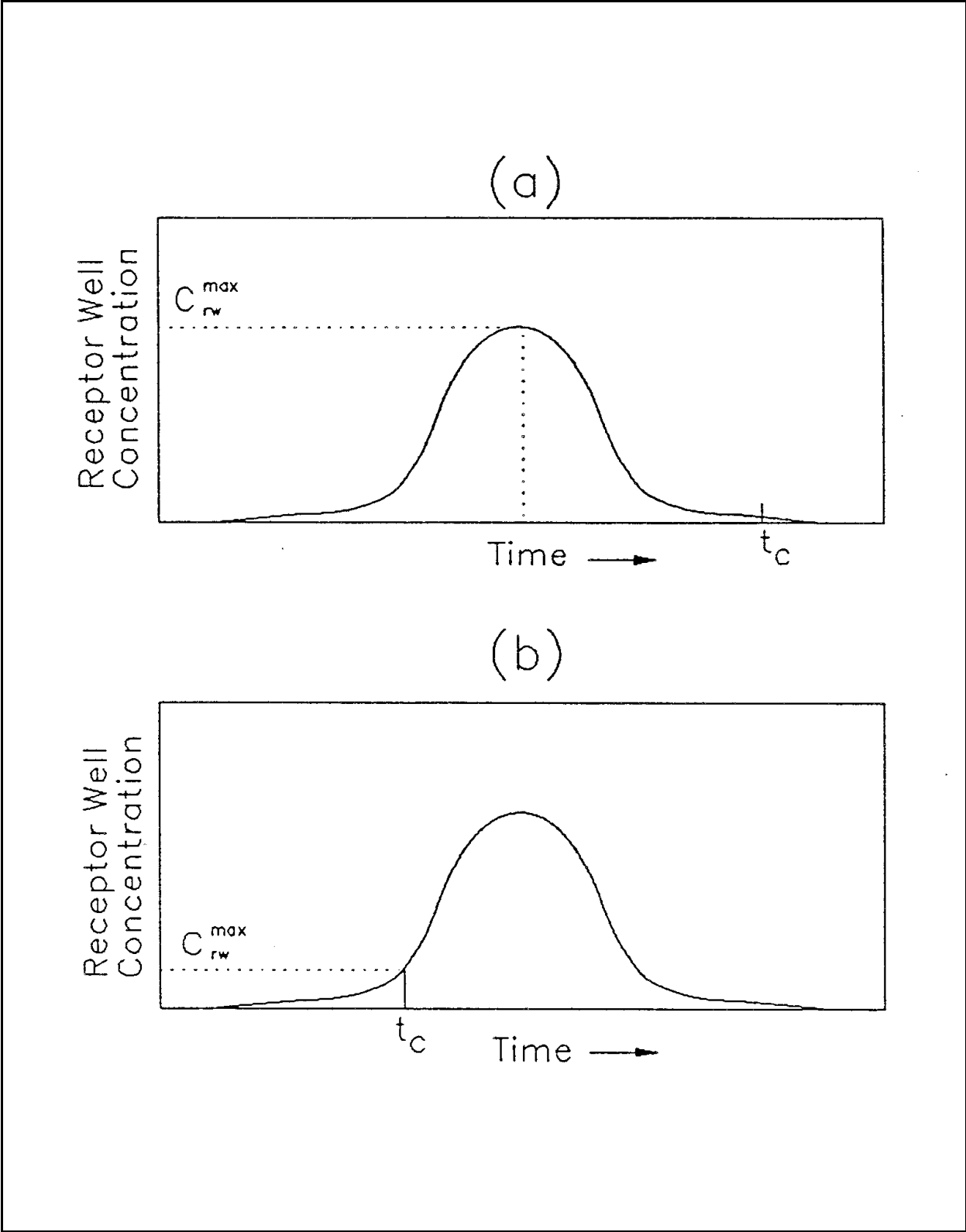
Figure 6.1   Maximum receptor well concentration with large time cutoff factor (a), and with short time cutoff factor (b).

ratio. Following the completion of all runs, isopleths of the percent exceedance of the health-based standard for different combinations of C_L and C_W can be constructed (Figure 6.2). Each Monte Carlo simulation, having been performed for a specific C_L, generates a set of C_W values associated with that C_L, each of which corresponds to different a percent exceedance outcome. This contrasts with transport modeling for linear partitioning cases, in which a single simulation applies to the entire leachate concentration range of interest (because the model is linear in its input concentration) and generates the entire set of C_W-C_L combinations used in constructing the isopleths. A sufficient number of simulations must be performed at specific values of C_L to define the C_W-C_L relation (isopleth) with the desired resolution. Because this relation is very smooth and regular, a polynomial can easily be fitted to the C_W-C_L pairs for each level of protection to develop the desired curves. From these curves, combinations of C_W and C_L that result in a desired protection level can be read directly using the fact that the percent protection is equal to 100 - % exceedance.

When nonlinear adsorption modeling is performed in the fate and transport simulations, the above procedure can no longer be used. Instead, it will be necessary to conduct Monte Carlo runs for different input values of C_L and C_w, spanning the concentration range of interest. The percentage exceedance of the appropriate health-based groundwater standard recorded at the end of each Monte Carlo run. Following completion of all runs, isopleths of the percent exceedance of the health-based level, as a function of C_L and C_w can be directly constructed, see Figure 6.2. From these graphs, the combinations of C_L and C_w that result in a desired protection level, can be read directly using the fact that the percent protection is equal to (100 - % exceedance).

In conclusion, the overall framework for the finite source analysis is applicable to metals with nonlinear sorption. However, the implementation will require a much greater number of Monte Carlo runs as compared to cases with a linear or linearized isotherm.

6.3   IMPLEMENTATION OF FINITE SOURCE METHODOLOGY FOR HWIR

For the proposed Hazardous Waste Identification Rule (HWIR), EPACMTP was used to determine waste and leachate concentration (C_w and C_L) limits for the 15 metals mentioned in the preceding chapters (i.e., page 3-1). Linear, pH dependent adsorption isotherms were used for As^{III}, Cr^{VI}, Sb^{V}, Se^{VI}, and TI. Hence they were treated similar to the organic constituents that were considered for the ground water exposure pathway. For further details refer to the finite source background document (EPA, 1996). For the remaining eight metals, nonlinear adsorption isotherms were used.

The procedure of determining asymptotic limits of C_w and C_L for non-linear adsorption metals discussed in the preceding section is laborious and computationally intensive. Therefore, a simplified procedure was used which is suitable for determining the limiting values of C_w and C_L needed for HWIR. The C_w and C_L limits correspond to the highest C_L and C_w values, respectively. Therefore to determine the C_w limit, the source concentration was set to a very high value and C_w values were varied over a range to determine the C_w value which would give the required level of protection. Similarly for C_L, C_w was set to a very high value and C_L was varied over a range of C_L values. This procedure saved significant time and computational effort.
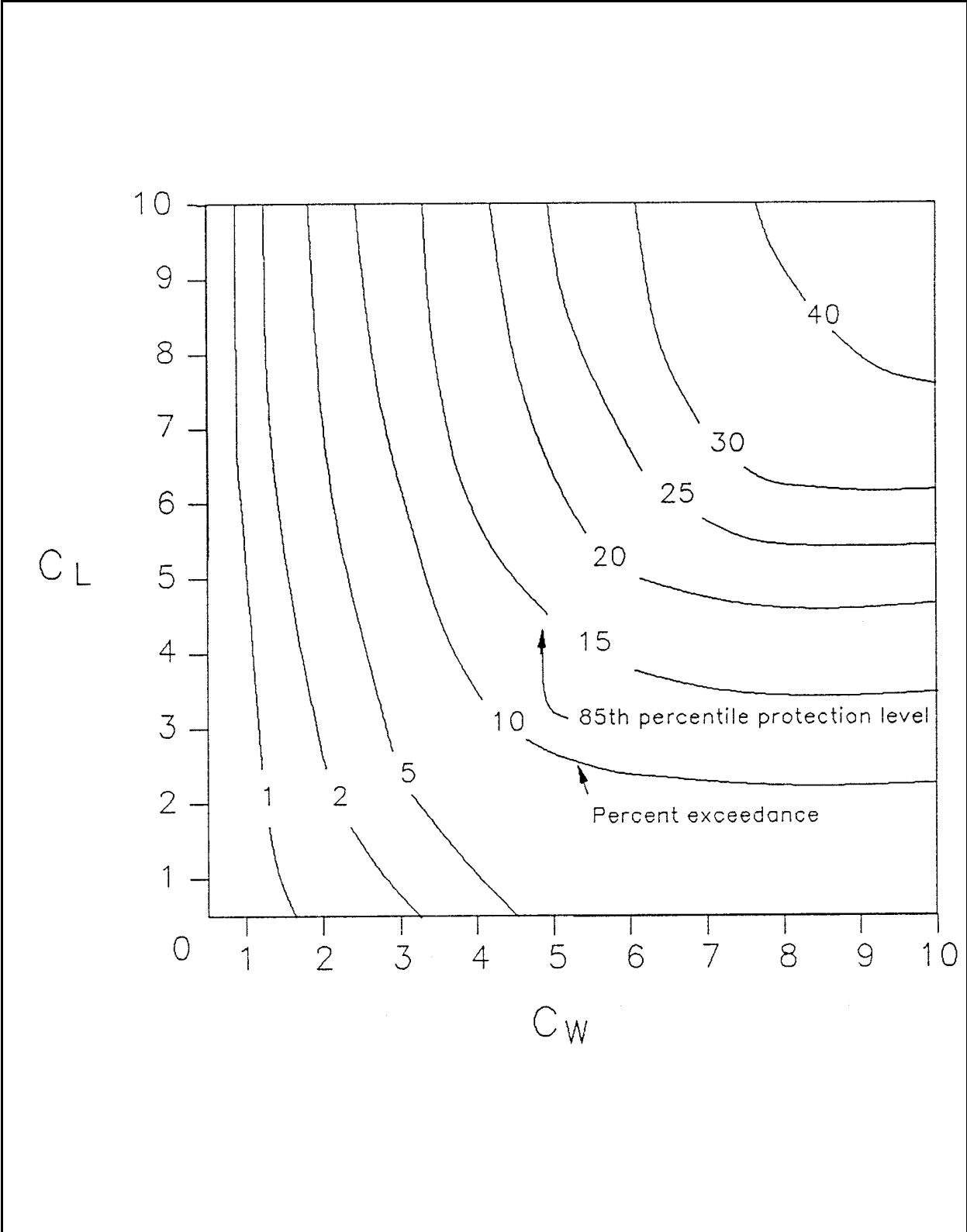
Figure 6.2   Example isopleths of the percentage exceedance of the health-based groundwater concentration level as a function of C_L and C_w.

6-4

7.0 VERIFICATION OF EPACMTP-METALS UNSATURATED ZONE MODULE

In this section modifications made to EPACMTP for simulating the transport of metal species are verified. Since the major modifications were made to the unsaturated zone modules, verification problems are limited to the unsaturated zone.

7.1   VERIFICATION OF TRANSPORT NUMERICAL SOLUTION

7.1.1   Linear Adsorption Case

In the first verification problem, the linear adsorption partitioning capability was exercised. For this problem, an analytical solution can be obtained for comparison with the EPACMTP result. The selected problem involves continuous release of a non-sorbing solute in a fully saturated column. Comparison of the EPACMTP result with the analytical solution was made at t= 20 d (Figure 7.1). Input transport parameters for this problem are provided in Table 7.1.

7.1.2   Nonlinear Freundlich Adsorption Isotherm Case

When the adsorption isotherm is nonlinear, an exact analytical solution is generally not available. Therefore, results from EPACMTP using the Freundlich isotherm were compared with those from HYDRUS, an numerical code known to produce good results for the Freundlich equation (Kool and Genuchten, 1991).

The test problem was solved two different ways using EPACMTP. First, the Freundlich isotherm was represented by its usual closed function form (see Equation 2.19). In the second approach, the closed form equation was used to compute K_d and C_d pairs which were presented to EPACMTP in tabular form. This approach tests the numerical algorithm in a manner consistent with the way the MINTEQA2 nonlinear isotherms are presented to the model.

In the remainder of this section, comparisons between the HYDRUS result (using the closed-functional form of the Freundlich equation) and EPACMTP are presented for two Freundlich isotherms.

7.1.2.1 Freundlich Exponent Greater Than One

The input transport parameters for this example problem are reported in Table 7.2. The tabular form of the Freundlich isotherm used by EPACMTP-Metals is presented in Table 7.3. Two different source conditions were used: continuous and finite sources. Figure 7.2 shows depth distributions of the concentration for the continuous source case at 40 years. The HYDRUS and EPACMTP results (both functional and tabular representations) are in good agreement. Figure 7.3 shows depth distributions of the concentration for the finite source case at 40 years. The source duration was 10 years. Overall agreement among the three solutions is good, although the result from the tabular form indicates that the contaminant front has advanced farther than in the HYDRUS and EPACMTP with function form, simulations. The difference reflects the approximation in representing the continuous Freundlich isotherm function using a table of discrete values.

Table 7.1   Parameter Values for the Linear Adsorption Transport Verification Problem

Source concentration, C_o	1 ppm
Flow rate, q	91.25 m/yr
Saturated hydraulic conductivity, K_{sat}	91.25 m/yr
Porosity, N	0.25
Column length, L	20 m
Dispersivity, $''_L$	4 m
Bulk Density, D_b	1.65 g/cm^3
Distribution coefficient, K_d	0.0
Simulation time	20 d
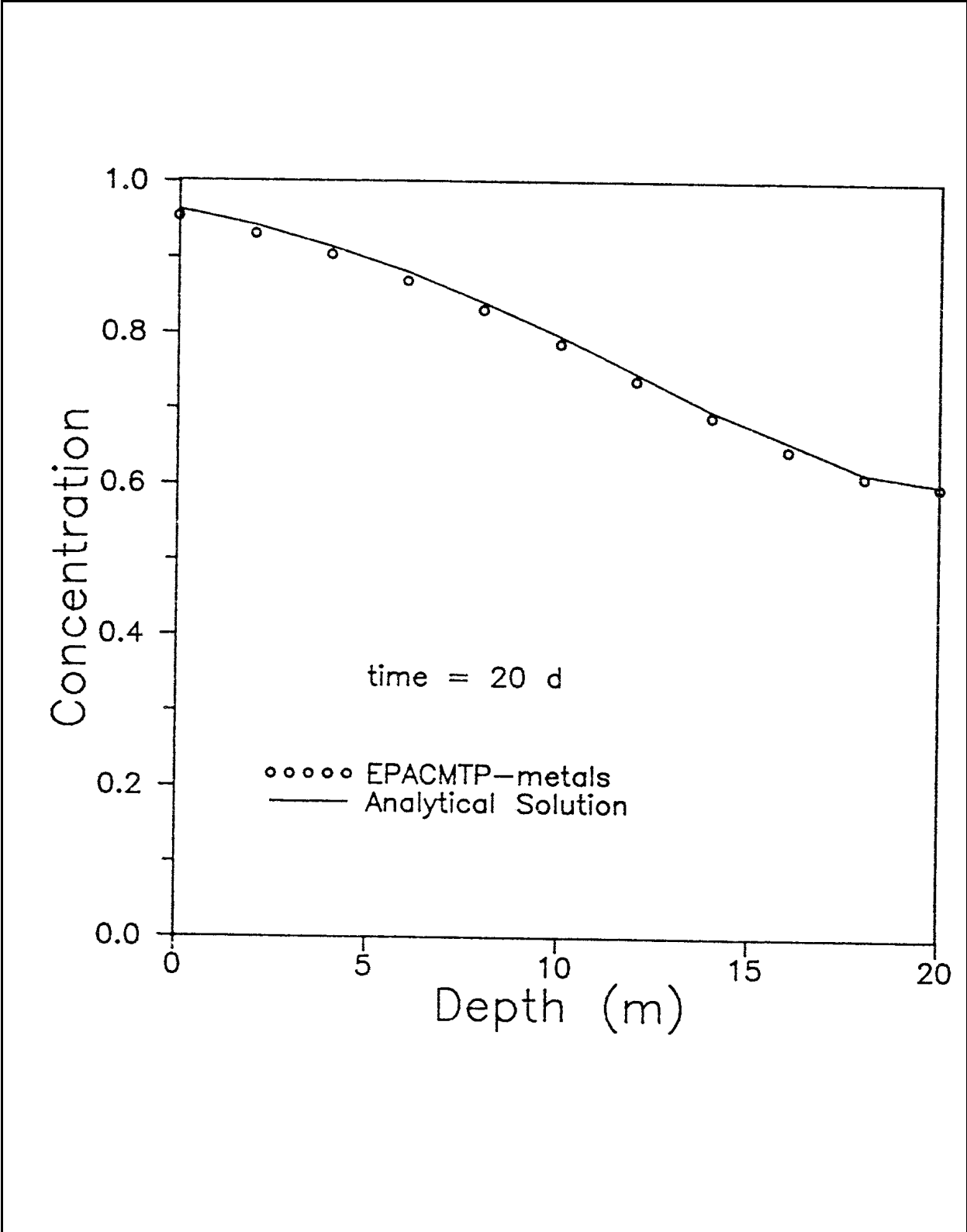
Figure 7.1   Comparison of EPACMTP-Metals result with analytical solution for the unsaturated-zone
verification problem with linear adsorption isotherm.

Table 7.2   Parameter Values for the Nonlinear Adsorption Verification Problem with Freundlich Isotherm

Source concentration C_o	5 ppm
Flow rate, q	0.15 m/yr
Saturated hydraulic conductivity, K_{sat}	0.00171 cm/hr
van Genuchten first parameter, "	0.01 m^{-1}
van Genuchten second parameter, \$	2.00
Residual water content, 2_r	0.10
Porosity, N	0.25
Thickness of unsaturated zone, L	25 m
Dispersivity, $"_L$	1 m
Soil bulk density, D_b	1.65 g/cm^3
Coefficient of Freundlich isotherm, k	$0.285 \text{ cm }^{3O}/\text{g}^O$
Exponent of Freundlich isotherm, O	1.5 and 0.5

Table 7.3   Tabular Form of Freundlich Isotherm (O = 1.5)

Total Concentration	Partitioning Coefficient
0.000	0.000
0.018	0.034
0.051	0.032
0.107	0.074
0.393	0.127
0.484	0.140
0.618	0.153
1.096	0.194
1.967	0.243
2.966	0.285
4.680	0.338
8.571	0.423
10.634	0.457
15.632	0.527
25.806	0.633
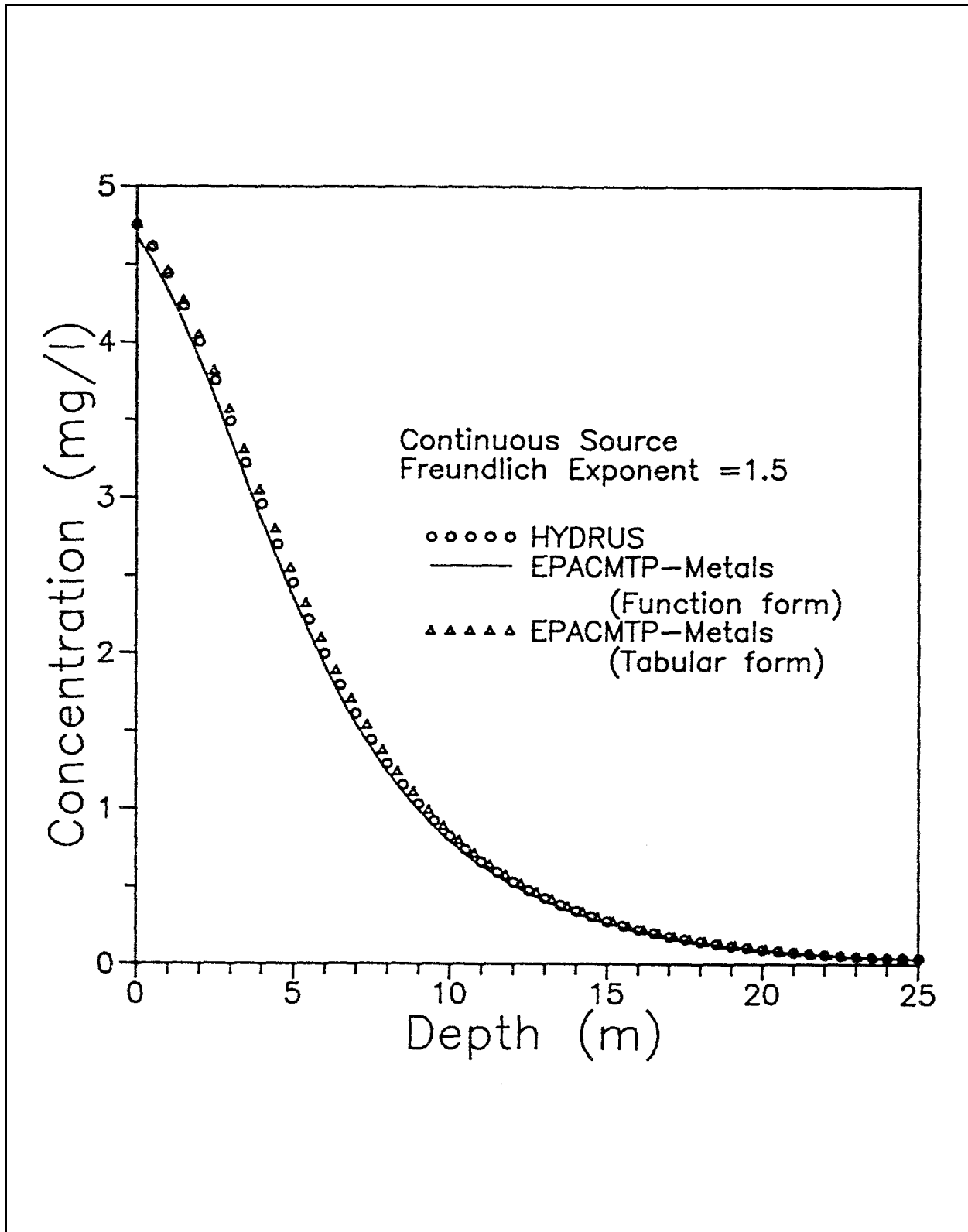
Figure 7.2   Comparison of unsaturated zone concentration profiles of HYDRUS and EPACMTP-Metals
for nonlinear adsorption with Freundlich exponent = 1.5; Continuous source case.
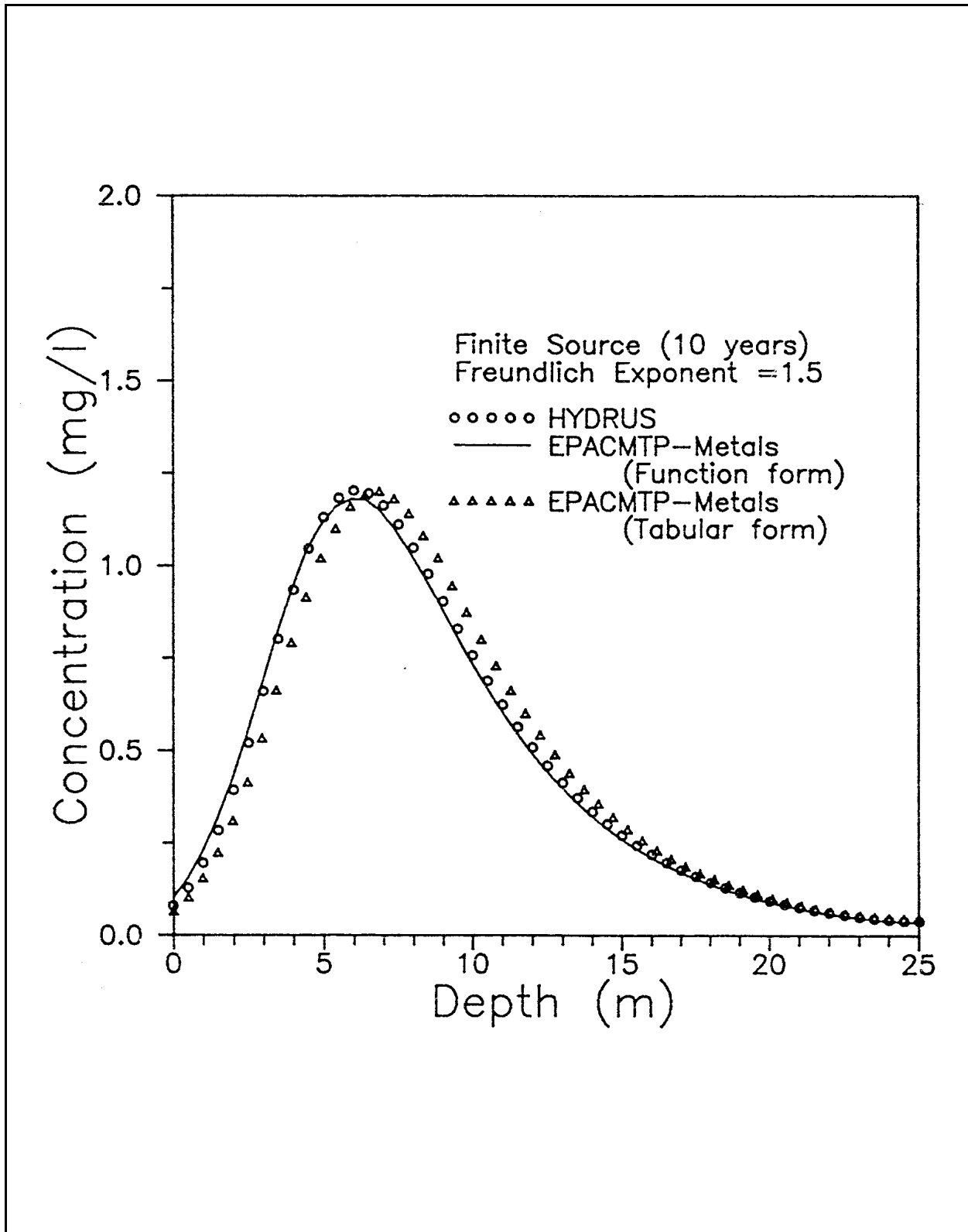
Figure 7.3   Comparison of unsaturated zone concentration profiles of HYDRUS and EPACMTP-Metals
for nonlinear adsorption with Freundlich exponent = 1.5; Finite source case.

7.1.2.2 <u>Freundlich Exponent Less Than One</u>

The input transport parameters for this example problem are identical to those reported in Table 7.2 except for the Freundlich exponent. For this example the exponent was 0.5. The tabular form of Freundlich isotherm used by EPACMTP-Metals is presented in Table 7.4. Two different source conditions were again used: continuous and finite sources. Figure 7.4 contains depth distributions of concentration for the continuous source case at 40 years. The results from HYDRUS and the functional and tabular forms of EPACMTP are in very good agreement. Figure 7.5 contains depth distributions of the concentration for the finite source at 40 years. Again, the source duration was 10 years. All three results are in good agreement. Mass balance calculation considering both dissolved and sorbed phase mass indicated that the mass balance error in the result from the tabular form is less than 1%.

7.1.3 MINTEQA2 Adsorption Isotherm Case

For this example problem, the EPACMTP-Metals code was used to simulate the transport of lead in the unsaturated zone. However, the accuracy of the model result cannot be verified due to the lack of reference codes. Reproduction of the test problems reported by Tetra Tech (1993) was not possible, since they did not provide input parameter values for the examples. Therefore, as a check on the simulation results, computed cumulative mass is compared with total input mass.

Two MINTEQA2-generated isotherms (#3 and #61) for lead were selected for testing. The first isotherm corresponds to low organic acids (LOA), low HFO, low POM, and low pH. The partitioning coefficient for this isotherm is highly nonlinear and varies from 144 to over 100,000 liters kg^{-1}. Other transport parameters used for the simulation are presented in Table 7.5. For simplicity, the flow rate and saturated soil conductivity are selected such that the soil column is fully saturated. Figure 7.6 presents concentration profiles obtained using all three options for the metals adsorption isotherm (i.e., Loux's pH-K_d relationship, and nonlinear and linearized MINTEQA2 isotherms). The cumulative contaminant mass versus depth profile, including metal in the dissolved and sorbed phases, is shown in Figure 7.7. EPACMTP-Metals resulted in slightly more mass in the soil column than the total contaminant input at the source. However, the difference was less than 1%.

The second isotherm corresponds to high leachate organic acid (LOA, low HFO, high POM, and low pH). The partitioning coefficient for this isotherm is almost linear and varies from 44 to 56 liters kg^{-1}. Other transport parameters are identical to those reported in Table 7.5. Concentration profiles obtained from all options are presented in Figure 7.8. The cumulative total mass versus depth profile, including metal in the dissolved and sorped phases, is shown in Figure 7.9. Again, EPACMTP-Metals resulted in slightly more mass than the total contaminant input at the source. As in the previous case, the error is less than 1%.

7.2 VERIFICATION OF TRANSPORT ANALYTICAL SOLUTION

The results from the analytical solution derived in Section 2.2.3 has been compared with results from HYDRUS (Kool and Genuchten, 1991) to verify the analytical solution. The Freundlich isotherm is used in the verification cases for both numerical and analytical simulations. The test case involves a one-dimensional vertical transport of solute, with a pulse source of 10 days, followed by continuous water infiltration from the surface. The parameters used for soil and solute properties and numerical simulation are given in Table 7.6.

Table 7.4   Tabular Form of Freundlich Isotherm (O = 0.5)

Total Concentration	Partitioning Coefficient
0.000	9592.792
0.001	3574.758
0.004	540.626
0.023	96.077
0.150	27.991
0.939	1.385
1.516	0.684
2.118	0.458
3.923	0.251
5.973	0.177
7.418	0.150
8.314	0.138
9.007	0.130
9.155	0.128
9.198	0.128
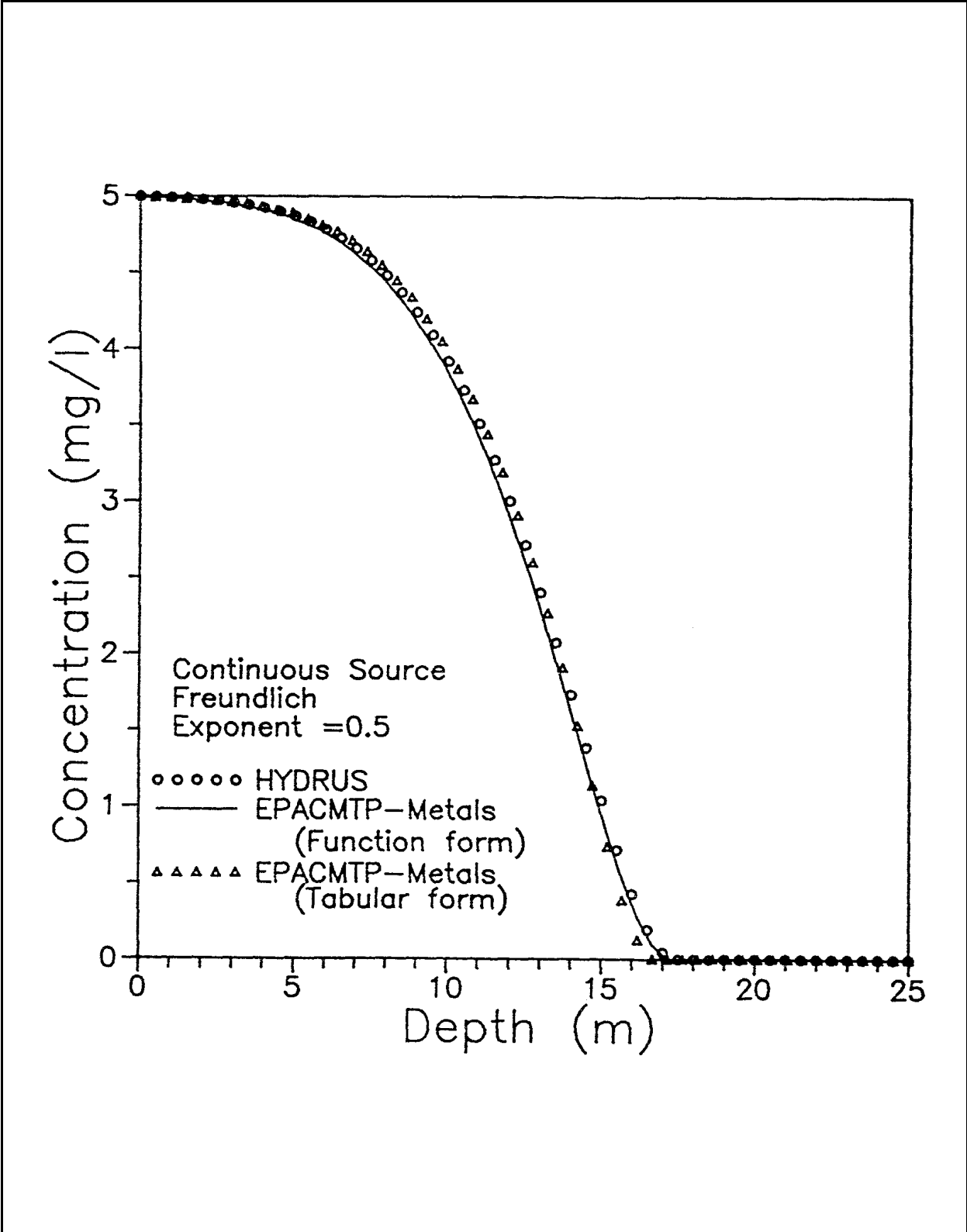
Figure 7.4   Comparison of unsaturated zone concentration profiles of HYDRUS and EPACMTP-Metals for nonlinear adsorption with Freundlich exponent = 1.5; Continuous source case.
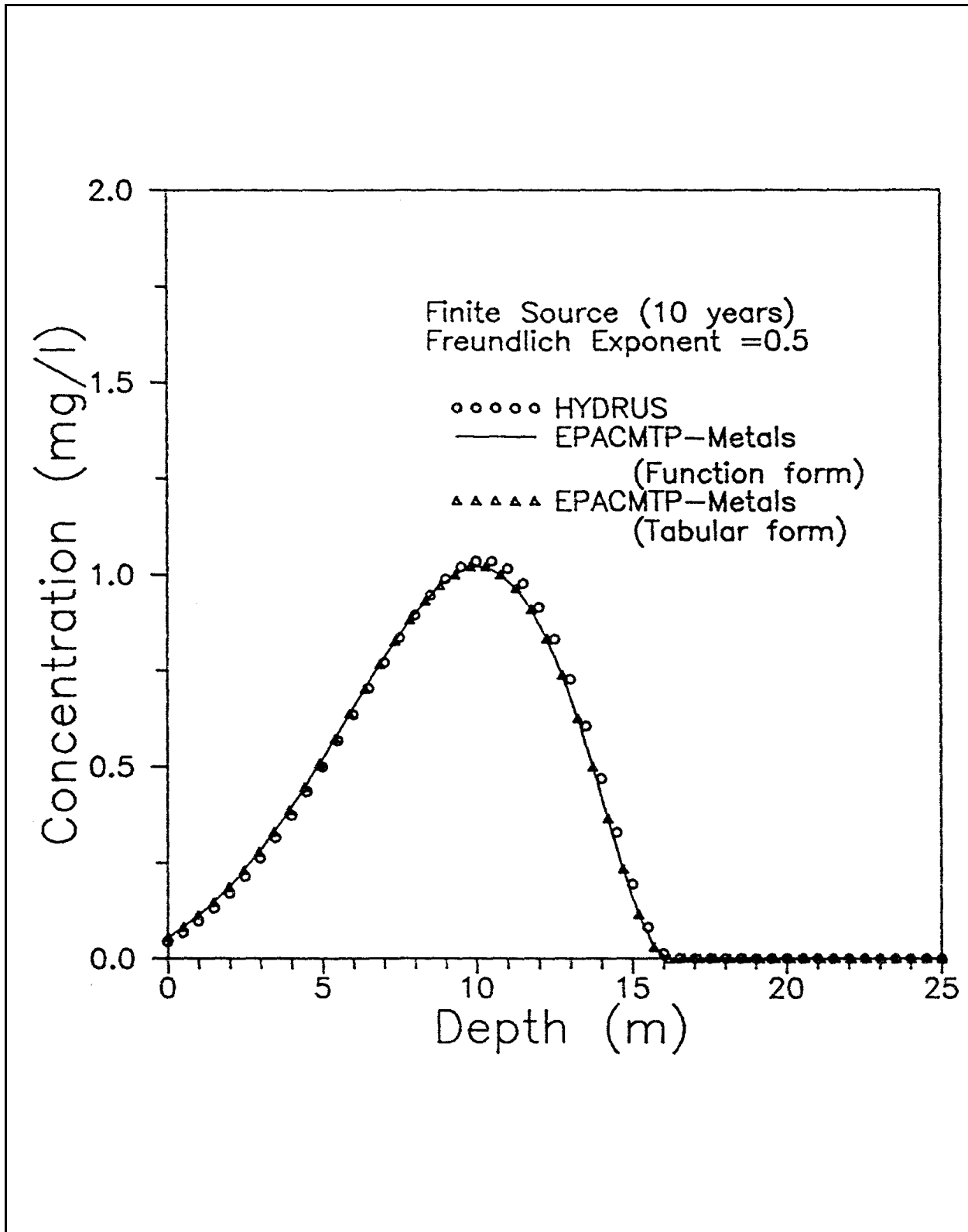
Figure 7.5   Comparison of unsaturated zone concentration profiles of HYDRUS and EPACMTP-Metals
              for nonlinear adsorption with Freundlich exponent = 0.5; Finite source case.

Table 7.5   Parameter Values for the Example using the MINTEQA2 - generated Nonlinear Lead Isotherm

Source concentration, C_o	5 ppm
Flow rate, q	0.15 m/yr
Saturated hydraulic conductivity, K_{sat}	0.15 m/yr
Porosity, N	0.25
Column Length, L	10. m
Dispersivity, $"_L$	0.5 m
Bulk density, D_b	1.65 g/cm^3
Source duration	50 years
Simulation time	1000 years
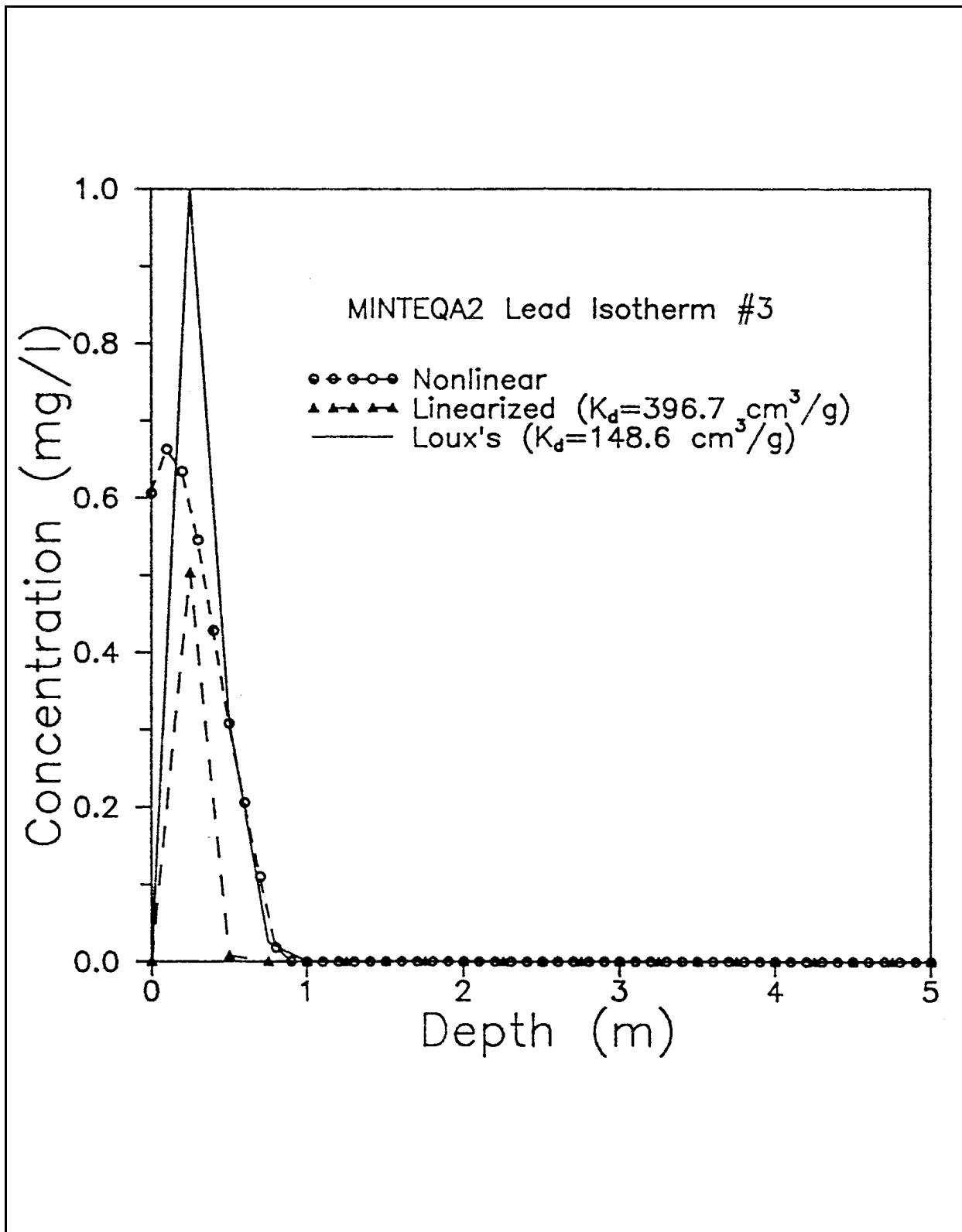
Figure 7.6   Unsaturated zone lead concentration profile low LOA, low HFO, low POM, and high pH
(= 8.1) condition.

7-13
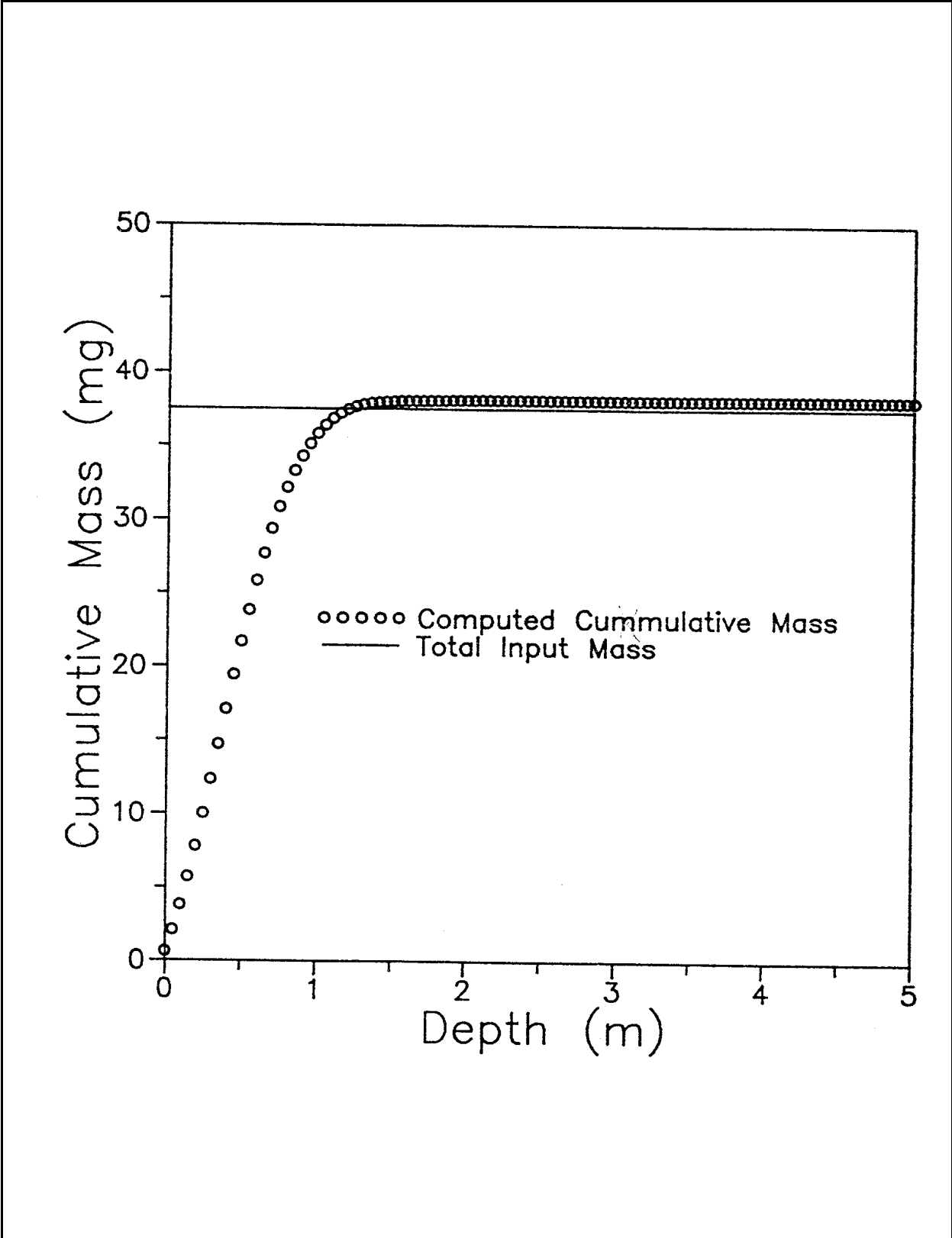
Figure 7.7   Cumulative mass in the unsaturated zone and total input mass.
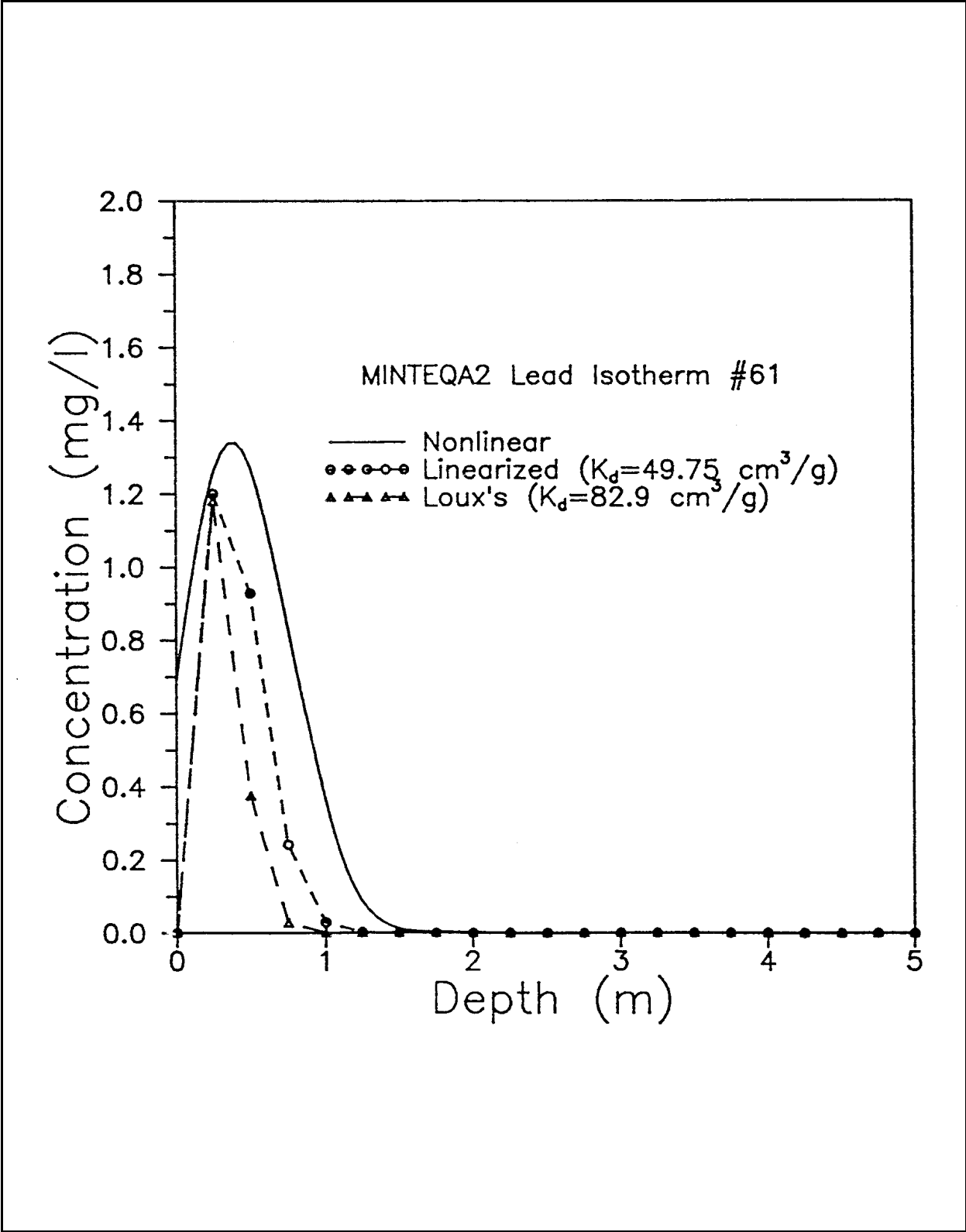
Figure 7.8 Unsaturated zone lead concentration profile for high LOA, low HFO, high POM, and low pH (= 4.8) condition.
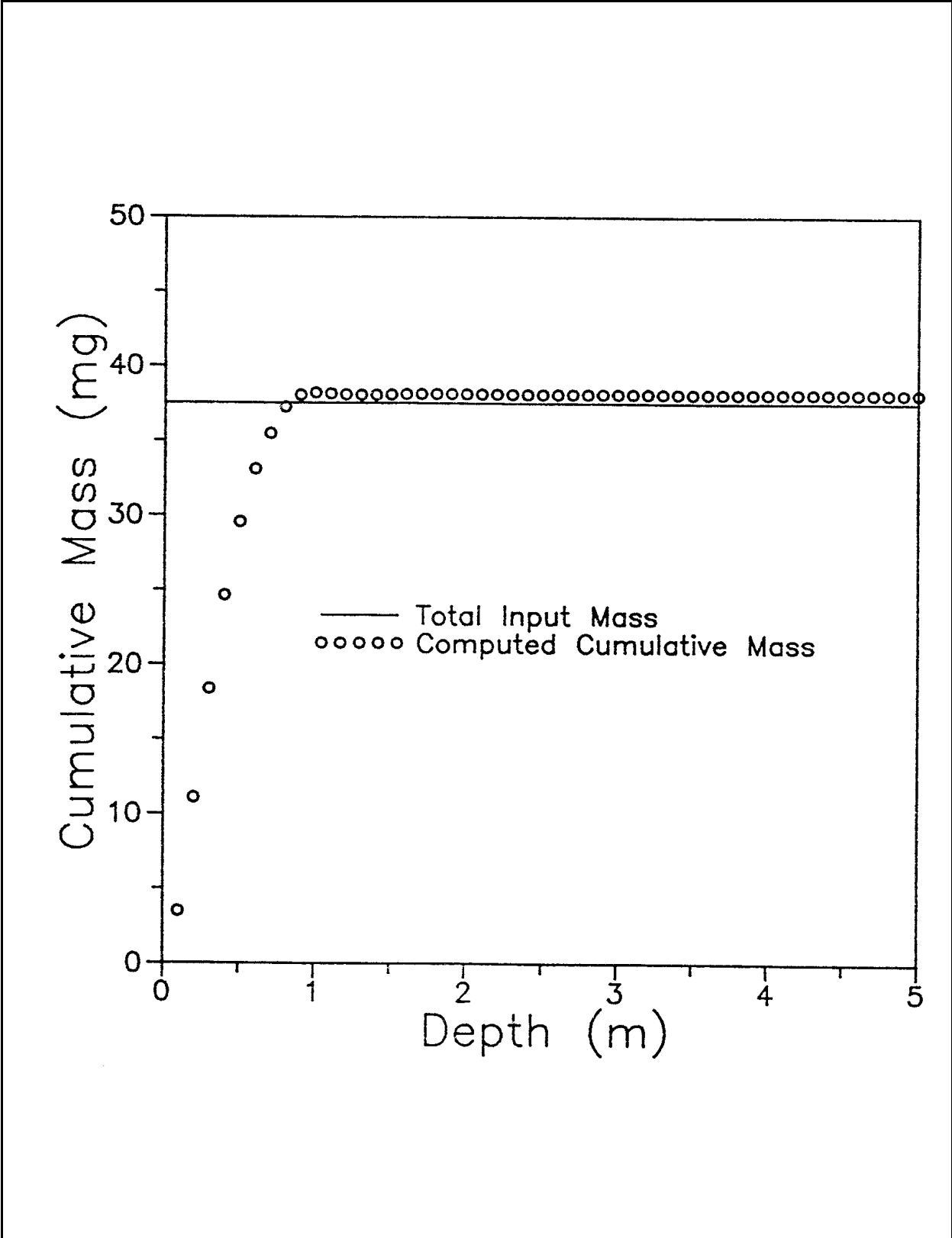
Figure 7.9   Cumulative mass in the unsaturated zone and total input mass.

Table 7.6   Values of Transport Parameters Used in Verification Examples

Parameter		Value
Pore velocity, V (cm/d)		0.444
Water content, θ		0.45
Bulk density D_b (g/cm^3)		1.5
Pulse duration, T (d)		10
Source concentration, c_o (mg liter^{-1})		1.0
Initial concentration, c_i (mg liter^{-1})		0.0
Freundlich exponent, β	Case 1:	0.8
	Case 2:	0.5
	Case 3:	1.5
Freundlich coefficient, K_1	Case 1: (cm^3/g)(L/mg)$^{-0.2}$	1.0
	Case 2: (cm^3/g)(L/mg)$^{-0.5}$	1.0
	Case 3: (cm^3/g)(L/mg)$^{0.5}$	1.0
Dispersivity, α_L (cm)	Case 1:	0.005
	Case 2:	0.005
	Case 3:	0.01
Spacial discretization, Δz (cm)	Case 1:	0.02
	Case 2:	0.01
	Case 3:	0.05

7.2.1   Comparison with 0 = 0.8

In this case 0 = 0.8, a sharp displacement front will develop for advection-dominated transport, as discussed before. A comparison between numerical and analytical predictions of solute plumes at t= 10, 50, and 100 days is shown in Figure 7.10. Excellent agreement was obtained between the numerical and analytical solutions. The sharp fronts and the dispersed tails of concentration profiles have been captured very well by both solutions. It should also be mentioned that a very small grid spacing of)z= 0.02 cm was used in the numerical model to avoid numerical oscillations and to attain reasonable accuracy.

7.2.2   Comparison with 0 = 0.5

For the case 0= 0.5, increased nonlinear behavior is expected relative to the 0= 0.8 case. Figure 7.11 shows the comparison of the numerical and analytical solutions. Agreement between the two solutions is excellent. Also, even smaller grids are needed for this case for the numerical solution because of highly nonlinear adsorption at lower concentration. Mesh spacing of)z= 0.01 cm was used in the numerical simulation.

7.2.3   Comparison with 0 = 1.5

For the 0 = 1.5 case, the solute plume should have a different shape than with 0 < 1, and a diffusive front and sharp tail should develop. This can be confirmed by a numerical solution. Figure 7.12 demonstrates good agreement in the plumes produced by both analytical and numerical solutions.

7.3   TESTING OF MONTE CARLO IMPLEMENTATION

The EPACMTP model was tested to examine the frequency distribution of randomly generated geochemical master variables. Since the distribution of natural organic matter in the unsaturated zone depends on the soil type, silt loam was selected as the soil type. Two thousand Monte Carlo iterations were conducted. The statistics for the sample parameters are reported in Table 7.7.
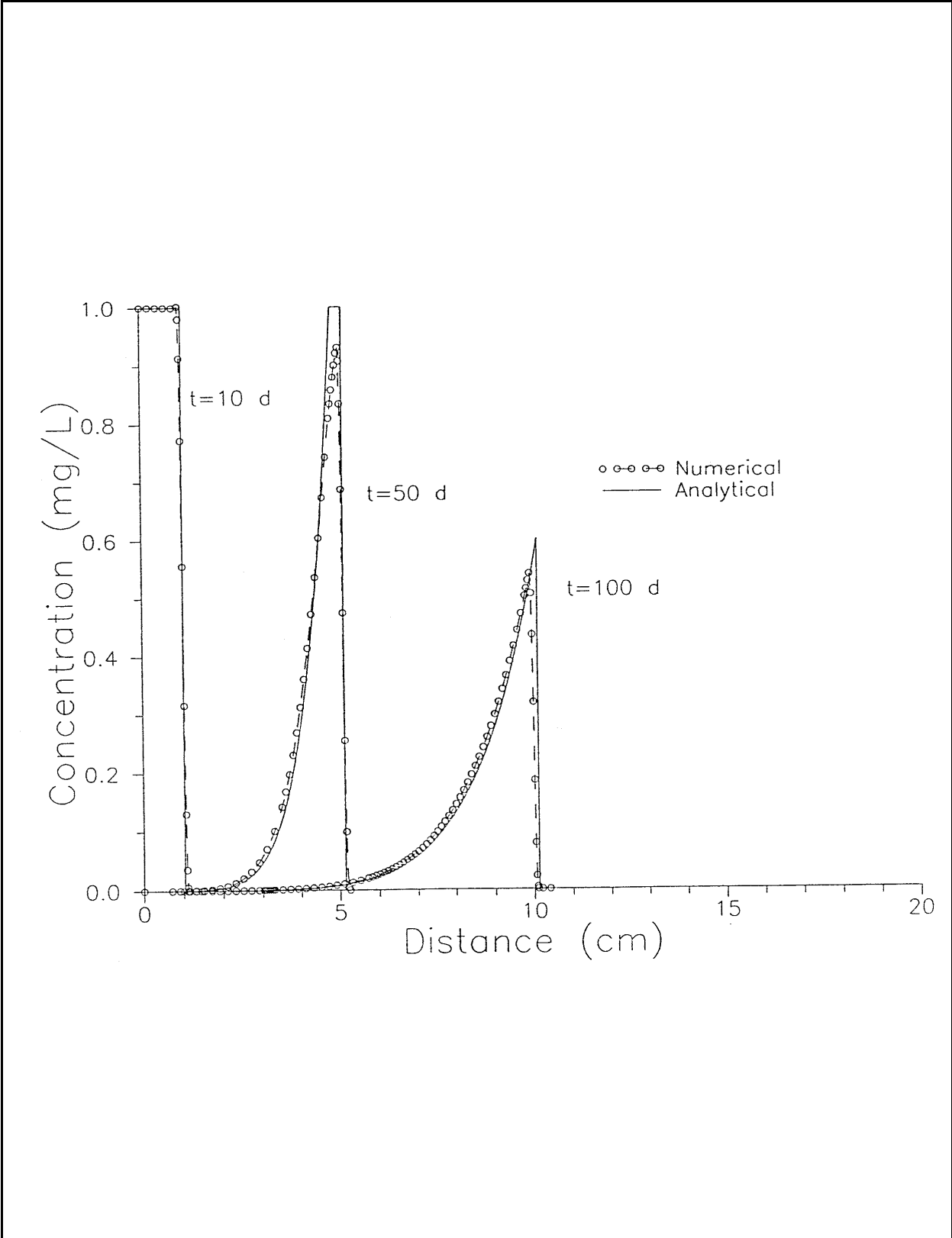
Figure 7.10   Comparison of concentration profiles for O= 0.8.
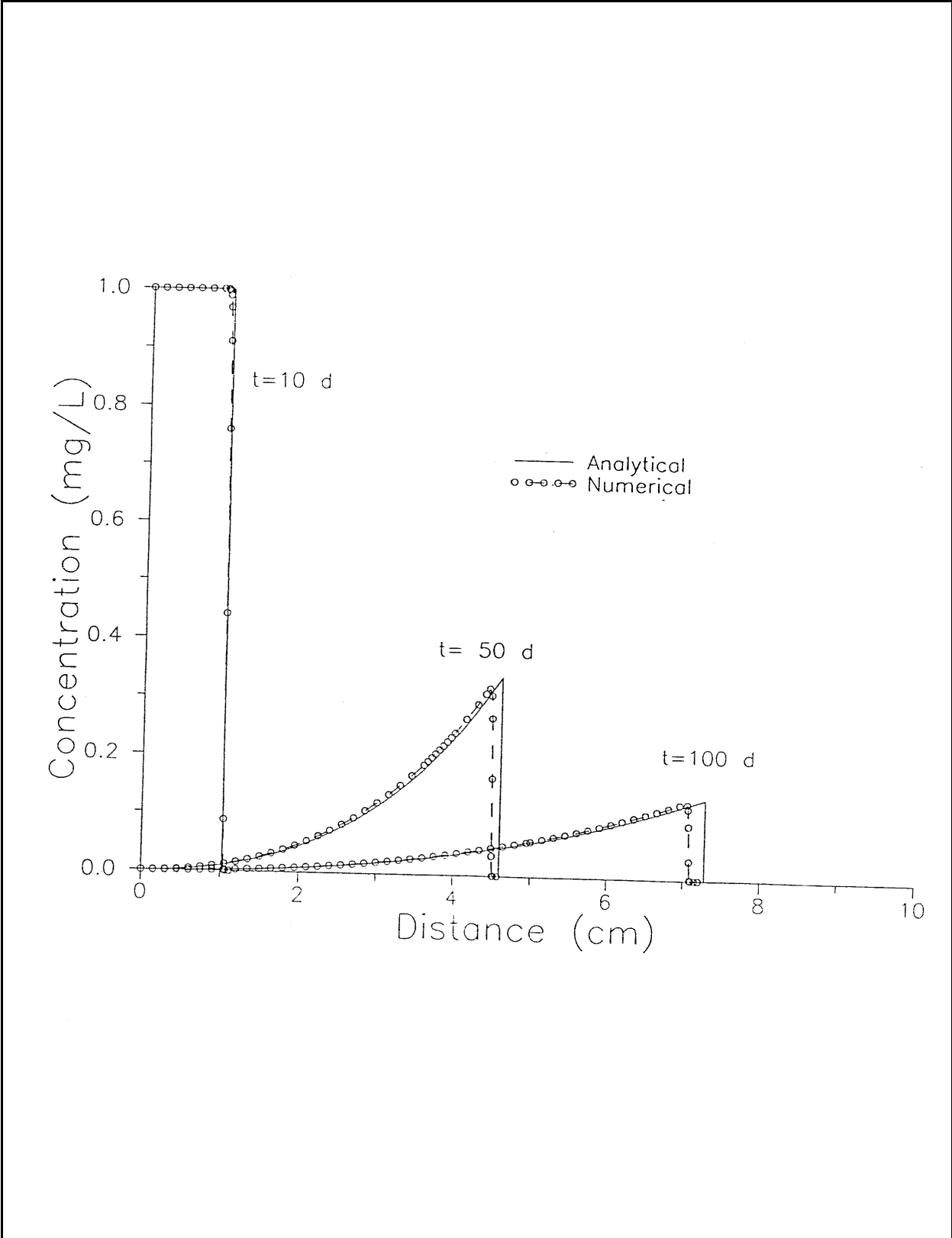
Figure 7.11   Comparison of concentration profiles for O= 0.5.
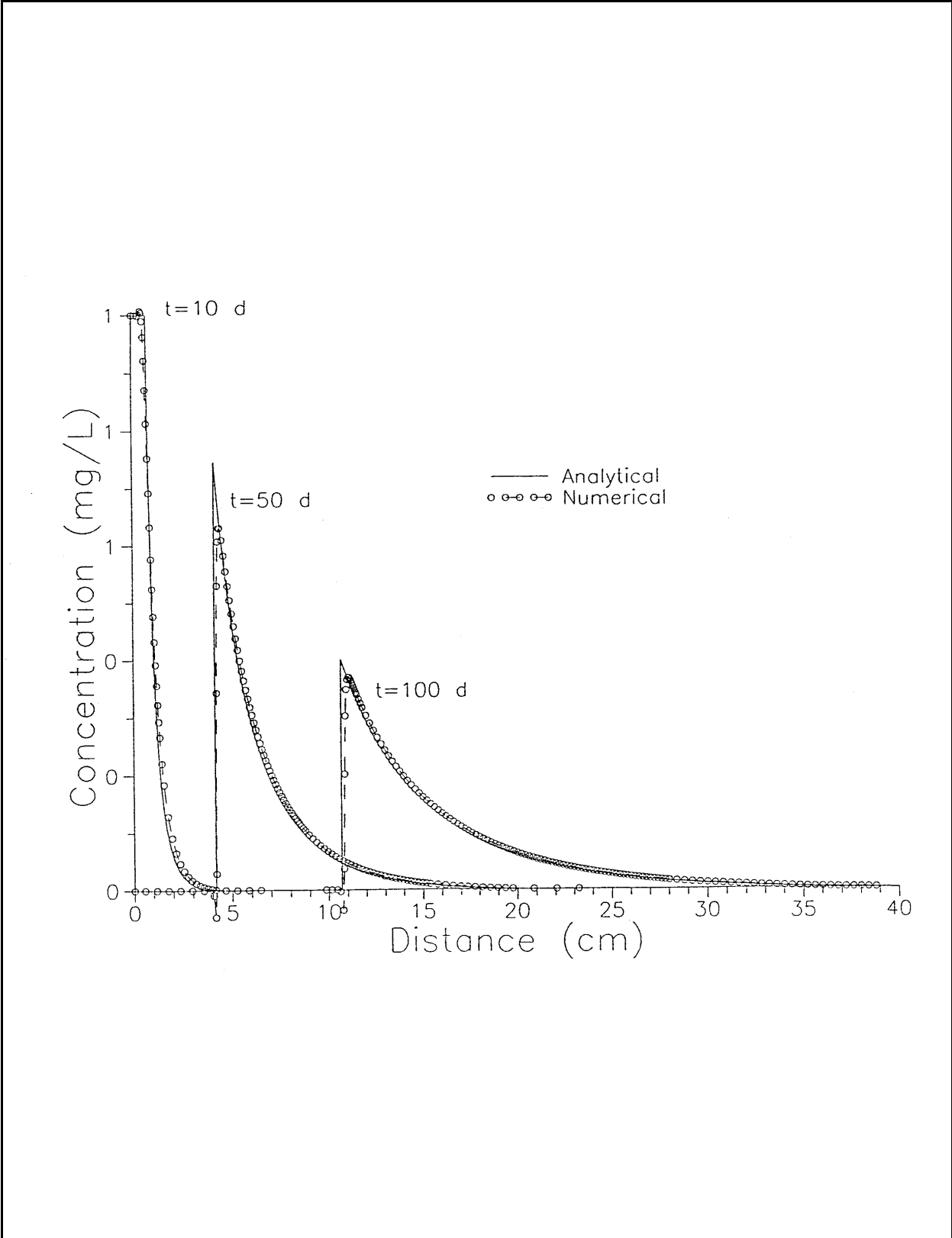
Figure 7.12   Comparison of concentration profiles for O= 1.5.

Table 7.7   Statistics for randomly generated first-type parameters (n= 2000).

	UNSATURATED ZONE				SATURATED ZONE	
	pH	**POM**	**HFO**	**LOA**	**POM**	**LOA**
Average	0.6633E+ 01	0.1436E+ 00	0.5692E+ 00	0.4924E-02	0.6200E-03	0.7035E-03
Std. dev	0.1151E+ 01	0.1374E+ 00	0.3193E+ 00	0.2198E-02	0.6128E-03	0.3140E-03
Minimum	0.3210E+ 01	0.8768E-02	0.1291E-01	0.1184E-02	0.1723E-04	0.1691E-03
Maximum	0.9597E+ 01	0.2072E+ 01	0.1110E+ 01	0.8778E-02	0.5806E-02	0.1254E-02
% Lows	22	31	13	16	33	16
% Meds	53	51	49	50	39	50
% Highs	25	18	37	34	27	34

REFERENCES

Allison, J.D., D.S. Brown, and K.H. Novo-Gradic, 1991. MINTEQA2/PRODEFA2, A Chemical Assessment Model for Environmental Systems: Version 4.0 User's Manual. EPA/600/3-91/021. U.S. Environmental Protection Agency, Athens, GA.

Allison, J.D., B.R. Bicknell, T.L. Allison, and K.J. Novo-Gradic, 1992. Development of the Finite Source Methodology for Wastes Containing Metals. Prepared for U.S. Environmental Protection Agency, Athens, GA.

CRC, 1970. Handbook of chemistry and physics, 51st edition. Chemical Rubber Company, Cleveland, OH 44128.

EPA, 1996a. EPA's Composite Model for Leachate Migration with Transformation Products and Background Document, U.S. Environmental Protection Agency, Office of Solid Waste, Washington, DC.

EPA, 1996b. Background document for EPACMTP: Finite Source Methodology for Degrading Chemicals with Transformation Products, U.S. Environmental Protection Agency, Office of Solid Waste, Washington, DC.

Helfferich, F., 1981, Theory of multicomponent, multiphase displacement in porous media, Soc. Pet. Eng. J., pp. 51-62.

Hildebrand, F.B., 1976, Advanced Calculus for Application, Second Edition, Prentice-Hall, Inc., Engelwood Cliffs, New Jersey.

Hirasaki, G.J., 1981, Application of the theory of multicomponent, multiphase displacement to three-component, two-phase surfactant flooding, Soc. Pet. Eng. J., pp. 191-204.

Kool, J.B. and M.Th. van Genuchten, 1991. HYDRUS, One-Dimensional Variably Saturated Flow and Transport Model, Including Hysteresis and Root Water Uptake, prepared for USDA-ARS Salinity Lab, Riverside, CA.

Loux, N.T., C.R. Chafin, and S.M Hassan, 1990. Statistics of Aquifer Material Properties and Empirical pH-dependent Partitioning Relationships for As(III), As(V), BA(II), Cd(II), Cr(VI), Cu(II), Hg(II), Ni(II), Pb(II), Sb(V), Se(IV), Tl(I), and Zn(II). U.S. Environmental Protection Agency, Athens, GA.

Tetra Tech, 1993. Review, Evaluation, and Verification of EPAMMM—Metals Model, Prepared for U.S. EPA Environmental Research Laboratory, Athens, GA.

van Der Zee, S.E.A.T.M., 1990. Analytical Traveling Wave Solutions for Transport with Non-linear and nonequilibrium adsorption. Water Resource Research, 26(10):2563-2578.

Yeh, G.T. and V.S. Tripathi, 1989. A Critical Evaluation of Recent Developments in Hydrogeochemical Transport Models of Reactive Multichemical Components. Water Resources Res. 25: 93-108.

APPENDIX A

HYDROUS FERRIC OXIDE AND PARTICULATE ORGANIC MATTER ADSORPTION

REACTIONS USED IN THE MINTEQA2 MODEL

The following compilation gives all adsorption reactions pertinent to the hydrous ferric oxide (HFO) and particulate organic matter (POM) surfaces used in the MINTEQA2 model runs. Reactions for the trace metals and other species that are competitively adsorbed are included.

HYDROUS FERRIC OXIDE ADSORPTION

As indicated in the description of MINTEQA2 modeling in Section 3.1.3, the HFO surface was treated as having two types of adsorbing sites. In distinguishing the two sites, site type 1 is regarded as a lower population density, higher affinity site. The MINTEQA2 component identifying number for this site is 811. Site type 2 is regarded as a higher population density, lower affinity site relative to site 1. The component identifying number for site 2 is 812. The relative population densities of the two sites are reflected in the site concentrations entered for these two components. The relative affinities of the two sites for a particular sorbate are reflected in the log K values associated with the adsorption reactions as shown below. For example, the high affinity site (site 1) has a log K of 0.97 for zinc. (See reaction 8119500 below.) The log K for this reaction is a composite constant for the deprotonation of the neutral site (S1OH) and adsorption of Zn^{2+}. The same adsorption reaction occurring at site 2 (see reaction 8129500) has an algebraically smaller log K of -1.99. For some sorbates, there is no difference in affinity for the two sites (e.g., protonation and deprotonation and all anions).

The source of all HFO adsorption reactions used in the MINTEQA2 modeling is a unified HFO database compiled by Dzombak (1986). In the paragraphs below, each reaction is shown in the format required for MINTEQA2. In some cases, the MINTEQA2 formatted reaction differs from the Dzombak reaction. This occurs when the reaction as given by Dzombak is not expressed in terms of MINTEQA2 components. For example, the Dzombak reaction for the adsorption of Hg^{2+} onto site 1 (S1OH) has this form:

$$S1OH^o \ + \ Hg^{2+} \ + \ H_2O \ \text{W} \ S1OHgOH_2^+ \ + \ H^+ \qquad \log K \ = \ 7.76$$

This reaction cannot be entered directly into MINTEQA2 because it is not written in terms of MINTEQA2 components. The component for Hg^{2+} in MINTEQA2 is $Hg(OH)_2^o$. The Dzombak reaction must be reformulated in terms of $Hg(OH)_2^o$ in order to be used in MINTEQA2. This is accomplished by adding the following reaction:

$$Hg(OH)_2^o \ + \ 2H^+ \ \text{W} \ Hg^{2+} \ + \ 2H_2O \qquad \log K \ = \ 6.10$$

The reformulated reaction is the sum of the above reactions; its log K value is likewise the sum of the log K values of the above reactions. As each MINTEQA2 reaction can have one and only one product, all species on the right side except the species to be added ($S1OHgOH_2^+$) are moved to the left side and given negative stoichiometry:

$$S1OH^o \ + \ Hg(OH)_2^o \ - \ H_2O \ + \ H^+ \ \text{W} \ S1OHgOH_2^+ \qquad \log K \ = \ 13.86$$
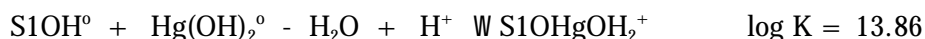
The MINTEQA2 reaction as entered in the input file must have an additional component to represent the electrostatic term in the Diffuse-Layer adsorption model. The electrostatic term is artificially treated as a MINTEQA2 reaction component with identifying number 813 and is assigned a stoichiometry equal to the change in charge of the surface site due to adsorption. For the above example, the change in charge at the surface site due to adsorption is + 1.0. Thus, the stoichiometry of component 813 is 1.0 as the reaction is entered in the MINTEQA2 input file. If the change in charge at the site due to adsorption is equal to zero, the 813 component is omitted.

In the paragraphs below, each reformulated MINTEQA2 reaction is shown in the format of a chemical reaction, and as required for entry in the MINTEQA2 input file. In most cases, the input file entry is already included in the file FEO-DLM. DBS distributed with MINTEQA2. This file containing the entries for the adsorption reactions must be appended to the MINTEQA2 input file if HFO adsorption is to be included in the calculations. The pre-processor PRODEFA2 was used to append FEO-DLM.DBS to the input files and to add adsorption reactions not currently included in FEO-DLM.DBS.

Protonation
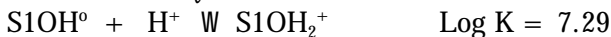
   Site 1- MINTEQA2 reaction:
   $S1OH^o + H^+ \ W \ S1OH_2^+$ Log K = 7.29
   Site 1- MINTEQA2 input file entry:
   8113302 = S1OH2+   0.0000   7.2900   0.000   0.000 1.00 0.00 0.00   0.0000
    0.00 3   1.000 811   1.000 330   1.000 813   0.000   0   0.000   0   0.000   0
     0.000   0   0.000   0   0.000   0   0.000   0   0.000   0   0.000   0
    0 0.000   0   0.000   0   0.000   0
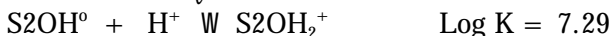
   Site 2- MINTEQA2 reaction:
   $S2OH^o + H^+ \ W \ S2OH_2^+$ Log K = 7.29
   Site 2- MINTEQA2 input file entry:
   8123302 = S2OH2+   0.0000   7.2900   0.000   0.000 1.00 0.00 0.00   0.0000
    0.00 3   1.000 812   1.000 330   1.000 813   0.000   0   0.000   0   0.000   0
     0.000   0   0.000   0   0.000   0   0.000   0   0.000   0   0.000   0
    0 0.000   0   0.000   0   0.000   0

Deprotonation

   Site 1- MINTEQA2 reaction:
   $S1OH^o - H^+ \ W \ S1O^-$ Log K = -8.93
   Site 1- MINTEQA2 input file entry:
   8113301 = S1O-   0.0000   -8.9300   0.000   0.000-1.00 0.00 0.00   0.0000
    0.00 3   1.000 811 -1.000 330 -1.000 813   0.000   0   0.000   0   0.000   0
     0.000   0   0.000   0   0.000   0   0.000   0   0.000   0   0.000   0
    0 0.000   0   0.000   0   0.000   0

   Site 2- MINTEQA2 reaction:
   $S2OH^o - H^+ \ W \ S2O^-$ Log K = -8.93
   Site 2- MINTEQA2 input file entry:
   8123301 = S2O-   0.0000   -8.9300   0.000   0.000-1.00 0.00 0.00   0.0000
    0.00 3   1.000 812 -1.000 330 -1.000 813   0.000   0   0.000   0   0.000   0
     0.000   0   0.000   0   0.000   0   0.000   0   0.000   0   0.000   0
    0 0.000   0   0.000   0   0.000   0

Silver(I) adsorption

   Site 1- MINTEQA2 reaction:

A-2

S1OH° + Ag⁺ + H₂O - H⁺ W S1OAgOH₂   Log K = -1.72

$S1OH^o + Ag^+ + H_2O - H^+ \; W \; S1OAgOH_2$ Log K = -1.72

Site 1- MINTEQA2 input file entry:
8110200 = S1OAgOH2   0.0000 -1.7200 0.000 0.000 0.00 0.00 0.00 0.0000
 0.00 4 1.000 811 -1.000 330 1.000 20 1.000 2 0.000 0 0.000 0
  0.000 0 0.000 0 0.000 0 0.000 0 0.000 0 0.000 0
0 0.000 0 0.000 0 0.000 0

Site 2- MINTEQA2 reaction:
$S2OH^o + Ag^+ + H_2O - H^+ \; W \; S2OAgOH_2$ Log K = -5.3
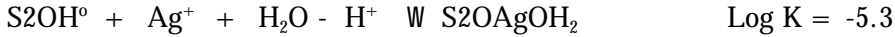
Site 2- MINTEQA2 input file entry:
8120200 = S2OAgOH2   0.0000 -5.3000 0.000 0.000 0.00 0.00 0.00 0.0000
 0.00 4 1.000 812 -1.000 330 1.000 20 1.000 2 0.000 0 0.000 0
  0.000 0 0.000 0 0.000 0 0.000 0 0.000 0 0.000 0
0 0.000 0 0.000 0 0.000 0

Mercury (II) adsorption

Site 1- MINTEQA2 reaction:
$S1OH^o + Hg(OH)_2^o - H_2O + H^+ \; W \; S1OHgOH_2^+$ log K = 13.86

Site 1- MINTEQA2 input file entry:
8113610 = S1OHgOH2+   0.0000 13.8600 0.000 0.000 1.00 0.00 0.00 0.0000
 0.00 5 1.000 811 1.000 361 -1.000 2 1.000 330 1.000 813 0.000 0
  0.000 0 0.000 0 0.000 0 0.000 0 0.000 0 0.000 0
0 0.000 0 0.000 0 0.000 0

Site 2- MINTEQA2 reaction:
$S2OH^o + Hg(OH)_2^o - H_2O + H^+ \; W \; S2OHgOH_2^+$ log K = 12.55

Site 2- MINTEQA2 input file entry:
8123610 = S2OHgOH2+   0.0000 12.5500 0.000 0.000 1.00 0.00 0.00 0.0000
 0.00 5 1.000 812 1.000 361 -1.000 2 1.000 330 1.000 813 0.000 0
  0.000 0 0.000 0 0.000 0 0.000 0 0.000 0 0.000 0
0 0.000 0 0.000 0 0.000 0

Chromium(III) adsorption

Site 1- MINTEQA2 reaction:
$S1OH^o + Cr(OH)_2^+ - H_2O \; W \; S1OCrOH^+$ log K = 11.56

Site 1- MINTEQA2 input file entry:
8112110 = S1OCrOH+   0.0000 11.5600 0.000 0.000 1.00 0.00 0.00 0.0000
 0.00 4 1.000 811 1.000 211 1.000 813 -1.000 2 0.000 0 0.000 0
  0.000 0 0.000 0 0.000 0 0.000 0 0.000 0 0.000 0
0 0.000 0 0.000 0 0.000 0

Zinc(II) adsorption

Site 1- MINTEQA2 reaction:
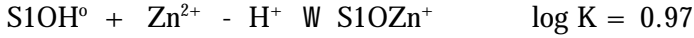
S1OH^o + Zn^{2+} - H$^+$ W S1OZn$^+$ log K = 0.97
Site 1- MINTEQA2 input file entry:
8119500 = S1OZn+   0.0000   0.9700   0.000   0.000 1.00 0.00 0.00   0.0000
 0.00 4   1.000 811 -1.000 330   1.000 813   1.000 950   0.000   0   0.000   0
  0.000   0   0.000   0   0.000   0   0.000   0   0.000   0   0.000   0
0 0.000   0   0.000   0   0.000   0

Site 2- MINTEQA2 reaction:
S2OH^o + Zn^{2+} - H$^+$ W S2OZn$^+$ log K = -1.99
Site 2- MINTEQA2 input file entry:
8129500 = S2OZn+   0.0000 -1.9900   0.000   0.000 1.00 0.00 0.00   0.0000
 0.00 4   1.000 812 -1.000 330   1.000 813   1.000 950   0.000   0   0.000   0
  0.000   0   0.000   0   0.000   0   0.000   0   0.000   0   0.000   0
0 0.000   0   0.000   0   0.000   0

Cadmium(II) adsorption

Site 1- MINTEQA2 reaction:
S1OH^o + Cd^{2+} - H$^+$ W S1OCd$^+$ log K = 0.43
Site 1- MINTEQA2 input file entry:
8111600 = S1OCd+   0.0000   0.4300   0.000   0.000 1.00 0.00 0.00   0.0000
 0.00 4   1.000 811 -1.000 330   1.000 813   1.000 160   0.000   0   0.000   0
  0.000   0   0.000   0   0.000   0   0.000   0   0.000   0   0.000   0
0 0.000   0   0.000   0   0.000   0

Site 2- MINTEQA2 reaction:
S2OH^o + Cd^{2+} - H$^+$ W S2OCd$^+$ log K = -2.90
Site 2- MINTEQA2 input file entry:
8121600 = S2OCd+   0.0000 -2.9000   0.000   0.000 1.00 0.00 0.00   0.0000
 0.00 4   1.000 812 -1.000 330   1.000 813   1.000 160   0.000   0   0.000   0
  0.000   0   0.000   0   0.000   0   0.000   0   0.000   0   0.000   0
0 0.000   0   0.000   0   0.000   0

Copper(II) adsorption

Site 1- MINTEQA2 reaction:
S1OH^o + Cu^{2+} - H$^+$ W S1OCu$^+$ log K = 2.85
Site 1- MINTEQA2 input file entry:
8112310 = S1OCu+   0.0000   2.8500   0.000   0.000 1.00 0.00 0.00   0.0000
 0.00 4   1.000 811 -1.000 330   1.000 813   1.000 231   0.000   0   0.000   0
  0.000   0   0.000   0   0.000   0   0.000   0   0.000   0   0.000   0
0 0.000   0   0.000   0   0.000   0

Site 2- MINTEQA2 reaction:
S2OH^o + Cu^{2+} - H$^+$ W S2OCu$^+$ log K = 0.60
Site 2- MINTEQA2 input file entry:
8122310 = S2OCu+   0.0000   0.6000   0.000   0.000 1.00 0.00 0.00   0.0000

```
0.00 4   1.000 812  -1.000 330   1.000 813   1.000 231   0.000   0   0.000   0
  0.000   0   0.000   0   0.000   0   0.000   0   0.000   0   0.000   0
 0 0.000   0   0.000   0   0.000   0
```

Nickel(II) adsorption

Site 1- MINTEQA2 reaction:
S1OH° + Ni²⁺ - H⁺ W S1ONi⁺   log K = 0.15
Site 1- MINTEQA2 input file entry:
```
8115400 = S1ONi+        0.0000   0.1500   0.000   0.000 1.00 0.00 0.00   0.0000
 0.00 4   1.000 811  -1.000 330   1.000 813   1.000 540   0.000   0   0.000   0
  0.000   0   0.000   0   0.000   0   0.000   0   0.000   0   0.000   0
 0 0.000   0   0.000   0   0.000   0
```
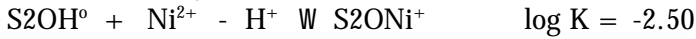
Site 2- MINTEQA2 reaction:
S2OH° + Ni²⁺ - H⁺ W S2ONi⁺   log K = -2.50
Site 2- MINTEQA2 input file entry:
```
8125400 = S2ONi+        0.0000   -2.5000   0.000   0.000 1.00 0.00 0.00   0.0000
 0.00 4   1.000 812  -1.000 330   1.000 813   1.000 540   0.000   0   0.000   0
  0.000   0   0.000   0   0.000   0   0.000   0   0.000   0   0.000   0
 0 0.000   0   0.000   0   0.000   0
```

Lead(II) adsorption
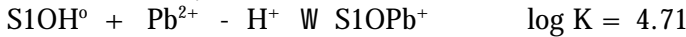
Site 1- MINTEQA2 reaction:
S1OH° + Pb²⁺ - H⁺ W S1OPb⁺   log K = 4.71
Site 1- MINTEQA2 input file entry:
```
8116000 = S1OPb+        0.0000   4.7100   0.000   0.000 1.00 0.00 0.00   0.0000
 0.00 4   1.000 811  -1.000 330   1.000 813   1.000 600   0.000   0   0.000   0
  0.000   0   0.000   0   0.000   0   0.000   0   0.000   0   0.000   0
 0 0.000   0   0.000   0   0.000   0
```
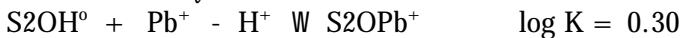
Site 2- MINTEQA2 reaction:
S2OH° + Pb⁺ - H⁺ W S2OPb⁺   log K = 0.30
Site 2- MINTEQA2 input file entry:
```
8126000 = S2OPb+        0.0000   0.3000   0.000   0.000 1.00 0.00 0.00   0.0000
 0.00 4   1.000 812  -1.000 330   1.000 813   1.000 600   0.000   0   0.000   0
  0.000   0   0.000   0   0.000   0   0.000   0   0.000   0   0.000   0
 0 0.000   0   0.000   0   0.000   0
```

Calcium adsorption

Site 1- MINTEQA2 reaction:
S1OH° + Ca²⁺ W S1OHCa⁺⁺   log K = 4.97
Site 1- MINTEQA2 input file entry:
```
8111500 = S1OHCa+ +     0.0000   4.9700   0.000   0.000 2.00 0.00 0.00   0.0000
 0.00 3   1.000 811   1.000 150   2.000 813   0.000   0   0.000   0   0.000   0
```

```
   0.000  0  0.000  0  0.000  0  0.000  0  0.000  0  0.000  0
  0 0.000  0  0.000  0  0.000  0
```
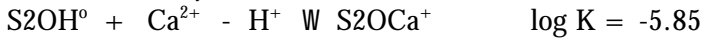
Site 2- MINTEQA2 reaction:
S2OH^o + Ca^{2+} - H$^+$ W S2OCa$^+$ log K = -5.85
Site 2- MINTEQA2 input file entry:
```
8121500 = S2OCa+        0.0000  -5.8500  0.000   0.000 1.00 0.00 0.00  0.0000
 0.00 4  1.000 812  -1.000 330  1.000 813  1.000 150  0.000  0  0.000  0
  0.000  0  0.000  0  0.000  0  0.000  0  0.000  0  0.000  0
 0 0.000  0  0.000  0  0.000  0
```

Barium adsorption

Site 1- MINTEQA2 reaction:
S1OH^o + Ba^{2+} W S1OHBa^{++} log K = 5.46
Site 1- MINTEQA2 input file entry:
```
8111000 = S1OHBa+ +       0.0000    5.4600   0.000   0.000 2.00 0.00 0.00   0.0000
 0.00 3  1.000 811  1.000 100  2.000 813  0.000  0  0.000  0  0.000  0
  0.000  0  0.000  0  0.000  0  0.000  0  0.000  0  0.000  0
 0 0.000  0  0.000  0  0.000  0
```
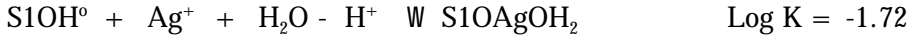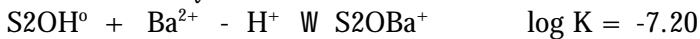
Site 2- MINTEQA2 reaction:
S2OH^o + Ba^{2+} - H$^+$ W S2OBa$^+$ log K = -7.20
Site 2- MINTEQA2 input file entry:
```
8121000 = S2OBa+        0.0000  -7.2000   0.000   0.000 1.00 0.00 0.00   0.0000
 0.00 4  1.000 812  -1.000 330  1.000 813  1.000 100  0.000  0  0.000  0
  0.000  0  0.000  0  0.000  0  0.000  0  0.000  0  0.000  0
 0 0.000  0  0.000  0  0.000  0
```

Sulfate adsorption
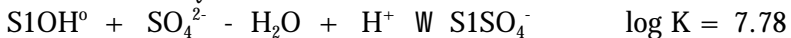
Site 1- MINTEQA2 reaction:
S1OH^o + SO$_4^{2-}$ - H$_2$O + H$^+$ W S1SO$_4^-$ log K = 7.78
Site 1- MINTEQA2 input file entry:
```
8117320 = S1SO4-        0.0000    7.7800   0.000   0.000-1.00 0.00 0.00   0.0000
 0.00 5  1.000 811  1.000 330  -1.000 813  1.000 732  -1.000  2  0.000  0
  0.000  0  0.000  0  0.000  0  0.000  0  0.000  0  0.000  0
 0 0.000  0  0.000  0  0.000  0
```
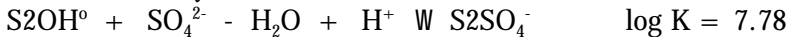
Site 2- MINTEQA2 reaction:
S2OH^o + SO$_4^{2-}$ - H$_2$O + H$^+$ W S2SO$_4^-$ log K = 7.78
Site 2- MINTEQA2 input file entry:
```
8127320 = S2SO4-        0.0000    7.7800   0.000   0.000-1.00 0.00 0.00   0.0000
 0.00 5  1.000 812  1.000 330  -1.000 813  1.000 732  -1.000  2  0.000  0
  0.000  0  0.000  0  0.000  0  0.000  0  0.000  0  0.000  0
 0 0.000  0  0.000  0  0.000  0
```

Site 1- MINTEQA2 reaction:

$S1OH^o + SO_4^{2-}$ W $S1OHSO_4^{2-}$ log K = 0.79

Site 1- MINTEQA2 input file entry:

8117321 = S1OHSO4-2   0.0000   0.7900   0.000   0.000-2.00 0.00 0.00   0.0000
 0.00 3   1.000 811 -2.000 813   1.000 732   0.000   0   0.000   0   0.000   0
  0.000   0   0.000   0   0.000   0   0.000   0   0.000   0   0.000   0
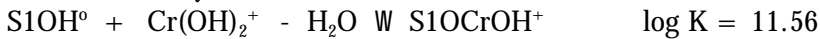0 0.000   0   0.000   0   0.000   0

Site 2- MINTEQA2 reaction:

$S2OH^o + SO_4^{2-}$ W $S2OHSO_4^{2-}$ log K = 0.79

Site 2- MINTEQA2 input file entry:

8127321 = S2OHSO4-2   0.0000   0.7900   0.000   0.000-2.00 0.00 0.00   0.0000
 0.00 3   1.000 812 -2.000 813   1.000 732   0.000   0   0.000   0   0.000   0
  0.000   0   0.000   0   0.000   0   0.000   0   0.000   0   0.000   0
0 0.000   0   0.000   0   0.000   0

Phosphate adsorption

Site 1- MINTEQA2 reaction:

$S1OH^o + PO_4^{3-} - H_2O + 3H^+$ W $S1H_2PO_4$ log K = 31.29
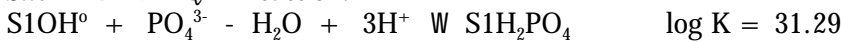
Site 1- MINTEQA2 input file entry:

8115800 = S1H2PO4   0.0000   31.2900   0.000   0.000 0.00 0.00 0.00   0.0000
 0.00 4   1.000 811   1.000 580   3.000 330 -1.000   2   0.000   0   0.000   0
  0.000   0   0.000   0   0.000   0   0.000   0   0.000   0   0.000   0
0 0.000   0   0.000   0   0.000   0

Site 2- MINTEQA2 reaction:

$S2OH^o + PO_4^{3-} - H_2O + 3H^+$ W $S2H_2PO_4$ log K = 31.29
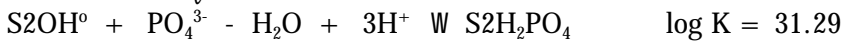
Site 2- MINTEQA2 input file entry:

8125800 = S2H2PO4   0.0000   31.2900   0.000   0.000 0.00 0.00 0.00   0.0000
 0.00 4   1.000 812   1.000 580   3.000 330 -1.000   2   0.000   0   0.000   0
  0.000   0   0.000   0   0.000   0   0.000   0   0.000   0   0.000   0
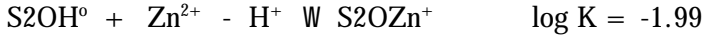0 0.000   0   0.000   0   0.000   0

Site 1- MINTEQA2 reaction:

$S1OH^o + PO_4^{3-} - H_2O + 2H^+$ W $S1HPO_4^-$ log K = 25.39
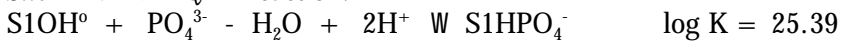
Site 1- MINTEQA2 input file entry:

8115801 = S1HPO4-   0.0000   25.3900   0.000   0.000-1.00 0.00 0.00   0.0000
 0.00 5   1.000 811 -1.000 813   1.000 580   2.000 330 -1.000   2   0.000   0
  0.000   0   0.000   0   0.000   0   0.000   0   0.000   0   0.000   0
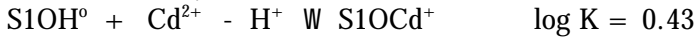0 0.000   0   0.000   0   0.000   0

Site 2- MINTEQA2 reaction:

$S2OH^o + PO_4^{3-} - H_2O + 2H^+$ W $S2HPO_4^-$ log K = 25.39
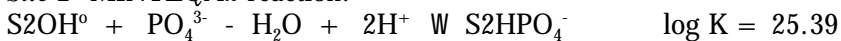
Site 2- MINTEQA2 input file entry:

8125801 = S2HPO4-   0.0000   25.3900   0.000   0.000-1.00 0.00 0.00   0.0000
 0.00 5   1.000 812 -1.000 813   1.000 580   2.000 330 -1.000   2   0.000   0

0.000 0 0.000 0 0.000 0 0.000 0 0.000 0 0.000 0
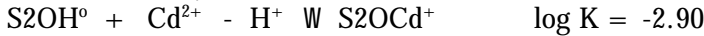   0 0.000 0 0.000 0 0.000 0
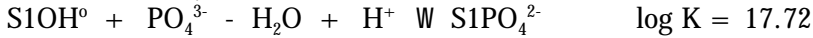
   Site 1- MINTEQA2 reaction:
   $S1OH^o + PO_4^{3-} - H_2O + H^+ \ \text{W} \ S1PO_4^{2-}$ log K = 17.72
   Site 1- MINTEQA2 input file entry:
   8115802 = S1PO4-2   0.0000 17.7200 0.000 0.000-2.00 0.00 0.00 0.0000
    0.00 5 1.000 811 1.000 580 1.000 330 -2.000 813 -1.000 2 0.000 0
     0.000 0 0.000 0 0.000 0 0.000 0 0.000 0 0.000 0
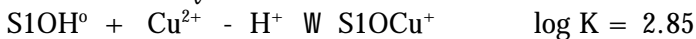   0 0.000 0 0.000 0 0.000 0
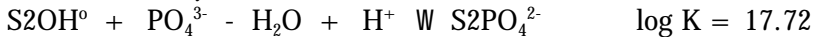
   Site 2- MINTEQA2 reaction:
   $S2OH^o + PO_4^{3-} - H_2O + H^+ \ \text{W} \ S2PO_4^{2-}$ log K = 17.72
   Site 2- MINTEQA2 input file entry:
   8125802 = S2PO4-2   0.0000 17.7200 0.000 0.000-2.00 0.00 0.00 0.0000
    0.00 5 1.000 812 1.000 580 1.000 330 -2.000 813 -1.000 2 0.000 0
     0.000 0 0.000 0 0.000 0 0.000 0 0.000 0 0.000 0
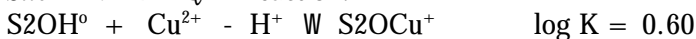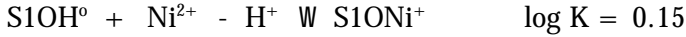   0 0.000 0 0.000 0 0.000 0

Vanadium (V) adsorption

   Site 2- MINTEQA2 reaction:
   $S2OH^o + VO_2^+ + 2H_2O - 4H^+ \ \text{W} \ S2OHVO_4^{3-}$ log K = -16.53
   Site 2- MINTEQA2 input file entry:
   8129030 = SOHVO4-3   0.0000 -16.5300 0.000 0.000-3.00 0.00 0.00 0.0000
    0.00 5 1.000 812 1.000 903 2.000 2 -4.000 330 -3.000 813 0.000 0
     0.000 0 0.000 0 0.000 0 0.000 0 0.000 0 0.000 0
    0 0.000 0 0.000 0 0.000 0


PARTICULATE ORGANIC MATTER ADSORPTION

As discussed in Section 3.1.3, the particulate organic matter (POM) surface was treated as undergoing the same reactions as dissolved organic matter (DOM). After converting weight percent POM to concentration of particulate organic carbon (POC) in mg liter^{-1}, a conversion factor of 1.2 μmol mg^{-1} organic matter was used to compute the molar site concentration (see section 3.1.3). POM was represented in the modeling by component number 146. This component, like component 145 (used for DOM), is specially designed to represent substances that are complex mixtures of functional groups (sub-ligands) as opposed to pure substances representable by a single ligand. MINTEQA2 has special routines that treat components 145 and 146 as behaving in accord with a Gaussian distribution of sub-ligand concentration versus binding affinity (Susetyo, et al., 1991; Allison and Perdue, 1994). The database of reactions for DOM is provided with the MINTEQA2 model in the database file COMPLIG.DBS. The database of reactions for POM, identical to the DOM database except for component and species identifying numbers, must be added by the user. POM reactions were added by editing COMPLIG.DBS and copying the reactions for DOM. The POM reactions were placed immediately after the DOM reactions and their component and species identifying numbers were changed to reflect component 146 rather than 145. The charge on the POM component and all POM-metal complexes was set to zero in the MINTEQA2 modeling.

In the paragraphs below, each POM adsorption reaction is shown in the format of a chemical reaction, and as required for entry in the MINTEQA2 input file. The mean log K (μ) of the Gaussian distribution of binding affinity is given for each reaction. The standard deviation in binding affinity is 1.7 log K units for all cations bound.

Protonation

    POM- MINTEQA2 reaction:
    POM + H$^+$ W H POM   μ = 3.87
    POM- MINTEQA2 input file entry:
    1463300 H POM   1.7000   3.8700 0.000 0.000 0.00 0.00 0.000000.0000
    0.00 2   1.000 146   1.000 330

Aluminum adsorption

    POM- MINTEQA2 reaction:
    POM + Al^{3+} W Al POM   μ = 5.2
    POM- MINTEQA2 input file entry:
    1460300 Al POM   1.7000   5.2000 0.000 0.000 0.00 0.00 0.000000.0000
    0.00 2   1.000 146   1.000 030

Barium adsorption

    POM- MINTEQA2 reaction:
    POM + Ba^{2+} W Ba POM   μ = 3.1
    POM- MINTEQA2 input file entry:
    1461000 Ba POM   1.7000   3.1000 0.000 0.000 0.00 0.00 0.000000.0000
    0.00 2   1.000 146   1.000 100

Calcium adsorption

    POM- MINTEQA2 reaction:
    POM + Ca^{2+} W Ca POM   μ = 2.9
    POM- MINTEQA2 input file entry:
    1461500 Ca POM   1.7000   2.9000 0.000 0.000 0.00 0.00 0.000000.0000
    0.00 2   1.000 146   1.000 150

Cadmium adsorption

    POM- MINTEQA2 reaction:
    POM + Cd^{2+} W Cd POM   μ = 3.3
    POM- MINTEQA2 input file entry:
    1461600 Cd POM   1.7000   3.3000 0.000 0.000 0.00 0.00 0.000000.0000
    0.00 2   1.000 146   1.000 160

Chromium(III) adsorption
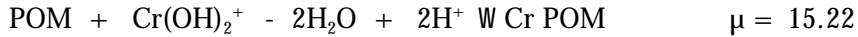
POM- MINTEQA2 reaction:
$POM + Cr(OH)_2^+ - 2H_2O + 2H^+ \ W \ Cr \ POM$ $\qquad \mu = 15.22$
POM- MINTEQA2 input file entry:
1462110 Cr POM   1.7000 15.2200 0.000 0.000 0.00 0.00 0.000000.0000
 0.00 4   1.000 146   1.000 211   2.000 330   -2.000 002

Copper(II) adsorption

POM- MINTEQA2 reaction:
$POM + Cu^{2+} \ W \ Cu \ POM$ $\qquad \mu = 4.9$
POM- MINTEQA2 input file entry:
1462310 Cu POM   1.7000   4.9000 0.000 0.000 0.00 0.00 0.000000.0000
 0.00 2   1.000 146   1.000 231

Iron(III) adsorption

POM- MINTEQA2 reaction:
$POM + Fe^{3+} \ W \ Fe \ POM$ $\qquad \mu = 7.7$
POM- MINTEQA2 input file entry:
1462810 Fe POM   1.7000   7.7000 0.000 0.000 0.00 0.00 0.000000.0000
 0.00 2   1.000 146   1.000 281

Magnesium adsorption

POM- MINTEQA2 reaction:
$POM + Mg^{2+} \ W \ Mg \ POM$ $\qquad \mu = 1.9$
POM- MINTEQA2 input file entry:
1464600 Mg POM   1.7000   1.9000 0.000 0.000 0.00 0.00 0.000000.0000
 0.00 2   1.000 146   1.000 460

Nickel adsorption

POM- MINTEQA2 reaction:
$POM + Ni^{2+} \ W \ Ni \ POM$ $\qquad \mu = 3.3$
POM- MINTEQA2 input file entry:
1465400 Ni POM   1.7000   3.3000 0.000 0.000 0.00 0.00 0.000000.0000
 0.00 2   1.000 146   1.000 540

Lead adsorption

POM- MINTEQA2 reaction:
$POM + Pb^{2+} \ W \ Pb \ POM$ $\qquad \mu = 5.2$

POM- MINTEQA2 input file entry:
1466000 Pb POM   1.7000   5.2000   0.000   0.000 0.00 0.00 0.000000.0000
 0.00 2   1.000 146   1.000 600

Zinc adsorption

POM- MINTEQA2 reaction:
POM + Zn^{2+} W Zn POM $\mu = 3.5$
POM- MINTEQA2 input file entry:
1469500 Zn POM   1.7000   3.5000   0.000   0.000 0.00 0.00 0.000000.0000
 0.00 2   1.000 146   1.000 950

REFERENCES

Allison, J.D. and E.M. Perdue. 1994. Modeling metal-humic interactions with MINTEQA2 *in:* Humic Substances in the Global Environment and Implications on Human Health, N. Senesi and T.M. Miano, *eds.,* Elsevier Science, B.V, pp. 927-942.

Susetyo, W., L.A. Carreira, L.V. Azarraga and D.M. Grimm. 1991. Fluorescence techniques for metal-humic interactions, Fresenius J Anal Chem, **339**, 624-635.

Dzombak, D.A. 1986. Toward a Uniform Model for the Sorption of Inorganic Ions on Hydrous Oxides. Ph.D Thesis. Massachusetts Institute of Technology, Cambridge, MA.

APPENDIX B

MINTEQA2 DATABASE UPDATE
for SELECTED REACTIONS
USING DATA from
NIST STANDARD REFERENCE DATABASE 46:
Critical Stability Constants of Metal Complexes,
Version 1.0

TABLE OF CONTENTS

SUMMARY

Thermodynamic parameters from the NIST Standard Reference Database 46: *Critical Stability Constants for Metal Complexes, Version 1.0* (NIST, 1993) were used in updating the thermodynamic database for the U.S. EPA geochemical speciation model MINTEQA2 v3.11 (Allison *et al.*, 1991). Eighty-three species given in the NIST database were not present in the MINTEQA2 database and have been added. In addition, the equilibrium constants (log K) and/or the standard enthalpies of reaction (ΔH^{o}_{r}) for 178 existing MINTEQA2 species were updated with NIST values. The thermodynamic constants for 21 other species were checked and found to agree with NIST values. All 282 species involved in this review and update of the MINTEQA2 database represent reaction products between the metals: Ag^{+}, Pb^{2+}, Cr^{3+}, Cd^{2+}, Ba^{2+}, Hg^{2+}, Ni^{2+}, Zn^{2+}, H^{+}, Al^{3+}, Fe^{3+}, Ca^{2+}, Mg^{2+}, Na^{+}, K^{+}, and Mn^{2+} and the ligands: OH^{-}, CO_3^{2-}, Br^{-}, Cl^{-}, NO_3^{-}, PO_4^{3-}, SO_4^{2-}, acetate, propanoate, and butanoate. Atomic and molecular weights given in the MINTEQA2 component database were updated with widely accepted standard values (IUPAC, 1984) so as to give a consistent basis for the calculation of molar masses of added and modified species.

Updated computer files (THERMO.DBS, TYPE6.DBS, COMP.DBS, THERMO.UNF, and TYPE6.UNF) were generated for use with MINTEQA2. Model runs were conducted to ensure that the modified files are properly read by the model and that model output reflects the new thermodynamic data.

This report was prepared by Allison Geoscience Consultants, Inc. for the U.S. EPA Office of Solid Waste, Contract Number 68-W4-0017, under sub-contract to HydroGeoLogic, Inc.

1.0 INTRODUCTION

MINTEQA2 is a geochemical speciation model available from the U.S. Environmental Protection Agency (EPA) that can be used to calculate the equilibrium composition of dilute aqueous solutions in the laboratory or in natural aqueous systems. The model is useful for calculating the equilibrium mass distribution between the dissolved, adsorbed, and multiple solid phases under a variety of conditions, including a gas phase with constant partial pressure. A database is included that is adequate for solving a broad range of problems without need for additional user-supplied equilibrium constants. However, the thermodynamic database for the EPA's latest version (v3.11) has not been reviewed and compared with critical compilations since the first release of the model in the mid 1980's. The purpose of this project was to update the thermodynamic constants for a specific set of metals and ligands using the National Institute of Standards Reference Database 46: *Critical Stability Constants for Metal Complexes, Version 1.0*. This database (referred to hereafter as the NIST database), is the electronic-media successor to the multi-volume standard reference work *Critical Stability Constants* (Smith and Martell, 1976).

The scope of the database update included the trace metals Ag^+, Pb^{2+}, Cr^{3+}, Cd^{2+}, Ba^{2+}, Hg^{2+}, Ni^{2+}, and Zn^{2+}. These metals are the subject of current speciation modeling studies being conducted on behalf of the EPA Office of Solid Waste. The MINTEQA2 modeling runs in which these metals are the primary focus have as their aim the estimation of the distribution coefficient for adsorption, K_d, in groundwater systems impacted by municipal landfill leachate. The groundwater systems of interest include major cations and anions and three leachate organic acids. Thus, the total set of competing cations and the set of ligands for which they compete were the subject of the database update. These include the eight trace metals previously mentioned and eight secondary metals: H^+, Al^{3+}, Fe^{3+}, Ca^{2+}, Mg^{2+}, Na^+, K^+, and Mn^{2+}. The NIST database was searched for reactions between these sixteen metals and the ten ligands: OH^-, CO_3^{2-}, Br^-, Cl^-, NO_3^-, PO_4^{3-}, SO_4^{2-}, acetate, propanoate, and butanoate. All retrieved data that met criteria for ionic strength and temperature (discussed below) were incorporated in MINTEQA2.

2.0 METHODOLOGY

The NIST database is accessed through a data retrieval program called CRITICAL. This program runs on an IBM compatible PC and is executed under DOS. CRITICAL can also be executed in a DOS window running under WINDOWS 3.1. The organizational approach used in the database and in CRITICAL is such that the user specifies keywords to identify the ligand of interest in response to a user prompt. For example, one may specify "carbonate" as a ligand search word. CRITICAL will respond by displaying successive screens of one ligand per screen whose names include the word "carbonate". The user moves forwards and backwards through these screens until the particular carbonate ligand of interest is found (for this study, hydrogen carbonate). The chemical formula and/or structure of the ligand is displayed on the computer screen along with a menu of database retrieval options. The "Display" option shows reactions between the selected ligand and the first metal listed in the database. From the screen that displays reactions with the first metal, the "Metals" option allows the user to search the database for reactions involving other specific metals with the selected ligand. Each reaction between a particular metal and the ligand is displayed on a separate screen. Each screen may have the log K and $)H^o_r$ (kcal mol^{-1}) reported at several different temperatures and ionic strengths. The mass law which defines the reaction to which the thermodynamic constants pertain is also displayed. Bibliographic information is available by selecting the appropriate menu option. The user transcribes the mass law defining the reaction and the corresponding thermodynamic constants and experimental conditions.

Accept/reject criteria for NIST data

MINTEQA2 database values are referenced to an ionic strength of zero (an ideal solution) at 25°C. Many experimentally determined constants reported in the NIST database were measured in solutions of higher ionic strength (> 1.0 M) or at a temperature other than 25°C. As explained in the data reduction section below, values reported at ionic strength greater than zero must be corrected to zero ionic strength. Activity coefficients estimated by the Davies equation become progressively less accurate as the ionic strength increases above 0.5 M. For this reason, the preferred log K is that reported at the lowest ionic strength. Log K values reported at ionic strength greater 0.7 M were not used in updating the database.

Thermodynamic constants reported at temperatures other than 25°C should be adjusted to 25°C prior to use in MINTEQA2. The most common method of adjustment employs the van't Hoff equation (detailed below) which requires the standard enthalpy of reaction, $)H^o_r$. As pointed out in Smith and Martell (1976), this relationship assumes constant heat capacity. The larger the temperature correction to be made, the greater the probability of significant error. Also, many compilations give equilibrium constants without specifying a value for $)H^o_r$. For both of these reasons, preference was given to constants determined at or near 25°C.

Correction to zero ionic strength

Log K values reported at ionic strength greater than zero must be corrected using estimates of activity coefficients for reactants and products. MINTEQA2 computes activity coefficients to recalculate the log K for any given ionic strength as it solves equilibrium problems. It is reasonable to use the same method to estimate the activity coefficients in this data correction step as is used in MINTEQA2 to adjust the constants during calculations. The most universally applicable estimator available in MINTEQA2 is the Davies equation. Equilibrium constants reported at ionic strengths between zero and 0.7 M were corrected using activity coefficients (() computed from the Davies equation:

$$\log (_i \quad ' \quad \&0.509 \, z_i^2 \; [\frac{\sqrt{\mu^)}}{1 \% \sqrt{\mu^)}} \quad \& \quad 0.24 \, mul^) \,]$$

where the subscript *i* refers to each of the reactants and products in the reaction, z_i is the ionic charge of each reactant or product, and μ' is the ionic strength reported for the experimental data. Once computed, the activity coefficients are used in the following relationship to correct the equilibrium constant to an ionic strength of zero:

$$K_{\mu' \, 0} \quad ' \quad K_{\mu^)} \; \frac{\mathbf{k}_i \; (_{i,products}}{\mathbf{k}_i \; (_{i,reactants}}$$

Correction to 25°C

The van't Hoff equation was used to correct those equilibrium constants reported at temperatures other than 25°C if a corresponding standard enthalpy of reaction value was available. For some reactions,

ΔH_r^o is simply not available and zero is entered for enthalpy in the MINTEQA2 database. In such cases, the reported equilibrium constant was incorporated without correction. MINTEQA2 also uses the van't Hoff equation to adjust equilibrium constants during speciation calculations for those reactions having non-zero enthalpy when the user specifies a system temperature other than 25°C. When ΔH_r^o is given in kcal mol^{-1}, the van't Hoff equation is:

$$\log K_{25} \;=\; \log K_T + \Delta H_r^o \,(25 - T_1)\,(0.00246)$$

where T is the temperature at which log K is reported in degrees Celsius.

Reformulation in terms of MINTEQA2 components

All reactions in MINTEQA2 must be written as formation reactions from the MINTEQA2 components. For solid species, the log K and ΔH_r^o given here may be of opposite sign to that reported in the literature (usually reported as a solubility product constant). Also, both solid and dissolved reactions and their associated thermodynamic constants have been added or subtracted from other reactions as required to reformulate the reaction in terms of MINTEQA2 components. An example is the species $CaOH^+$, given in the NIST database by the reaction:

$$Ca^{2+} + OH^- \rightarrow CaOH^+ \qquad\qquad \log K = 1.3; \; \Delta H_r^o = 2.0$$

As written, this reaction cannot be used in MINTEQA2. To reformulate the reaction for MINTEQA2, the existing MINTEQA2 reaction for the formation of OH^- from the MINTEQA2 components H_2O and H^+ must be added to this reaction:

$$Ca^{2+} + OH^- \rightarrow CaOH^+ \qquad \log K = \quad 1.3 \quad \Delta H_r^o = \quad 2.0$$
$$+ H_2O - H^+ \rightarrow OH^- \qquad \log K = -13.997 \qquad \Delta H_r^o = 13.34$$

$$Ca^{2+} + H_2O - H^+ \rightarrow CaOH^+ \quad \log K = -12.6 \quad \Delta H_r^o = 15.3$$
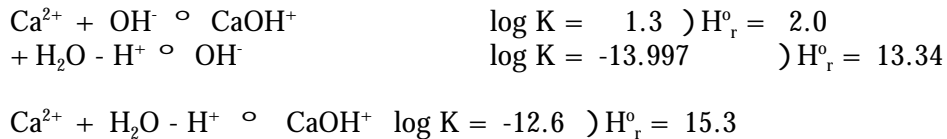
The last reaction and its associated thermodynamic constants are now expressed in terms of MINTEQA2 components and are ready to be entered in the MINTEQA2 database. Note that reactions used to reformulate other reactions (i.e., reactions such as the OH^- reaction in this example) were themselves updated with NIST data prior to use in reformulation. Note also that standard rules of significant figures were used in determining how many decimal places to retain in the result of reformulation operations. Similar manipulations were performed for other species as required to reduce the reactions and their thermodynamic constants to MINTEQA2 basis components.

3.0 RESULTS OF NIST DATABASE SEARCH

The table below lists all species added, changed, or checked during this review. For each species, the table shows the seven digit MINTEQA2 ID number, the MINTEQA2 name, the MINTEQA2 v3.11 ΔH^o_r (if applicable), the corresponding NIST ΔH^o_r reduced for use in MINTEQA2, the v3.11 log K value, the corresponding NIST log K value reduced for use in MINTEQA2, and the status of the entry: A = added, C = corrected, U = checked but not changed.

Table 3.1

MINTEQ ID No.	Name	MINTEQ ΔH^o_r	NIST ΔH^o_r	MINTEQ Log K	NIST Log K	STATUS
DISSOLVED SPECIES						
3300020	OH-	13.3450	13.34	-13.9980	-13.997	C
3301400	HCO3 -	-3.6170	-3.50	10.3300	10.329	C
3301401	H2CO3*	-2.2470	-5.69	16.6810	16.681	C
3301403	CO2(g)	-0.5300	-0.97	18.1600	18.147	C
3305800	HPO4 -2	-3.5300	-3.8	12.3460	12.375	C
3305801	H2PO4 -	-4.5200	-4.7	19.5530	19.573	C
3305802	H3PO4	0.0000	-2.8	21.7000	21.721	C
3307320	HSO4 -	4.9100	5.4	1.9870	1.99	C
3309921	H Acetate	0.0000	0.10	4.7600	4.757	C
3309711	H Propanoate	0.0000	0.2	4.8740	4.874	C
3309721	H Butanoate	0.0000	0.64	4.7300	4.819	C
4603300	MgOH +	15.9350		-11.7900	-11.19	C
4601400	MgCO3 AQ	2.0220	3.	2.9800	2.92	C
4601401	MgHCO3 +	-2.4300	-2.	11.4000	11.33	C
4601402	Mg2CO3+2				3.76	A
4601800	MgCl+				0.6	A
4605801	MgH2PO4 +	-1.1200		21.0660	21.22	C
4605802	MgHPO4 AQ	-0.2300	-0.9	15.2200	15.17	C
4607320	MgSO4 AQ	1.3990	1.4	2.2500	2.23	C
4609920	MgAcetate	0.0000		1.2700	1.27	U
4609710	MgPropanoate	0.0000		0.5400	0.98	C
4609720	MgButanoate	0.0000		0.5300	0.97	C
1003300	BaOH +	15.0950	14.4	-13.3580	-13.3	C
1001400	BaCO3(aq)		4.		2.71	A
1001401	BaHCO3+		2.		11.30	A
1004920	BaNO3+				0.7	A
1007320	BaSO4(aq)				2.2	A
1009921	BaAcetate	0.0000		1.0700	1.07	U
1009711	BaPropanoate	0.0000		0.3400	0.78	C
1009721	BaButanoate	0.0000		0.9400	0.75	C
1503300	CaOH +	14.5350	15.3	-12.5980	-12.6	C
1501400	CaHCO3 +	1.7900	1.	11.3300	11.59	C
1501401	CaCO3 AQ	4.0300	4.	3.1500	3.20	C

Table 3.1 (cont.)

MINTEQ ID No.	Name	MINTEQ ΔH^o_r	NIST ΔH^o_r	MINTEQ Log K	NIST Log K	STATUS
1501800	CaCl+				0.6	A
1504920	CaNO3+		-1.3		0.5	A
1505800	CaHPO4 AQ	-0.2300	0.0	15.0850	15.03	C
1505802	CaH2PO4 +	-1.1200	-1.	20.9600	20.98	C
1507320	CaSO4 AQ	1.4700	1.6	2.3090	2.30	C
1509920	CaAcetate	0.0000	1.0	1.1800	1.18	C
1509710	CaPropanoate	0.0000		0.5000	0.94	C
1509720	CaButanoate	0.0000		0.5100	0.95	C
5003300	NaOH		13.34		-13.8	A
5001400	NaCO3 –	8.9110		1.2680	1.27	C
5001401	NaHCO3 AQ	0.0000		10.0800	10.07	C
5001800	NaCl (aq)		-2.		-0.5	A
5004920	NaNO3 (aq)				-0.55	A
5005800	NaHPO4 –	0.0000	4.	12.6360	13.22	C
5005801	NaPO4-2				1.49	A
5005802	NaH2PO4(aq)				19.97	A
5007320	NaSO4 –	1.1200	0.3	0.7000	0.72	C
5009920	NaAcetate	0.0000	3.	-0.1800	-0.18	C
4103300	KOH				-13.7	A
4101800	KCl (aq)		-1.		-0.5	A
4104920	KNO3 (aq)		-3.		-0.19	A
4105800	KHPO4 –	0.0000	3.2	12.6400	13.16	C
4105801	KPO4-2				1.3	A
4105802	KH2PO4(aq)				20.0	A
4107320	KSO4 –	2.2500	1.8	0.8500	0.85	C
4109920	K Acetate		1.		-0.18	A
303300	AlOH +2	11.8990	12.	-4.9900	-4.98	C
303301	Al(OH)2 +	0.0000		-10.1000	-10.1	U
303302	Al(OH)4 –	44.0600		-23.0000	-22.6	C
303303	Al(OH)3 AQ	0.0000		-16.0000	-16.4	C
303304	Al2(OH)2+4				-4.7	A
303305	Al3(OH)4+5				-13.8	A
303306	Al13O4(OH)24+7				-98.7	A
301400	Al2(OH)2CO3+2				4.4	A
301401	Al3(OH)4HCO3+4				1.8	A
307320	AlSO4 +	2.1500		3.0200	3.89	C
305800	AlPO4(aq)				18.1	A
305801	Al2PO4+3				23.3	A
305802	AlHPO4+				21.4	A
305803	AlH2PO4+2				24.4	A
305804	Al2(OH)2PO4+				18.7	A
305805	Al2(OH)3PO4				9.6	A
2813300	FeOH +2	10.3990		-2.1900	-2.18	C

| 2813301 | FeOH2 + | 0.0000 | | -5.6700 | -4.5 | C |

Table 3.1 (cont.)

MINTEQ ID No.	Name	MINTEQ)H°r	NIST)H°r	MINTEQ Log K	NIST Log K	STATUS
2813304	Fe2(OH)2+4	13.5000	13.	-2.9500	-2.85	C
2813305	Fe3(OH)4+5	14.3000		-6.3000	-6.2	C
2811300	FeBr+2		6.		0.6	A
2817320	FeSO4 +	3.9100	6.	3.9200	4.04	C
2817321	Fe(SO4)2 –	4.6000		5.4200	5.38	C
2811800	FeCl +2	5.6000	5.6	1.4800	1.48	U
2811801	FeCl2 +	0.0000		2.1300	2.13	U
2814920	FeNO3+2				1.0	A
2815800	FeHPO4 +	-7.3000		17.7800	22.0	C
2815801	FeH2PO4 +2	0.0000		24.9800	23.94	C
2819920	FeAcetate	0.0000		3.2100	4.04	C
2819921	FeAcetate2	0.0000		6.5000	7.6	C
2819922	FeAcetate3	0.0000		8.3000	9.6	C
4703300	MnOH +	14.3990	13.	-10.5900	-10.5	C
4703302	Mn(OH)4-2				-48.2	A
4703303	Mn2(OH)+3				-7.1	A
4703304	Mn2(OH)3+				-23.8	A
4701400	MnHCO3 +	0.0000	-2.	11.6000	11.62	C
4704921	MnNO3+				0.2	A
4704920	Mn(NO3)2(aq)	-0.3960		0.6000	0.6	U
4707320	MnSO4 AQ	2.1700	2.1	2.2600	2.26	C
4709920	MnAcetate	0.0000		1.4000	1.40	U
1603300	CdOH +	13.1000		-10.0800	-10.0	C
1603301	Cd(OH)2 AQ	0.0000		-20.3500	-20.2	C
1603303	Cd(OH)4 -2	0.0000		-47.3500	-47.2	C
1603304	Cd2OH +3	10.8990		-9.3900	-9.3	C
1603305	Cd4(OH)4+4				-32.7	A
1601400	CdHCO3 +	0.0000		12.4000	12.78	C
1601401	CdCO3 AQ	0.0000		5.3990	4.3	C
1601403	Cd(CO3)2-2				7.25	A
1601300	CdBr +	-0.8100		2.1700	2.17	U
1601301	CdBr2 AQ	0.0000		2.8990	3.0	C
1601302	CdBr3 –				3.1	A
1601303	CdBr4-2				2.9	A
1601800	CdCl +	0.5900		1.9800	1.98	U
1601801	CdCl2 AQ	1.2400		2.6000	2.6	U
1601802	CdCl3 –	3.9000		2.3990	2.4	C
1604920	CdNO3 +	-5.2000	-5.2	0.3990	0.5	C
1604921	Cd(NO3)2 (aq)				0.4	A
1605800	CdHPO4(aq)				16.16	A
1607320	CdSO4 AQ	1.0800	2.3	2.4600	2.46	C

MINTEQ ID No.	Name	MINTEQ)H°r	NIST)H°r	MINTEQ Log K	NIST Log K	STATUS
1609921	CdAcetate	0.0000	1.8	1.9300	1.93	C
1609922	CdAcetate2	0.0000	3.2	3.1500	3.15	C
1609923	CdAcetate3	0.0000		2.1700	3.07	C

Table 3.1 (cont.)

MINTEQ ID No.	Name	MINTEQ)H°r	NIST)H°r	MINTEQ Log K	NIST Log K	STATUS
6003300	PbOH +	0.0000		-7.7100	-7.5	C
6003301	Pb(OH)2 AQ	0.0000		-17.1200	-17.0	C
6003302	Pb(OH)3 –	0.0000		-28.0600	-28.0	C
6003303	Pb2OH +3	0.0000		-6.3600	-6.3	C
6003304	Pb3(OH)4+2	26.5000		-23.8800	-23.8	C
6003306	Pb4(OH)4+4				-19.9	A
6003307	Pb6(OH)8+4				-43.5	A
6001400	Pb(CO3)2-2	0.0000		10.6400	9.46	C
6001401	PbCO3 AQ	0.0000		7.2400	6.60	C
6001300	PbBr +	2.8800		1.7700	1.77	U
6001301	PbBr2 AQ	0.0000		1.4400	2.6	C
6001302	PbBr3 –				3.0	A
6001303	PbBr4-2				2.3	A
6001800	PbCl +	4.3800	2.1	1.6000	1.55	C
6001801	PbCl2 AQ	1.0800	3.	1.8000	2.2	C
6001802	PbCl3 –	2.1700	1.	1.6990	1.8	C
6004920	PbNO3 +	0.0000	-0.6	1.1700	1.17	C
6004921	Pb(NO3)2(aq)				1.4	A
6005800	PbHPO4 (aq)				15.4	A
6005801	PbH2PO4 +				21.0	A
6007320	PbSO4 AQ	0.0000		2.7500	2.69	C
6009921	PbAcetate	0.0000		2.8700	2.68	C
6009922	PbAcetate2	0.0000		4.0800	4.08	U
6009711	PbPropanoate	0.0000		2.6400	2.64	U
6009712	PbPropanoat2	0.0000		4.1500	4.15	U
5403300	NiOH +	12.4200	12.2	-9.8600	-9.8	C
5403301	Ni(OH)2 AQ	0.0000		-19.0000	-18.	C
5403302	Ni(OH)3 –	0.0000		-30.0000	-29.	C
5403303	Ni4(OH)4+4				-27.6	A
5401400	NiHCO3 +	0.0000		12.4700	12.49	C
5401401	NiCO3 AQ	0.0000		6.8700	4.74	C
5404920	NiNO3+				0.4	A
5405800	NiHPO4(aq)				15.36	A
5405801	NiH2PO4+				20.4	A
5407320	NiSO4 AQ	1.5200	1.4	2.2900	2.34	C
5409921	NiAcetate	0.0000		1.4300	1.43	U
3613300	Hg+2	-11.0600		6.0970	6.1	C
3613302	HgOH+1	0.0000		2.6974	2.7	C
3613303	Hg(OH)3-1	0.0000		-15.0042	-14.9	C
3613304	Hg2(OH)+3				8.9	A

MINTEQ ID No.	Name					STATUS
3613305	Hg3(OH)3+3				11.9	A
3611404	HgCO3(aq)				18.3	A
3611401	Hg(CO3)2-2				21.8	A
3611402	HgHCO3+				22.5	A

Table 3.1 (cont.)

MINTEQ ID No.	Name	MINTEQ ΔH^o_r	NIST ΔH^o_r	MINTEQ Log K	NIST Log K	STATUS
3611403	HgOHCO3-				11.4	A
3611301	HgBr+	0.0000		15.8347	16.0	C
3611302	HgBr2 (aq)	-30.8320	-31.9	23.6065	23.6	C
3611303	HgBr3-1	0.0000		25.7857	26.4	C
3611304	HgBr4-2	0.0000	-36.96	27.0633	27.4	C
3611306	HgBrOH (aq)	0.0000		11.5980	12.6	C
3611800	HgCl+1	0.0000		12.8500	13.4	C
3611801	HgCl2 (aq)	0.0000		19.2203	20.1	C
3611802	HgCl3-1	0.0000		20.1226	21.1	C
3611803	HgCl4-2	0.0000		20.5338	21.7	C
3617320	HgSO4 (aq)	0.0000		7.4911	8.6	C
3617321	Hg(SO4)2-2				9.7	A
3619920	HgAcetate	0.0000		9.4170	10.2	C
3619711	HgPropanoate	0.0000		9.4170	10.5	C
3619721	HgButanoate	0.0000		10.0970	10.1	C
2113300	Cr+3	-20.1400	-31.1	9.6200	9.5	C
2113301	CrOH+2	0.0000	18.7	5.6200	5.8	C
2111300	CrBr+2	-11.2110	-22.2	7.5519	--	C
2115801	CrHPO4+				16.24	A
2119921	CrAcetate	0.0000	-30.	14.2500	15.03	C
2119922	CrAcetate2	0.0000	-28.	16.6800	18.08	C
2119923	CrAcetate3	0.0000	-23	19.2000	20.9	C
2119711	CrPropanoate	0.0000		14.3200	15.1	C
2119712	CrPropanoat2	0.0000		16.6600	18.04	C
2119713	CrPropanoat3	0.0000		19.3200	21.0	C
0203300	AgOH(aq)	0.0000		-12.0000	-12.0	U
0203301	Ag(OH)2-	0.0000		-24.0000	-24.0	U
0201300	AgBr(aq)	0.0000		4.2400	4.7	C
0201301	Ag(Br)2-	0.0000		7.2800	7.5	C
0201302	Ag(Br)3-2	0.0000		8.7100	8.4	C
0201303	Ag(Br)4-3				8.5	A
0201800	AgCl(aq)	-2.6800	-2.7	3.2700	3.31	C
0201801	Ag(Cl)2-	-3.9300	4.	5.2700	5.25	C
0201802	Ag(Cl)3-2	0.0000		5.2900	5.20	C
0204920	AgNO3(aq)	0.0000		-0.2900	-0.1	C
0207320	AgSO4-	1.4900	1.5	1.2900	1.3	C
0209921	AgAcetate	0.0000	0.9	0.7300	0.73	U
0209922	Ag(Acetate)2	0.0000	0.9	0.6400	0.64	U
9503300	ZnOH+	13.3990	13.34	-8.96	-8.9	C

MINTEQ ID No.	Name	MINTEQ ΔH^o_r	NIST ΔH^o_r	MINTEQ Log K	NIST Log K	STATUS
9503301	Zn(OH)2(aq)	0.0000		-16.899	-17.7	C
9503302	Zn(OH)3-	0.0000		-28.399	-28.0	C
9503303	Zn(OH)4-2	0.0000		-41.199	-40.4	C
9501401	ZnCO3(aq)	0.0000		5.3	5.1	C
9501400	ZnHCO3+	0.0000		12.4	11.74	C

Table 3.1 (cont.)

MINTEQ ID No.	Name	MINTEQ ΔH^o_r	NIST ΔH^o_r	MINTEQ Log K	NIST Log K	STATUS
9507320	ZnSO4(aq)	1.3600	1.5	2.37	2.34	C
9505800	ZnHPO4(aq)				15.6	A
9505801	ZnH2PO4+				21.2	A
9504920	ZnNO3+				0.4	A
9504921	Zn(NO3)2(aq)				-0.3	A
9501800	ZnCl+	7.7900		0.43	0.46	C
9501801	Zn(Cl)2(aq)	8.5000		0.45	0.6	C
9509921	ZnAcetate	0.0000		1.57	1.58	C
9509922	Zn(Acetate)2	0.0000		1.90	2.0	C
9509711	ZnPropanoate	0.0000		0.72	1.45	C
9509712	ZnPropanoat2	0.0000		1.23	2.03	C
9509721	ZnButanoate	0.0000		0.983	1.44	C

SOLID SPECIES

MINTEQ ID No.	Name	MINTEQ ΔH^o_r	NIST ΔH^o_r	MINTEQ Log K	NIST Log K	STATUS
2003003	GIBBSITE (C)	22.8000		-8.7700	-8.4	C
7003000	AlPO4(s)				21.3	A
2015001	PORTLANDITE	30.6900	30.9	-22.6750	-22.80	C
5015000	ARAGONITE	2.6150	3.	8.3600	8.30	C
5015001	CALCITE	2.5850	2.	8.4750	8.48	C
5015004	VATERITE		4.		7.91	A
5015005	MONOHYDROCAL				7.60	A
6015000	ANHYDRITE	3.7690	-0.3	4.6370	4.62	C
7015004	CaHPO4(H2O)2		-4.		18.95	A
7015005	Ca3(PO4)2		13.2		28.92	A
7015006	Ca4H(PO4)3				61.6	A
2046000	BRUCITE	25.8400		-16.7920	-16.84	C
2046002	Mg(OH)2(act)				-18.7	A
5046002	MAGNESITE	6.1690	5.	8.0290	7.46	C
5046003	NESQUEHONITE	5.7890		5.6210	4.67	C
5046004	MgCO3.5H2O				4.54	A
7046001	MgHPO4(H2O)3				18.17	A
7046002	Mg3(PO4)2(s)				23.28	A
2010000	Ba(OH)2.8H2O		12.9		-24.3	A
5010000	WITHERITE	-0.3600	-1.	8.5850	8.57	C
6010000	BARITE	-6.2800	-5.5	9.9760	9.96	C
7010000	BaHPO4(s)				19.77	A

MINTEQ ID No.	Name	MINTEQ ΔH^o_r	NIST ΔH^o_r	MINTEQ Log K	NIST Log K	STATUS
2028100	FERRIHYDRITE	0.0000		-4.8910	-3.1	C
2028102	GOETHITE	14.4800		-0.5000	-0.4	C
3028100	HEMATITE	30.8450		4.0080	1.4	C
7028100	STRENGITE	2.0300		26.4000	26.4	U
2047003	PYROCROITE	22.5900		-15.0880	-15.1	C
5047000	RHODOCHROSIT	2.0790		10.4100	10.58	C

Table 3.1 (cont.)

MINTEQ ID No.	Name	MINTEQ ΔH^o_r	NIST ΔH^o_r	MINTEQ Log K	NIST Log K	STATUS
2016001	CD(OH)2 (C)	0.0000	22.5	-13.6500	-13.64	C
5016000	OTAVITE	0.5800		13.7400	12.00	C
2060000	MASSICOT	16.7800		-12.9100	-12.8	C
2060001	LITHARGE	16.3800		-12.7200	-12.6	C
2060005	PB2O(OH)2	0.0000		-26.2000	-26.1	C
4160000	COTUNNITE	-5.6000		4.7700	4.78	C
5060000	CERRUSITE	-4.8600		13.1300	13.13	U
5060003	HYDCERRUSITE	0.0000		17.4600	19.1	C
5060004	PLUMBONAERIT				8.76	A
6060003	ANGLESITE	-2.1500	-3.	7.7900	7.79	C
7060006	PBHPO4	0.0000		23.9000	23.8	C
7060007	PB3(PO4)2	0.0000		44.5000	43.53	C
2054000	NI(OH)2	-30.4500		-10.8000	-12.7	C
5054000	NICO3	9.9400		6.8400	6.87	C
2036101	Hg(OH)2(s)	0.0000		3.4963	3.5	C
4036100	HgBr2(s)	-34.452		25.373	25.9	C
5036101	Hg2O2CO3(s)				29.4	A
2021101	CR(OH)3 (C)	7.1150		-1.7005	-1.3	C
2002000	Ag2O(s)	10.4300	10.48	-12.5800	-12.57	C
5002000	Ag2CO3(s)	9.5300		11.0700	11.09	C
4002000	BROMYRITE	-20.1700	-20.26	12.2700	12.30	C
5102000	AgNO3(s)				-5.43	A
6002000	Ag2SO4(s)	-4.2500	-4.1	4.9200	4.83	C
7002000	Ag3PO4(s)	0.0000		17.5500	17.59	C
2095000	Zn(OH)2(s,am)	0.0000		-12.45	-12.47	C
2095002	Zn(OH)2(s,B1)	0.0000		-11.75	-11.75	U
2095007	Zn(OH)2(s,B2)				-11.79	A
2095003	Zn(OH)2(s,gm)	0.0000		-11.71	-11.73	C
2095008	Zn(OH)2(s,del)				-11.84	A
2095004	Zn(OH)2(s,eps)	0.0000		-11.50	-11.53	C
2095005	ZnO(s)	0.0000		-11.31	-11.33	C
5095000	ZnCO3(s)	4.3600		10.0	10.00	U
7095000	Zn3(PO4)2(s)	0.0000		32.42	35.42	C

4.0   UPDATING AND TESTING MINTEQA2 DATABASE FILES

The data for species shown in Table 3.1 having a status of (A)dded or (C)orrected were used to update the MINTEQA2 database files THERMO.DBS, TYPE6.DBS, and GASES.DBS. The latter two files are merely subsets of the overall thermodynamic database file THERMO.DBS. Therefore, all corrections were made in THERMO.DBS and new TYPE6.DBS and GASES.DBS files were created by duplication of the appropriate sections of the corrected THERMO.DBS file.

Two quality assurance (QA) measures were implemented to ensure that the final entries in THERMO.DBS reflected the intended changes and additions obtained from the NIST database through CRITICAL. For the first QA measure, a short Pascal program, DATACHEK was used to display all parameters for updated species on the computer screen. For corrected species, the old and new parameters were displayed side-by-side for comparison with each other and with notebook entries made as the NIST data was reduced to MINTEQA2 components, ionic strength zero, and 25° C. For added species, the displayed data was compared with notebook entries. In addition, DATACHEK automatically computed and updated the molar mass and charge for each corrected and added species from the stoichiometry of each component and the known component masses and charges (read from the component database COMP.DBS). Prior to use in DATACHEK, the component masses in COMP.DBS were checked and made to conform with atomic weight standards as given by IUPAC (1984).

In the second QA test, the MINTEQA2 model was executed with a test input file containing all ten ligands, all eight secondary metals, and one of the seven primary metals. Prior to executing the model, it was necessary to create new unformatted versions of the THERMO.DBS and TYPE6.DBS files. This was accomplished by using the UNFRMT program supplied with version 3.11 of MINTEQA2.   The new unformatted files, THERMO.UNF and TYPE6.UNF, were used in the test model runs in which the model output option was set to FULL so as to obtain a printout of the raw thermodynamic parameters as read from the corrected database files. The printout was then compared with Table 3.1 above to ensure that the information read by the model conforms to the intended updates. This test was repeated for each of the seven primary cations. All discrepancies were noted and corrected.

Finally, during the course of using CRITICAL, several apparent inconsistencies or errors in the NIST database were discovered. The questionable entries were brought to the attention of the user support group at Texas A&M University, Dept. of Chemistry as directed in the CRITICAL user guide.   The list below details the NIST database errors and our interpretation or course of action pertaining to each:

1.   Some mass law expressions displayed by CRITICAL use dots to separate reactants rather than enclosing reactants in square brackets as is traditionally done to indicate concentrations. Also, when dots are used, stoichiometric coefficients that should be exponents in the mass law may appear as subscripts. Subscripts may also appear in place of exponents even if square brackets are used. We interpreted each instance of these inconsistencies in the most reasonable way.

2.   There are multiple entries for $KHPO_4^-$ and KH_2PO_4(aq). The data displayed by CRITICAL for the second entry is not consistent with the first. We used the first data displayed. It always included the data with lowest ionic strength and temperature 25° C.

3.   The mass law for the Hg^{2+} solid species $HgBr_2$ (s) indicated a stoichiometry of one for Br^-. The NIST support person felt that this was simply an omission of the stoichiometric coefficient. We treated it as such; the computed log K was very close to the previous MINTEQA2 value which supports our interpretation.

4.   The mass law for the Al^{3+} solid species $Al(OH)_3$ (s,") was given as $[ML_3]/[ML_3(s,")]$.   The numerator portion of this expression should be $[M][L]^3$. We confirmed this by obtaining the article cited in the CRITICAL bibliography (Frink and Peech, 1962).

5.0   REFERENCES

Allison, J.D., D.S. Brown, and K.J. Novo-Gradac, 1991. MINTEQA2/PRODEFA2, A Geochemical Assessment Model for Environmental Systems: Version 3.0 User's Manual. U.S. Environmental Protection Agency, Athens, GA. EPA/600/3-91/021.

Frink, C. R. and M. Peech, 1962. *Soil Sci. Soc. Proc.* **26**, 346.

IUPAC Commission on Atomic Weights, 1984. *Pure and Appl. Chem.* **56**, 653.

NIST, 1993. *NIST Critical Stability Constants for Metal Complexes Database, Version 1.0.* Standard Reference Database 46, National Institute of Standards, U.S. Dept of Commerce, Gaithersburg, MD.

Smith, R.M. and A.E. Martell, 1976. *Critical Stability Constants*, Plenum Press, New York.

APPENDIX C

EXAMPLE MINTEQA2 INPUT FILE

```
PRODUCTION RUN.  PB  UNSAT ZONE, Water Saturation = 77.7%
LMML:  Lo Leachate Acids, Md FeO Sorbent, Md Natural Organic Matter, Lo pH
14.00 MG/L   0.000  4.57000E+00
0 0 1 1 3 0 0 0 1 0 2 1 2
TOTAL CONC 600 48
  1.000E-02  5.000E-02  1.000E-01  2.500E-01  5.000E-01  7.500E-01
  1.000E+00  2.000E+00  3.000E+00  4.000E+00  5.000E+00  6.000E+00
  8.000E+00  1.000E+01  1.200E+01  1.400E+01  1.600E+01  2.000E+01
  2.500E+01  3.000E+01  4.000E+01  5.000E+01  6.000E+01  7.000E+01
  9.000E+01  1.100E+02  1.300E+02  1.500E+02  1.700E+02  1.900E+02
  2.100E+02  2.300E+02  2.500E+02  2.750E+02  3.000E+02  3.500E+02
  4.000E+02  5.000E+02  7.500E+02  1.000E+03  2.500E+03  5.000E+03
  1.000E+04  2.500E+04  5.000E+04  7.500E+04  1.000E+05
PbLMMLux.prn      600
4   1   7
1.525E+01  600.00 0.000 0.000 81
    330  0.000E+00   -8.00 y                   /H+1
    600  1.000E-03   -6.24 y                   /Pb+2
     30  2.000E-01   -5.13 y                   /Al+3
    150  4.800E+01   -2.92 y                   /Ca+2
    281  2.000E-01   -5.45 y                   /Fe+3
    460  1.400E+01   -3.24 y                   /Mg+2
    470  4.000E-02   -6.14 y                   /Mn+2
    410  2.900E+00   -4.13 y                   /K+1
    500  2.200E+01   -3.02 y                   /Na+1
    140  1.870E+02   -2.51 y                   /CO3-2
    130  3.000E-01   -5.43 y                   /Br-1
    180  1.500E+01   -3.37 y                   /Cl-1
    492  1.000E+00   -4.79 y                   /NO3-1
    580  9.000E-02   -6.02 y                   /PO4-3
    732  2.500E+01   -3.58 y                   /SO4-2
    992  2.480E+01   -3.37 y                   /Acetate
    971  1.461E+01   -3.71 y                   /Prpanot
    972  1.568E+01   -3.75 y                   /Butanot
    145  2.439E-05   -6.50                     /DOM
    146  5.758E-03   -6.17                     /POM
    811  8.568E-04   -4.45 y                   /ADS1TYP1
    812  3.427E-02   -2.84 y                   /ADS1TYP2
    813  0.000E+00    0.00 y                   /ADS1PSIo

  3   1
    330     4.9000      0.0000                 /H+1
  6   3
    813     0.0000      0.0000                 /ADS1PSIo
2003002     0.0000      0.0000                 /DIASPORE
3028100     0.0000      0.0000                 /HEMATITE

  2  34
8123301 =SO2-          0.0000   -8.9300   0.000   0.000-1.00 0.00 0.00   0.0000
 0.00 3   1.000 812  -1.000 330  -1.000 813   0.000   0   0.000   0   0.000   0
  0.000   0   0.000   0   0.000   0   0.000   0   0.000   0   0.000   0
```

C-1

```
0  0.000   0   0.000   0   0.000   0
8123302 =SO2H2+          0.0000    7.2900   0.000   0.000 1.00 0.00 0.00   0.0000
 0.00 3   1.000 812   1.000 330   1.000 813   0.000   0   0.000   0   0.000   0
   0.000   0   0.000   0   0.000   0   0.000   0   0.000   0   0.000   0
0  0.000   0   0.000   0   0.000   0
8113301 =SO1-           0.0000   -8.9300   0.000   0.000-1.00 0.00 0.00   0.0000
 0.00 3   1.000 811  -1.000 330  -1.000 813   0.000   0   0.000   0   0.000   0
   0.000   0   0.000   0   0.000   0   0.000   0   0.000   0   0.000   0
0  0.000   0   0.000   0   0.000   0
8113302 =SO1H2+          0.0000    7.2900   0.000   0.000 1.00 0.00 0.00   0.0000
 0.00 3   1.000 811   1.000 330   1.000 813   0.000   0   0.000   0   0.000   0
   0.000   0   0.000   0   0.000   0   0.000   0   0.000   0   0.000   0
0  0.000   0   0.000   0   0.000   0
8120200 =SO2AgOH2        0.0000   -5.3000   0.000   0.000 0.00 0.00 0.00   0.0000
 0.00 4   1.000 812  -1.000 330   1.000  20   1.000   2   0.000   0   0.000   0
   0.000   0   0.000   0   0.000   0   0.000   0   0.000   0   0.000   0
0  0.000   0   0.000   0   0.000   0
8110200 =SO1AgOH2        0.0000   -1.7200   0.000   0.000 0.00 0.00 0.00   0.0000
 0.00 4   1.000 811  -1.000 330   1.000  20   1.000   2   0.000   0   0.000   0
   0.000   0   0.000   0   0.000   0   0.000   0   0.000   0   0.000   0
0  0.000   0   0.000   0   0.000   0
8123610 =SO2HgOH2+       0.0000   12.5500   0.000   0.000 1.00 0.00 0.00   0.0000
 0.00 5   1.000 812   1.000 361  -1.000   2   1.000 330   1.000 813   0.000   0
   0.000   0   0.000   0   0.000   0   0.000   0   0.000   0   0.000   0
0  0.000   0   0.000   0   0.000   0
8113610 =SO1HgOH2+       0.0000   13.8600   0.000   0.000 1.00 0.00 0.00   0.0000
 0.00 5   1.000 811   1.000 361  -1.000   2   1.000 330   1.000 813   0.000   0
   0.000   0   0.000   0   0.000   0   0.000   0   0.000   0   0.000   0
0  0.000   0   0.000   0   0.000   0
8112110 =SO1CrOH+        0.0000   11.5600   0.000   0.000 1.00 0.00 0.00   0.0000
 0.00 4   1.000 811   1.000 211   1.000 813  -1.000   2   0.000   0   0.000   0
   0.000   0   0.000   0   0.000   0   0.000   0   0.000   0   0.000   0
0  0.000   0   0.000   0   0.000   0
8129500 =SO2Zn+          0.0000   -1.9900   0.000   0.000 1.00 0.00 0.00   0.0000
 0.00 5   1.000 812  -1.000 330   1.000 813   1.000 950   1.000   2   0.000   0
   0.000   0   0.000   0   0.000   0   0.000   0   0.000   0   0.000   0
0  0.000   0   0.000   0   0.000   0
8119500 =SO1Zn+          0.0000    0.9700   0.000   0.000 1.00 0.00 0.00   0.0000
 0.00 5   1.000 811  -1.000 330   1.000 813   1.000 950   1.000   2   0.000   0
   0.000   0   0.000   0   0.000   0   0.000   0   0.000   0   0.000   0
0  0.000   0   0.000   0   0.000   0
8121600 =SO2Cd+          0.0000   -2.9000   0.000   0.000 1.00 0.00 0.00   0.0000
 0.00 5   1.000 812  -1.000 330   1.000 813   1.000 160   1.000   2   0.000   0
   0.000   0   0.000   0   0.000   0   0.000   0   0.000   0   0.000   0
0  0.000   0   0.000   0   0.000   0
8111600 =SO1Cd+          0.0000    0.4300   0.000   0.000 1.00 0.00 0.00   0.0000
 0.00 5   1.000 811  -1.000 330   1.000 813   1.000 160   1.000   2   0.000   0
   0.000   0   0.000   0   0.000   0   0.000   0   0.000   0   0.000   0
0  0.000   0   0.000   0   0.000   0
8112310 =SO1Cu+          0.0000    2.8500   0.000   0.000 1.00 0.00 0.00   0.0000
 0.00 5   1.000 811  -1.000 330   1.000 813   1.000 231   1.000   2   0.000   0
```

```
   0.000    0    0.000    0    0.000    0    0.000    0    0.000    0    0.000    0
0    0.000    0    0.000    0    0.000    0
8122310 =SO2Cu+        0.0000    0.6000    0.000    0.000 1.00 0.00 0.00    0.0000
 0.00 5    1.000 812   -1.000 330    1.000 813    1.000 231    1.000    2    0.000    0
   0.000    0    0.000    0    0.000    0    0.000    0    0.000    0    0.000    0
0    0.000    0    0.000    0    0.000    0
8115400 =SO1Ni+        0.0000    0.1500    0.000    0.000 1.00 0.00 0.00    0.0000
 0.00 5    1.000 811   -1.000 330    1.000 813    1.000 540    1.000    2    0.000    0
   0.000    0    0.000    0    0.000    0    0.000    0    0.000    0    0.000    0
0    0.000    0    0.000    0    0.000    0
8125400 =SO2Ni+        0.0000   -2.5000    0.000    0.000 1.00 0.00 0.00    0.0000
 0.00 5    1.000 812   -1.000 330    1.000 813    1.000 540    1.000    2    0.000    0
   0.000    0    0.000    0    0.000    0    0.000    0    0.000    0    0.000    0
0    0.000    0    0.000    0    0.000    0
8116000 =SO1Pb+        0.0000    4.7100    0.000    0.000 1.00 0.00 0.00    0.0000
 0.00 5    1.000 811   -1.000 330    1.000 813    1.000 600    1.000    2    0.000    0
   0.000    0    0.000    0    0.000    0    0.000    0    0.000    0    0.000    0
0    0.000    0    0.000    0    0.000    0
8126000 =SO2Pb+        0.0000    0.3000    0.000    0.000 1.00 0.00 0.00    0.0000
 0.00 5    1.000 812   -1.000 330    1.000 813    1.000 600    1.000    2    0.000    0
   0.000    0    0.000    0    0.000    0    0.000    0    0.000    0    0.000    0
0    0.000    0    0.000    0    0.000    0
8121500 =SO2Ca+        0.0000   -5.8500    0.000    0.000 1.00 0.00 0.00    0.0000
 0.00 4    1.000 812   -1.000 330    1.000 813    1.000 150    0.000    0    0.000    0
   0.000    0    0.000    0    0.000    0    0.000    0    0.000    0    0.000    0
0    0.000    0    0.000    0    0.000    0
8111500 =SO1HCa++      0.0000    4.9700    0.000    0.000 2.00 0.00 0.00    0.0000
 0.00 3    1.000 811    1.000 150    2.000 813    0.000    0    0.000    0    0.000    0
   0.000    0    0.000    0    0.000    0    0.000    0    0.000    0    0.000    0
0    0.000    0    0.000    0    0.000    0
8111000 =SO1HBa++      0.0000    5.4600    0.000    0.000 2.00 0.00 0.00    0.0000
 0.00 3    1.000 811    1.000 100    2.000 813    0.000    0    0.000    0    0.000    0
   0.000    0    0.000    0    0.000    0    0.000    0    0.000    0    0.000    0
0    0.000    0    0.000    0    0.000    0
8121000 =SO2Ba+        0.0000   -7.2000    0.000    0.000 1.00 0.00 0.00    0.0000
 0.00 4    1.000 812   -1.000 330    1.000 813    1.000 100    0.000    0    0.000    0
   0.000    0    0.000    0    0.000    0    0.000    0    0.000    0    0.000    0
0    0.000    0    0.000    0    0.000    0
8117320 =S1SO4-        0.0000    7.7800    0.000    0.000-1.00 0.00 0.00    0.0000
 0.00 5    1.000 811    1.000 330   -1.000 813    1.000 732   -1.000    2    0.000    0
   0.000    0    0.000    0    0.000    0    0.000    0    0.000    0    0.000    0
0    0.000    0    0.000    0    0.000    0
8127320 =S2SO4-        0.0000    7.7800    0.000    0.000-1.00 0.00 0.00    0.0000
 0.00 5    1.000 812    1.000 330   -1.000 813    1.000 732   -1.000    2    0.000    0
   0.000    0    0.000    0    0.000    0    0.000    0    0.000    0    0.000    0
0    0.000    0    0.000    0    0.000    0
8117321 =SO1HSO4-2     0.0000    0.7900    0.000    0.000-2.00 0.00 0.00    0.0000
 0.00 4    1.000 811   -2.000 813    1.000 732   -1.000    2    0.000    0    0.000    0
   0.000    0    0.000    0    0.000    0    0.000    0    0.000    0    0.000    0
0    0.000    0    0.000    0    0.000    0
8127321 =SO2HSO4-2     0.0000    0.7900    0.000    0.000-2.00 0.00 0.00    0.0000
```

```
  0.00 4   1.000 812  -2.000 813   1.000 732  -1.000   2   0.000   0   0.000   0
    0.000   0   0.000   0   0.000   0   0.000   0   0.000   0   0.000   0
0  0.000   0   0.000   0   0.000   0
8115800 =S1H2PO4        0.0000   31.2900   0.000   0.000 0.00 0.00 0.00   0.0000
  0.00 4   1.000 811   1.000 580   3.000 330  -1.000   2   0.000   0   0.000   0
    0.000   0   0.000   0   0.000   0   0.000   0   0.000   0   0.000   0
0  0.000   0   0.000   0   0.000   0
8125800 =S2H2PO4        0.0000   31.2900   0.000   0.000 0.00 0.00 0.00   0.0000
  0.00 4   1.000 812   1.000 580   3.000 330  -1.000   2   0.000   0   0.000   0
    0.000   0   0.000   0   0.000   0   0.000   0   0.000   0   0.000   0
0  0.000   0   0.000   0   0.000   0
8115801 =S1HPO4-        0.0000   25.3900   0.000   0.000-1.00 0.00 0.00   0.0000
  0.00 5   1.000 811  -1.000 813   1.000 580   2.000 330  -1.000   2   0.000   0
    0.000   0   0.000   0   0.000   0   0.000   0   0.000   0   0.000   0
0  0.000   0   0.000   0   0.000   0
8125801 =S2HPO4-        0.0000   25.3900   0.000   0.000-1.00 0.00 0.00   0.0000
  0.00 5   1.000 812  -1.000 813   1.000 580   2.000 330  -1.000   2   0.000   0
    0.000   0   0.000   0   0.000   0   0.000   0   0.000   0   0.000   0
0  0.000   0   0.000   0   0.000   0
8115802 =S1PO4-2        0.0000   17.7200   0.000   0.000-2.00 0.00 0.00   0.0000
  0.00 5   1.000 811   1.000 580   1.000 330  -2.000 813  -1.000   2   0.000   0
    0.000   0   0.000   0   0.000   0   0.000   0   0.000   0   0.000   0
0  0.000   0   0.000   0   0.000   0
8125802 =S2PO4-2        0.0000   17.7200   0.000   0.000-2.00 0.00 0.00   0.0000
  0.00 5   1.000 812   1.000 580   1.000 330  -2.000 813  -1.000   2   0.000   0
    0.000   0   0.000   0   0.000   0   0.000   0   0.000   0   0.000   0
0  0.000   0   0.000   0   0.000   0
8129030 =SOHVO4-3       0.0000  -16.5300   0.000   0.000-3.00 0.00 0.00   0.0000
  0.00 5   1.000 812   1.000 903   2.000   2  -4.000 330  -3.000 813   0.000   0
    0.000   0   0.000   0   0.000   0   0.000   0   0.000   0   0.000   0
```